The Rôle of Sponges in High-Antarctic Carbon and Silicon Cycling – a Modelling Approach

Die Rolle der Schwämme im hochantarktischen Kohlenstoff- und Silikatkreislauf – ein Modellierungsansatz

Susanne Gatti

Susanne Gatti
Stiftung Alfred-Wegener-Institut für Polar- und Meeresforschung
Am Handelshafen 12
27570 Bremerhaven

Contents

Summary

Antarctica is a sponge kingdom. Sponges clearly dominate many areas on the Antarctic shelf regarding abundance and biomass in terms of wet mass (>90% are comprised of sponges). Furthermore they are of known structural importance for benthic shelf communities. Nevertheless our knowledge about the sponge's contribution to energy and matter flow within the system is less than fragmentary. Despite a detailed 10-year *in situ* study growth rates could only be established for 2 of 11 studied sponges species. While calcareous sponges can be aged by carbon isotope ratios, no comparable methods are hitherto available for direct age determination of glass-sponges (Hexactinellida and Demospongiae).

In this study I used an indirect approach to estimate the age of slow growing Antarctic sponges: mass specific oxygen consumption rate – which depends on the size of an individual – was used as a proxy of metabolic rate. Not only metabolic rate depends on the size of an individual, also that part of available energy that is spent for growth ($P_s/\Sigma R$) varies with size of the individual. Based on experimentally established relationships between the metabolic rate and body mass on one hand and the $P_s/\Sigma R$ ratio and body mass on the other hand I developed a modelling routine (AMIGO: Advanced Modelling of Invertebrate Growth from Oxygen consumption data) to calculate growth rates of sponges of different initial body mass. In a test run of the model growth rates of *Halichondria panicea* (Baltic Sea) determined in a laboratory- and field-study were compared with those calculated by the model. Modelled growth rates were in good agreement with those observed in the field or laboratory.

To be able to use the model for Antarctic sponges I established a data set of respiration rates of the Demospongiae *Stylocordyla borealis* and *Cinachyra antarctica* as well as for the Hexactinellida *Rossella spp.* from the eastern Weddell Sea shelf (WSS). Weighted least square linear regression analysis was used to compensate for bias introduced by variable data quality. The upper and lower 95% confidence limits of these regressions were used as a basis for error propagation of subsequent calculations. Von Bertalanffy growth functions were fitted to growth curves as modelled for each species with AMIGO. Largest individuals on the eastern Weddell Sea Shelf were 152 years (*S. borealis*), 35 years (*C. antarctica*) and 1515 years (*Rossella spp.*) old. For the calculation of energy budgets based on modelled growth curves, I supplemented my own mass frequency distribution (MFD) data for *S. borealis* and *C. antarctica* with data from literature. For *Rossella spp.* I used MFD and abundance data from literature.

These data indicate a high standing stock of sponge biomass (45.3 gC m^{-2}) on the WSS with sponges clearly dominating communities not only in terms of wet mass but

also in terms of carbon. I found a mean annual production of 0.3 gC m^{-2} y^{-1} of the sponge community on the eastern WSS (depth range of 100 - 700 m) with an annual productivity (P$_s$/B) of 0.007. *S. borealis* – the lollypop sponge – is a known relatively early settler in iceberg scour marks and showed a markedly higher P$_s$/B of 0.106. Overall, sponges do not contribute substantially to carbon flow on the eastern WSS. Opal production (biogenic SiO$_2$) of sponges on the eastern WSS (100 - 700m water depth) amounted to ~1Mt y^{-1} (2.4 gSiO$_2$ m^{-2} y^{-1}). Estimates of opal from primary production that reaches the sea floor are hitherto uncertain and may on the WSS only account for less that 1g m^{-2} y^{-1} of opal. It can thus be concluded that locally sponges are the predominant pathway for dissolved silicic acid to opal.

Based on my modelling results it is now possible to age resettlement stages of iceberg scour marks by aging the largest hexactinellid sponge specimen in a study area. With the help of such data the disturbance regime on the eastern WSS can be described more clearly.

Independent validation of my modelling results with the fission track dating method that is also used in geology, may be possible in the near future. With this technique single sponge spicules can be analyzed and the age of a sponge individual may possibly be assessed by different number of fission tracks per area of old and young spicules. Sample analysis is presently ongoing.

Zusammenfassung

Die Antarktis ist ein Reich der Schwämme. Sie dominieren sowohl hinsichtlich der Biomasse als auch hinsichtlich der Abundanz (> 90% sind Schwämme) große Gebiete auf dem Schelf des östlichen Weddellmeeres. Die entscheidende Bedeutung des strukturierenden Einflusses der Schwämme auf benthische Gemeinschaften des Schelfes ist inzwischen gut untersucht. Dagegen beruhen unsere Kenntnisse über ihren Beitrag zu Energie- und Partikelfluss im System bis jetzt lediglich auf vagen Schätzungen. Trotz einer detaillierten 10-Jahres *in situ* Studie konnten bisher nur für zwei der untersuchten elf Arten Wachstumsraten ermittelt werden. Es stehen zur Zeit keine Methoden zur Altersbestimmung von Glasschwämmen (Hexactinellida und Demospongiae) zur Verfügung.

In dieser Arbeit wurde ein indirekter Ansatz gewählt mit dem Ziel, Wachstumsraten auch für die langsam wachsenden Arten abschätzen zu können: Massenspezifische Sauerstoffverbrauchsraten, die von der Größe eines Individuums abhängen, wurden als Proxy für die Stoffwechselrate benutzt. Neben der Stoffwechselrate hängt auch der Anteil der Energie, der für Wachstum genutzt wird ($P_s/\Sigma R$) von der Körpermasse ab. Basierend auf experimentell gefundenen Beziehungen zwischen der Stoffwechselrate und Körpermasse einerseits sowie zwischen dem $P_s/\Sigma R$-Verhältnis und der Körpermasse andererseits, habe ich eine Modellroutine (AMIGO: Advanced Modelling of Invertebrate Growth from Oxygen consumption data) entwickelt, mit der die Berechnung von Wachstumsraten verschieden großer Schwämme möglich ist. Ein Vergleich von Modelldaten mit experimentell ermittelten Labor- und Freilandwachstumsdaten des Brotkrummenschwamms *Halichondria panicea* (Ostsee) ergaben eine gute Übereinstimmung.

Für die Anwendung des Modells auf antarktische Schwämme habe ich experimentell Sauerstoffverbrauchsdaten für die Demospongiae *Stylocordyla borealis* und *Cinachyra antarctica* sowie für die Hexactinellida *Rossella spp.* des östlichen Weddellmeerschelfes ermittelt. Um Unterschiede in der Datenqualität zu kompensieren habe ich diese Datensätze mit gewichteter linearer Regression analysiert. Die obere und untere 95% Vertrauensgrenze dieser Regressionen habe ich mittels Fehlerfortpflanzung in allen folgenden Berechnungen zur Abschätzung der Zuverlässigkeit benutzt. Zur Beschreibung der mit AMIGO modellierten Wachstumskurven wurde für die jeweilige Art eine von Bertalanffy Wachstumsfunktion an die Modellergebnisse angepaßt. Die größten Individuen auf dem östlichen Weddellmeerschelfes sind danach 152 Jahre (*S. borealis*), 35 Jahre (*C. antarctica*) bzw. 1515 Jahre alt (*Rossella spp.*). Zur Berechnung der Energiebilanzen, die auf diesen Modellergebnissen basieren, habe ich meine eigenen Masse-Häufikeits-Verteilungsdaten für *S. borealis* und *C. antarctica* mit Abundanzdaten aus der Literatur

ergänzt. Für *Rossella spp.* stammen sowohl die Masse-Häufigkeitsverteilungen als auch die Abundanzdaten aus der Literatur.

Die Berechnungen ergeben eine hohe Schwammbestandsdichte (45.3 gC m^{-2}) bei gleichzeitiger niedriger Produktivität (P_s/B = 0.007) im Tiefenhorizont von 100 - 700m Wassertiefe. *S. borealis* – der 'Lollypop' Schwamm – zeigte als relativ früher Besiedler von Eisbergkratzern eine deutlich höhere Produktivität (P_s/B = 0.106). Im Mittel tragen die Schwämme des östlichen Weddellmeerschelfes nicht nennenswert zum Kohlenstofffluss in diesem Gebiet bei. Die Opalproduktion (biogenes Silikat) der Schwammgemeinschaft (100 - 700m Wassertiefe) beträgt ca. 1Mt y^{-1} (2.4 gSiO$_2$ m^{-2} y^{-1}). Abschätzungen des Opalanteils, der aus Primärproduktion den Boden des Schelfes erreicht sind bis heute unsicher und belaufen sich für das östliche Weddellmeerschelf möglicherweise auf weniger als 1g Opal pro Jahr. Daraus schließe ich, dass die Schwammgemeinschaft lokal den beherrschenden Stoffwechselweg vom gelöstem Silizium zu Opal darstellt.

Vor dem Hintergrund meiner Modellierungsergebnisse ist es nun möglich, Wiederbesiedlungsstadien von Eisbergkratzern anhand des Alters des größten hexactinelliden Schwammes einer Wiederbesiedlungszone zu datieren. Mithilfe solcher Daten können Störungsmuster der Fauna des östlichen Weddellmeerschelfes genauer als bisher beschrieben werden.

Die unabhängige Validierung meiner Modellergebnisse könnte in naher Zukunft mit Hilfe von Spaltspurdatierungen, einer Methode, die auch in der Geologie benutzt wird, möglich sein. Mit dieser Methode können einzelne Schwammspikulae analysiert werden. Das Alter eines Individuums kann möglicherweise aus der unterschiedlichen Dichte von Spaltspuren in alten und jungen Spikulae ermittelt werden. Die Analyse erster Proben wird gegenwärtig durchgeführt.

1 Introduction

1.1 Why work with sponges in Antarctica

Antarctica is a sponge kingdom (Koltun 1968). More than 300 different sponge species have been found in Antarctica (Barthel et al. 1997) and many of the rich and diverse benthic communities on the Antarctic shelf are clearly dominated by sponges (>90% of WM) (Beliaev & Ushakov 1957, Dayton et al. 1970, Dayton et al. 1974, Voß 1988, Barthel et al. 1990). Like trees in a rainforest or corals in a tropical reef, sponges play a major rôle in structuring the habitat. They serve as a "kindergarten" for juveniles of a large number of benthic invertebrates (Kunzmann 1996). Barthel (1997) found pentacrinoids, the sessile stage of comatulid crinoid development in the suboscular cavity of rossellid sponges. Also, fish eggs have been found in the suboscular cavity of larger rossellid sponges (Moreno 1980, Konecki & Targett 1989, Barthel 1997). Furthermore, sponges provide living quarters "on the second floor" (Arntz et al. 1994) on the otherwise essentially flat and soft sediment. Underwater photographs show that many motile invertebrates (e.g. crinoids, ophiurids and holothurians) are regularly sitting on top of sponges or fish are hiding inside sponges. Numerous benthic organisms choose sponges as their prime habitat (Dearborn et al. 1977, Wägele 1988, Barthel et al. 1991). Benthic life thrives in, on, around and under Antarctic sponges (Figure 1). After death of a sponge individual, the remaining spicule mat has substantial structuring influence in stabilizing the soft sediment. By accumulation over longer periods of time such spicule mats can reach a thickness of up to 1.5 m and provide a biogenic substrate that resembles hard substrata (Koltun 1968, own observation).

By active filter feeding, sponges on the Antarctic shelf closely link the pelagic system with the benthic system. Sponges are preyed upon by asteroids, and a nudibranch (Dayton et al. 1974). While our knowledge of the structural importance of sponges for the Antarctic benthic system has greatly extended over the last four decades, we still know next to nothing about the sponges' contribution to carbon and silicon cycling in Antarctica, nor about their basic population dynamic parameters such as growth rates, age or productivity. Such knowledge, however, is urgently needed for evaluating the sponges' contribution to energy flow patterns within the system and the time scales of recolonization processes in which sponges play a known structuring key rôle. Schalk (1993) and Jarre-Teichmann et al. (1997) modelled first estimates of energy flow patterns. The latter authors compiled data on primary production, zooplankton, benthic invertebrates and top predators to build a balanced model of trophic flow. The Antarctic benthic system, as also described in that model, is characterized by rather stable, albeit low water temperatures year round and an overall scarcity of food (Clarke 1985, Clarke 1988, Grebmeier & Barry 1991, Arntz et al. 1994).
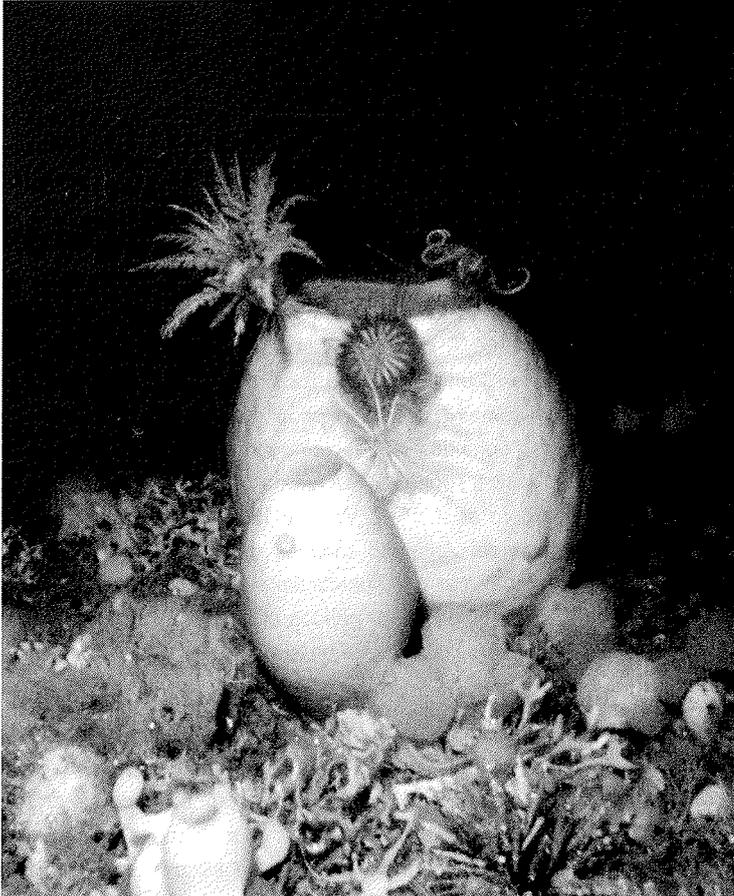
Figure 1 Typical community on the eastern Weddell Sea shelf (Station PS 39-32, depth ~140m). Sponges dominate many areas and are utilized by several invertebrates to access higher water layers. (Photo: J. Gutt, AWI)

The benthos experiences a distinct pulse of fresh food in summer (6-8 weeks of intense primary production - PP) with a relative scarcity of fresh input during the rest of the year. The benthos in general and sponges like other suspension feeders specifically have long been thought to experience dormancy-like stages of starving during long periods without PP (Barnes & Clarke 1995). Recently, however, an alternative feeding strategy has been documented: instead of intense feeding on fresh food particles each summer combined with starving in fall and winter some suspension feeders also utilize pico- and nanoplankton and detritus from resuspension events as a more constant food source throughout the year, albeit of lower nutritional value (Barnes & Clarke 1995, Orejas 2001).

Living under such conditions, polar benthic invertebrates commonly have slower growth rates and lower productivity when compared to temperate species (e. g. Brey & Clarke 1993, Bluhm et al. 1998 for sea urchins). Remarkably, they are often older and also reach larger maximum sizes than their close congeners in warmer waters (Atkinson & Sibly 1997, Chapelle & Peck 1999). Antarctic sponges are a good example for 'polar gigantism', and to find out whether or not they are also older than boreal, temperate, or tropical sponges is one of the objectives of this study. The species studied in this work – two demosponges *Stylocordyla borealis*, *Cinachyra antarctica*, and the hexactinellids *Rossella spp.* – are briefly described in the following paragraphs.

Stylocordyla borealis (Lovén, 1868) (Hadromerida, Demospongiae). Its shape and appearance closely resembles a lollypop: A spherical body is lifted into the water column by an elongated thin stalk. Stalks of *S. borealis* are often heavily overgrown by anthozoans, gorgonians and other sessile fauna, indicating their importance for structuring early resettlement stages. Members of the family Stylocordylidae are sometimes difficult to distinguish (Bergquist 1972) and have caused considerable taxonomic debate. Presently we must conclude that the same species *S. borealis* occurs throughout the Atlantic Ocean from north of Iceland down to the Weddell Sea, Antarctica. Single specimens can also be found in the Ross Sea near McMurdo Station (pers. comm. McClintock) and in New Zealand waters (Bergquist 1972). Our ecological knowledge about *S. borealis* is very limited. From underwater photographs Gutt et al. (1996) concluded that this species is one of the relatively early colonizers after iceberg scouring. Recently, Sarà et al. (2002) clarified *S. borealis*'s reproduction mode and documented that this species carries embryos, which never hatch into larvae. From this observation Sarà (pers. com.) concluded that *S. borealis* is most likely to recruit within the same patch rather than spread out over long distances.

Cinachyra antarctica (Carter, 1872) (Tetillidae, Demospongiae) is a spherical epibenthic sponge with spicule tufts protruding perpendicularly from the whole body. Oscular openings are evenly spread over the body. From the fact that *C. antarctica* contracts heavily when taken from the water Barthel et al. (1991) concluded that our estimates of space requirements of this species based on trawl catches would certainly underestimate true space requirements of relaxed sponges *in situ*.

Rossella spp.: All the often mentioned large, mass-occurring hexactinellids, and also the spectacular individual found by Dayton et al. (1974) near McMurdo Station, Ross Sea, which was ~2m high, are members of this family. With one exception the body of a member of this family is always vase-, sack-, or barrel-shaped. Eleven species are grouped in five genera, some of which are very difficult to distinguish (Barthel & Tendal 1994). As very small individuals are rarely found on the shelf of the eastern Weddell Sea and are even more difficult to distinguish than large specimens, all Rossellidae were grouped together for the purpose of this study.

The two demosponges were chosen as their life-maintenance was far more successful during the earlier EASIZ expedition ANT XIII than that of other sponge species (Barthel et al. 1997). The Rossellidae were chosen as they are the most important group regarding biomass on the Antarctic shelf.

- Sponges dominate many benthic communities on the eastern Weddell Sea shelf in terms of abundance and wet mass.
- Their structural importance for the habitat is well documented.
- The sponges' contribution to C- and Si-cycling is largely unknown.

1.2 Monthly samples of the deep Antarctic benthos – no way!

Antarctica is a truly fascinating continent holding numerous surprises for scientist among which the rich epibenthic fauna of many shelf areas is one of the most impressing ones. Research in Antarctica, however, differs fundamentally from research in boreal, temperate or tropical regions where studies of benthic fauna are often based on a year round sampling strategy (e.g. Ayling 1980, Ayling 1983, Graça et al. 1999, Coma et al. 2002, Tanaka 2002). From the latter studies we are used to expect a more or less complete picture of variability and dynamics within the system not only within the annual seasonal cycle but also in between consecutive years (e.g. Turon et al. 1998). Working in Antarctica one has to abandon such expectations. Studies in polar regions are logistically far more difficult as complete ice coverage can extent to 60°S in winter (Foster 1981). Even in summer some regions in the western and southern Weddell Sea are often impenetrable (Heygster et al. 1996, Comiso & Gordon 1998). The deep benthos can – at present – not be studied on the basis of monthly, three-monthly or even just annual sampling dates. Data that are collected are usually summer data (Baker et al. 1994, Ahn & Shim 1998, Kowalke 2000, Bluhm & Brey 2001) with a few exceptions of spring or autumn data. Data about winter conditions are scarce, usually stem from the eulittoral and shallow sublittoral around the Antarctic

peninsula and maritime Antarctica (Peck et al. 1997, Brockington & Clarke 2001, Brockington et al. 2001, Kim 2001) and do not extend into sublittoral depths. Thus our insights into reproductive strategies, annual cycles of nutrition and energetic requirements are strongly impeded. When comparing studies and results from warmer waters with those of polar regions one has to keep in mind that the latter were achieved under often adverse sampling conditions, sometimes massive logistic problems and usually with great time constraints due to the maximum time an expedition to the Antarctic can work in the study area. Despite the mentioned constrains, past and ongoing studies of the Antarctic benthos have contributed – and are contributing – substantially to further our knowledge of the system, albeit not with the same step-size that can be attained with year round studies in warmer areas.

● Studies of the deep benthos in polar regions and that of warmer waters cannot be assessed with the same measuring stick.

1.3   How can growth and age be determined? – Why is that impossible for Antarctic sponges?

Direct measurement

A straightforward approach to estimate growth and age is the direct measurement (e.g. Osinga et al. 1999a&b, Laudien et al. subm). Differently sized individuals of a species are marked; their size or mass is measured and re-measured after a suitable time interval. Ideally individuals should remain in their habitat but variations of this method include the mark/recapture approach (where individuals are captured, marked and need to be recaptured for the second measurement) and repeated size or mass measurements of laboratory cultured specimens. Dayton et al. (1974) and Dayton (1979) marked 13 species of sponges in the Ross Sea near McMurdo Station by SCUBA diving and reassessed height and diameter of the specimens for more than 10 consecutive summers. The authors could document measurable increase in size for two sponge species only: *Mycale acerata* and *Homaxinella sp.* For nine other species – among which were hexactinellid sponges and *Cinachyra antarctica* – growth was not measurable during the 10 year study.

Analyzing growth marks

Originally developed for trees this aging technique analyses growth marks laid down in permanent hard structures. Teleost fish (by otoliths: Campana & Neilson 1985), echinoderms (by vertebral ossicles in Ophiuroidea: Gage 1990a,b and by tests or

Aristotle laterns in Echinoidea: Gage 1991) as well as Cephalopoda (by statoliths: Rodhouse 1991) have successfully been aged by analysis of such growth marks. Glass sponges (Demospongiae and Hexactinellida) contain large numbers of spicules – the needed hard structure. Ring like structures in the cross section of spicules were found and analyzed by Schwab & Shore (1971a). However, such structures cannot be related to age (Schwab & Shore 1971b). Also it remains unclear, whether or not spicules are a "permanent" structure. Bavestrello et al. (1996) found that in living *Tethya omanensis* spicules can dissolve and it can be hypothesized that the dissolved silicon may be used elsewhere in the sponge for synthesis of new spicules. Also, Marliave (1992) found evidence for resorption of spicules in the hexactinellid *Rhabdocalyptus dawsoni*. By photographing and analyzing complete specimens of *Haliclona oculata* Kaandorp (1991), on the other hand, found layers of spicules which were deposited upon each other as the individual increased in length. Kaandorp's results indicate that at least some sponge species show accretive grow patterns i.e. young material is deposited upon older parts of an individual. One may conclude that spicules are indeed a long lasting – if not permanent – entity. Such knowledge about the growth form is a prerequisite for analysis of stable isotopes or radionuclides. A first study exploring complete spicule arrangement within Antarctic hexactinellids is ongoing (Gatti, unpub. data).

Stable isotopes

Stable isotopes of oxygen and carbon have been used successfully to analyze growth of skeletal carbonate of bivalves, bryozoans – also of polar origin. Mediterranean sponges belonging to the Calcarea have been aged successfully by analysis of their isotopic composition. While oxygen ($\delta^{18}O$) leaves a temperature change dominated signal within hard structures, fluctuations in PP can be inferred from changes in the carbon-signal ($\delta^{13}C$). From the change in signal as documented in the hard structures of individuals the annual cycle of such temperature and/or PP-cycles can be interpreted and subsequently age can be estimated. Siliceous spicules of sponges are composed of >99% of opal (biogenic SiO_2) and contain less than 0.2% of carbon (Schwab & Shore 1971a) which renders them unsuitable for analysis of carbon isotopic composition. Water temperature of water masses close to the bottom of the Antarctic shelf hardly fluctuates during the annual cycle (variation <0.8°C Hellmer & Bersch 1985, Fahrbach et al. 1992) so that changes in oxygen isotopic composition may be difficult to interpret.

Radionuclides

Analysis of naturally occurring radionuclides have been used successfully to determine the age of water masses (time since last contact with the atmosphere) and geological structures such as rocks or sediment. Generally a time-span of up to 5 times the half-life of the analyzed radionuclide can be used for reliable age estimates. If, as

has been concluded by Dayton (1979), big hexactinellid sponges are several hundred years old, they may certainly be within the age range that would be analyzable with radionuclides. There are three indispensable prerequisites for this type of analysis. Firstly, a suitable radionuclide needs to be present in sufficient quantity within the structure to analyze. Secondly knowledge about the growth form of sponges is required to be able to distinguish old parts from young parts and finally the structure to analyze should not be in contact with seawater after its deposition. Cosmogenic ^{32}Si, is a naturally occurring radionuclide of silicon in the atmosphere and in seawater. Its half-life has been subject to intense research which yielded controversial results (Lal et al. 1970: 200-300 years; Clausen 1973: ~650 years; DeMaster 1980: 276±32 years) with the latter study considered to be the most reliable one (Faure 1986). ^{32}Si has been found within sponge spicules (Lal et al. 1970, Lal et al. 1976, Lal & Somayajulu 1980). However, sponge spicules have very low ^{32}Si-concentrations (Lal & Somayajulu 1980) and suitable samples need to contain >5g spicule mass. Such a large sample is a mixed sample of older and more recent material and yields the age of youngest material only. Present analysis techniques are not sufficient to analyze very small sample – ideally one single spicule (pers. comm. M. Rutgers v. d. Loeff).

Analysis of size-frequency-distributions (SFD)

When age classes of a population can be distinguished in SFD histograms and when data about the mean time span of one reproduction cycle are available, it is possible to estimate growth of individuals by comparing mean size of cohorts (Brey 1999). However, for Antarctic sponges two problems arise from this method: (1) Our knowledge about reproduction in general is limited and we have no insight whatsoever into reproduction cycles. (2) For many polar invertebrates we can observe a pile up of most individuals in larger size classes (Brey et al. 1995ab, Dahm 1996, Piepenburg & Schmid 1996, Bluhm et al. 1998, Bluhm & Brey 2001, Bluhm et al. 2001). The peak of such histograms is composed of many age classes, which can not be resolved. It is thus impossible to estimate growth of Antarctic sponges from analysis of SFD histograms.

Indirect approach via metabolism

Reliable data about metabolic activity throughout the season can be used to estimate accumulated production (Lampert 1984). Based on

Equation 1 $P = A - R - E$

(where P = production, A = assimilation, R = respiration and E = excretion) a relationship between P and R can be established. Engelmann (1966) was the first to suggest a linear relationship between annual production and respiration (per unit area) in animal populations. Estimates were recalculated for poikilotherms after separation for longevity by McNeil & Lawton (1970). After extraction of 235 energy budgets from literature Humphreys (1979) could separate distinct groups of poikilotherms and homoiotherms.

All of the mentioned studies dealt with the relationship between respiration and production on the basis of animal populations per area and on the time scale of a year. Individual variations as they occur throughout the lifecycle of an individual can not be inferred from such relationships. However, a prerequisite to modelling of individual growth rates is the shift of energy expenditure primarily for growth in younger individuals towards increasing energy expenditure for reproduction in mature individuals. Such a shift of energy expenditure in sponges can be inferred from respiration rates and growth rates for the breadcrumb sponge *Halichondria panicea* (Thomassen & Riisgård 1995).

- Well established techniques to estimate age and growth cannot be used for Antarctic sponges.
- The development of an indirect approach using metabolic rates was needed for this study.

1.4 What's to find out? – Objectives of this study

The major aims of this study are

(i)   to develop and validate a model for calculation of individual growth rates from oxygen consumption data,

(ii) to generate a data set of respiration data of Antarctic sponges to which the model can be applied, and

(iii) to assess the sponges' contribution to C- and Si-flow patterns within the Antarctic trophic system.

The demosponges *Stylocordyla borealis* and *Cinachyra antarctica* and the hexactinellids *Rossella spp.* were chosen for respiration experiments. Present knowledge about Antarctic sponges led to the formulation of the following hypotheses:

- Hypothesis 1: Large hexactinellid sponges on the eastern Weddell Sea shelf are up to ~500 years old.
- Hypothesis 2: Sponges are of structural importance only and are no major component of carbon or silicon flow patterns on the eastern Weddell Sea shelf.

2 Material and Methods

2.1 How and where to catch a sponge and keep it alive

All sampling was performed within the EASIZ (Ecology of the Antarctic Sea Ice Zone) framework on R/V Polarstern during expeditions ANT XV/3 and XV/4 to the eastern Weddell Sea using Agassiz trawl and bottom trawl. Figure 2 shows the sampling area in the eastern Weddell Sea. Details of each station such as geographical position, water depth, and deployed gear are given in Arntz & Gutt (1999) and in Publication II (p 63).

Sponges that were in excellent condition (undamaged and not covered with sediment) were taken for life-maintenance and the remainder was frozen at -30°C until further sample processing in the laboratory.

Sponges are marred when exposed to air and usually great care is taken to handle sponges constantly submerged (e.g. Thomassen & Riisgård 1995, MacMillan 1996). However, when caught with a trawl sponges inevitably get exposed to air upon arrival on the deck. The most important problem seems to be the air caught inside the sponge which can apparently not be removed by the sponge itself. Life-maintenance during the first EASIZ expedition (ANT XIII) had been impeded by air trapped inside sponges (pers. obs.). Initially I chose the demosponges *Stylocordyla borealis* and *Cinachyra antarctica* for the respiration experiments because they contract heavily when exposed to air (Barthel et al. 1991 and pers. obs.). Upon submersion in an aquarium the sponges relax again and water is sucked into the water carrying system. Thus contractible sponges do not have the problem to rid themselves of air. Subsequently I developed an easy method to aid a sponge in releasing the air, and thus facilitated respiration experiments also with rossellid sponges: Sponges were placed in a large (ca. 200 liter) container filled with seawater of ambient salinity and temperature.
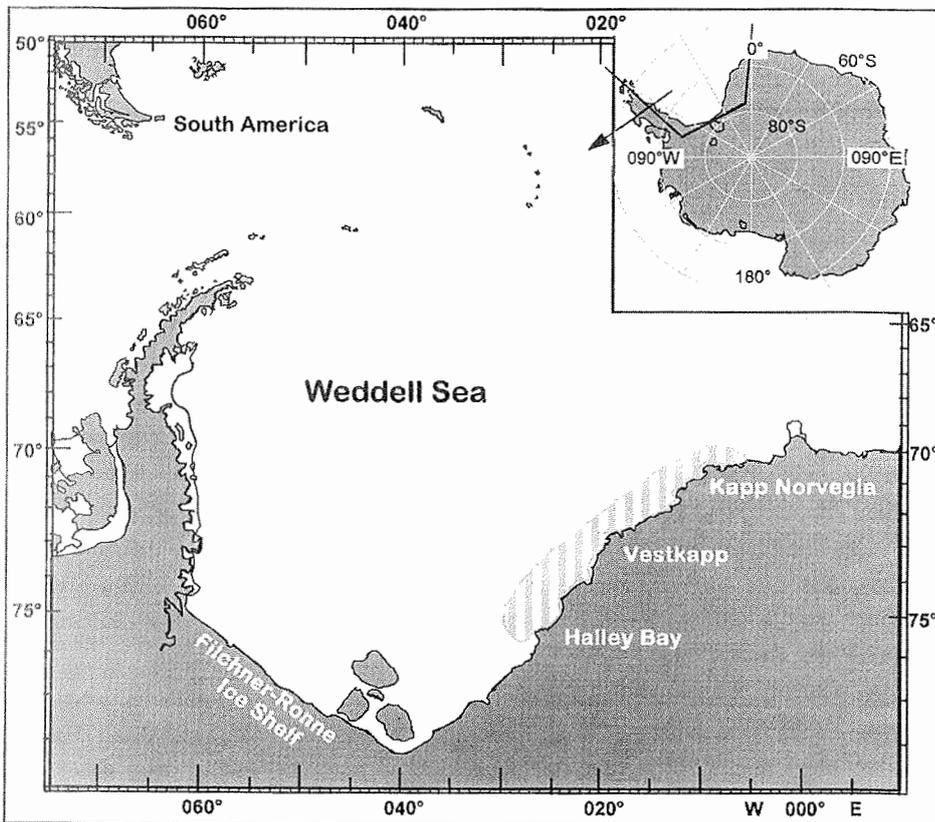
Figure 2 Schematic map of Antarctica (inlet) and the Weddell Sea. Sampling area on the eastern Weddell Sea shelf (WSS) is hatched.

By directing a moderately strong current from a hose running with cold seawater towards the inhalant side of the sponge and gently turning the sponge with the osculum up I could observe numerous air bubbles leaving the osculum. I considered the procedure finished when (a) no more bubbles were leaving the osculum and (b) the sponge would sit on the bottom of the container by itself and not float to the surface any more. It was possible to keep sponges for up to three month in an aquarium after that treatment. Sponges were kept in running natural unfiltered seawater of ambient temperature and salinity in a temperature controlled room. As water was pumped constantly from a water depth of 5m, no additional feeding was applied. Most sponges were in good condition throughout the maintenance period of 5 month (see also Publication III p 78).

- Air that is trapped within the sponge tissue can be evacuated by moderately strong water currents applied externally.

2.2 Work in the laboratory

Respiration experiments were performed on board R/V Polarstern. Respiration chambers were specifically designed to accommodate a large variety of animal sizes (details of chamber design are given in Publication I p 44). Chamber size was limited by maximum pump performance. Flow through chambers >14 liters would not have been sufficient to ensure that sponges are not affected by low flow speed during respiration experiments. Respiration experiments with rossellid sponges could thus not be performed on a large scale as most individuals caught during ANT XV/3 and /4 were too large for the largest respiration chambers. Details of experimental protocol are given in Publication I (pp 44-46). The activity of the electron transport system (ETS) was determined following commonly used procedures. Details are given in Publication III (pp 78-81). Mass and length parameters of sponges were determined. For *Stylocordyla borealis* separate analysis of body and stalk parts was performed. Details are given in Publication II (p 64).

- Morphometrics of *Cinachyra antarctica* and *Stylocordyla borealis* were determined. For *S. borealis* measurements were taken for stalks and bodies separately.
- Respiration experiments were performed with *S. borealis, C. antarctica* and *Rossella spp.*
- Activity of the electron transport system (ETS) was determined in *S. borealis, C. antarctica* and *Rossella spp.* following common procedures.

2.3 Analysis of respiration data

Plots of oxygen consumption data vs. body mass with both axes on a logarithmic scale were analyzed with linear least square regressions. As the slope of the linear regression through all respiration data of one species was of paramount importance for the modelling approach thorough care had to applied to calculate an unbiased regression of body mass and respiration rate. Repeated measurements of respiration rates of the same individual yielded data with different intra-individual variation — thus data of different quality. By using weighted linear least square regression (Draper & Smith 1980) repeated measurements with higher quality (i. e. lower intra-individual variance) have a greater influence on the regression line than have those of lower quality (i. e. higher intra-individual variance). A detailed explanation and discussion of the technique of weighted linear least square regression is given in Publication III (p 79). By using this method of regression analysis I was able to calculate an unbiased regression of respiration data.

⊛   Oxygen consumption data were analyzed with the weighted linear least square
    regression technique.

2.4 Modelling with AMIGO

The modelling routine AMIGO (Advanced Modelling of Invertebrate Growth from Oxygen consumption) was developed for the software ME10 (Hewlett & Packard: Student Version 7.1). The model calculates somatic production from oxygen consumption data. Figure 3 shows a flow chart of the modelling routine.

Details of the theoretical background of this modelling approach are given in Publication III (pp 80-82), the complete modelling routine is given in the Appendix (pp 111-127). The model calculates growth rates when oxygen consumption data are available for a wide size range of individuals of one species and when the species' maximum observed body mass is known. $P_s/\Sigma R$ ratios follow

Equation 2 $$\frac{P_s}{\Sigma R} = a'' + b'' \times \log(M_e)$$

where: P_s = somatic production, ΣR is oxygen consumption and M_e is the energy equivalent of body mass [kJ]. The boundary value for this function is given as $P_s/\Sigma R = 0$ at $M_e = M_{emax}$, where M_{emax} is defined as the energy equivalent of maximum body mass observed in the field increased by 10% to account for incomplete sampling of the population.

The modelling routine was validated by comparing growth rates of the temperate sponge *Halichondria panicea* as observed in the field and in an aquarium (Thomassen & Riisgård 1955) with those resulting from the model. AMIGO 4.04 was used for all calculations of this study.

```
┌─────────────────────────┐
│ Addition of production   │
│ from previous time       │◄──┐
│ interval to body mass    │   │
└───────────┬─────────────┘   │
            │                  │
            ▼                  │
         ◇ final              │
         body mass    YES ──► ( End of calculations
         reached ?            output of results )
            │ NO              │
            ▼                  │
┌─────────────────────────┐   │
│ Calculation of oxygen    │   ( INPUT
│ consumption per given    │◄── e.g. starting body mass,
│ body mass & time         │    step-size (time) etc. )
│ intervall                │   │
└───────────┬─────────────┘   │
            ▼                  │
┌─────────────────────────┐   │
│ Calculation of Ps/ΣR     │   │
│ ratio for given body     │   │
│ mass                     │   │
└───────────┬─────────────┘   │
            ▼                  │
┌─────────────────────────┐   │
│ Conversion of oxygen     │   │
│ consumption to energy    │   │
│ equivalent               │   │
└───────────┬─────────────┘   │
            ▼                  │
┌─────────────────────────┐   │
│ Conversion of energy     │───┘
│ equivalent to production │
│ (Ps)                     │
└─────────────────────────┘
```

Figure 3 Flow chart of the AMIGO modelling routine. All data that are entered prior to a modelling run and all results that accumulate during calculations are written to a tab-delimited output-file. The output-file can be imported into commonly used software for further calculations.

● With the model AMIGO (Advanced Modelling of Invertebrate Growth from Oxygen consumption) it is possible to calculate growth rates from the mass specific oxygen consumption rate of individual specimens when the maximum body mass is known.

2.5 Population energy budgets

Using the excel-solver provided by Brey's Virtual Handbook (2001) a von Bertalanffy growth function (VBGF) was fitted to mass at age data as obtained from the modelling output. Infinite body mass (M_∞) was set equal to M_{max} of the model. Mean

annual biomass, production and productivity (P_s/B) were calculated using mass frequency distributions and model results.

To assess overall carbon requirements of sponges on the eastern Weddell Sea shelf (WSS), I used my own results for *Stylocordyla borealis* and *Cinachyra antarctica* and *Rossella spp.* wherever appropriate. Data and conversions that were not part of this study were taken from the following sources:

- Estimates of total sponge WM per area are based on data by Gerdes et al. (in press).

- Abundance data of *C. antarctica* are based on results of Gutt & Starmans (1998).

- Abundance and MFD-data of *Rossella spp.* are based on unpublished results of an ongoing study by N. Teixidó.

- To convert WM of hexactinellid sponges or of sponges of unknown species composition into AFDM the mean (0.06088) of all available data for Antarctic sponges (Dayton et al. 1974, McClintock 1987, Barthel 1995, this study) was used.

- Assimilation efficiencies were calculated as mean (36.3%, SD: 25.92 - 44.2%) of those of 188 herbivorous suspension feeding species (Brey, unpubl. data compilation).

- To calculate opal (biogenic SiO_2) content of sponges all ash was assumed to be opal (Dayton et al. 1974, McClintock 1987).

To assess the reliability of energy budget calculations I used the following error propagation procedure: Growth curves modelled with the upper and lower 95% confidence limit of the slope of regression through oxygen consumption data were the basis for the calculation of upper and lower production and productivity limits.

- Modelling results were used to calculate population energy budgets.
- For fitting of von Bertalanffy growth functions infinite body mass was set equal to maximum attainable body mass of the model.
- Reliability of calculations was assessed by error propagation.

3 Results

3.1 *Stylocordyla borealis*

Results for *S. borealis* are described in detail in Publications II (pp 66-69) and III (pp 82-85) and are only briefly summarized here.

Morphometrics

● Stalk and body of one individual differed markedly in their tissue composition.

● About 8% of the individuals carried disproportional small bodies.

● Mass frequency distribution plots could not be separated into annual modes.

Reproduction

● All embryos were found in the body, none in the stalk.

● 29% of all individuals carried embryos.

● Individuals ≥ 120 mm length or ≥ 0.2 g AFDM carried embryos.

● Larger individuals tended to carry more embryos.

Metabolic rate

● The activity of the electron transport system (ETS_{tot}) increased with body mass: $\log ETS_{tot} = 0.289 + 0.948 \times \log AFDM$.

● The mass specific parameter ETS' was independent of body mass.

● The ratio of oxygen consumption to ETS was high (0.47) for small individuals and low (0.04) for large individuals.

Modelling with AMIGO

● Parameters of the von Bertalanffy growth function were: M_∞ = 4.38 g C, k = 0.015, D = 1.182, t_0 = 0.0, r^2=1.0.

● Averaged sized *Stylocordyla borealis* (0.414 gC) were **10.4 years** old.

● Biggest *S. borealis* (3.9 gC) were **152.3 years** old.

Population energy budget

● Average abundance of *S. borealis* was **3.02 ind m^{-2}** (max = 48 ind m^{-2}).

● Average somatic production: P_s = **0.133 g C m^{-2} y^{-1}**.

● Average assimilation: A = **1.63 gC m^{-2} y^{-1}** (max = 25.95 gC m^{-2} y^{-1}).

● Average consumption: C = **4.5 gC m^{-2} y^{-1}** (max = 71.5 gC m^{-2} y^{-1}).

● Productivity: P_s/B = **0.106**.

● Opal deposition: **1.19 gSiO$_2$ m^{-2} y^{-1}**.

3.2 *Cinachyra antarctica*

Morphometrics

The biggest and smallest *Cinachyra antarctica* found during this study had a diameter of 64.5 and 7.5 mm, respectively (mean ± SE: 27.8 ± 1.49 mm). Conversion factors for diameter (D) and mass parameters of *C. antarctica* are given in Table 1. The size-frequency-distribution histogram (SFD) of *C. antarctica* derived from catches during ANT XV are shown in Figure 4 (grey filled graph) and compared with the SFD based on catches from other studies.

x	y	a	b	N	R^2_{adj}	p
D	V	4.784×10^{-4}	2.846	68	0.930	<0.0001
D	WM	1.888×10^{-4}	3.100	70	0.901	<0.0001
D	DM	1.476×10^{-4}	2.806	68	0.901	<0.0001
D	AFDM	3.768×10^{-5}	2.848	67	0.880	<0.0001
V	WM	1.227	0.814	81	0.952	<0.0001
V	DM	0.390	0.205	81	0.943	<0.0001
V	AFDM	0.149	0.056	81	0.866	<0.0001
WM	DM	0.109	0.249	80	0.968	<0.0001
WM	AFDM	0.063	0.069	80	0.909	<0.0001
DM	AFDM	0.038	0.275	80	0.925	<0.0001

Table 1 *Cinachyra antarctica*. Conversions between the different diameter and mass parameters. Conversion of diameter (D) [mm] to volume (V) [cm^3] or mass [g] follows the function $y = ax^b$ while conversion of volume to mass or mass to mass the parameters follow linear regression ($y = bx + a$). (WM = wet mass, DM = dry mass, AFDM = Ash free dry mass).
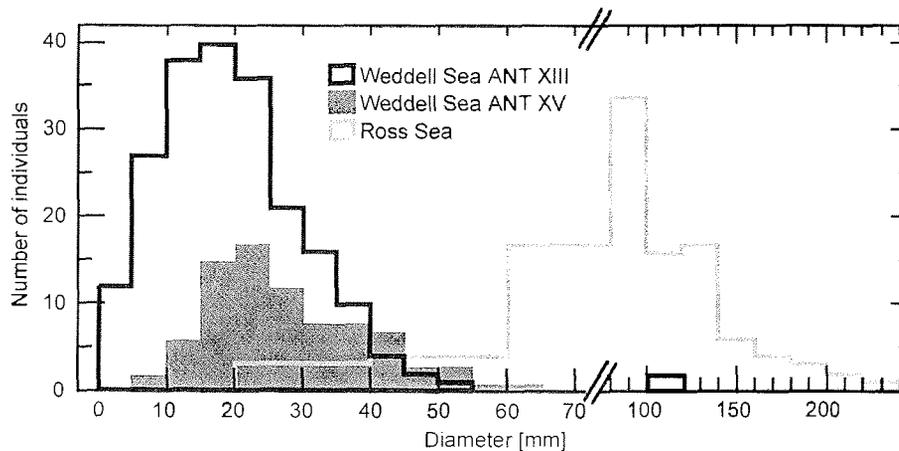
Figure 4 *Cinachyra antarctica*. Size-frequency-distribution histogram of individuals sampled in the eastern Weddell Sea in grey blocks (n=83, ANT XV), and outlined in black (n=207, ANT XIII) and the Ross Sea near McMurdo Station (n=107) outlined in grey. Size of classes for the Weddell Sea samples is 5 mm each, while for the Ross Sea samples class size is 20 mm each. Graph for ANT XIII is modified after Barthel et al. 1997, graph for the Ross Sea samples is modified after Dayton et al. 1974.

Metabolic rate

The relationship between body mass (AFDM) and oxygen consumption rate of *Cinachyra antarctica* is shown in Figure 5. Individual oxygen consumption rate increased with body mass (AFDM) of the specimens (Figure 5A): $\log V_{O_2} = -1.095 + 0.426 \times \log AFDM$. Mass specific oxygen consumption rate decreased with increasing body mass (Figure 5B) following the equation $\log V'_{O_2} = -1.095 - 0.574 \times \log AFDM$.
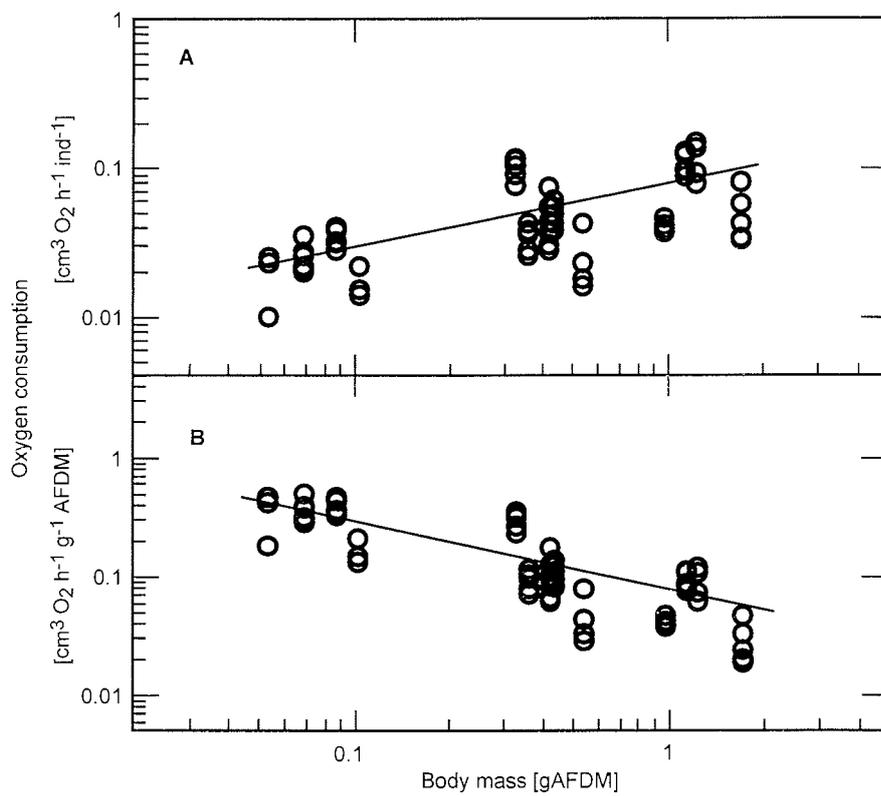
Figure 5AB *Cinachyra antarctica*. Total individual (A) and mass specific (B) respiration rates. Regressions shown are weighted least square linear regressions. For discussion of regression technique see text. (A): $\log V_{O_2} = -1.095 + 0.426 \times \log AFDM$; (B): $\log V'_{O_2} = -1.095 - 0.574 \times \log AFDM$.

Individual ETS activity increased exponentially with body mass (Figure 6A) but there
was no significant relation between the mass specific parameter ETS' and body mass
(Figure 6B). The ratio of oxygen consumption rate over individual ETS activity
(V_{O2}/ETS) decreased exponentially with body mass (Figure 7) from V_{O2}/ETS = 1.5 for
small sponges (2.6 mgC) to 0.02 for large individuals (1.56 gC).
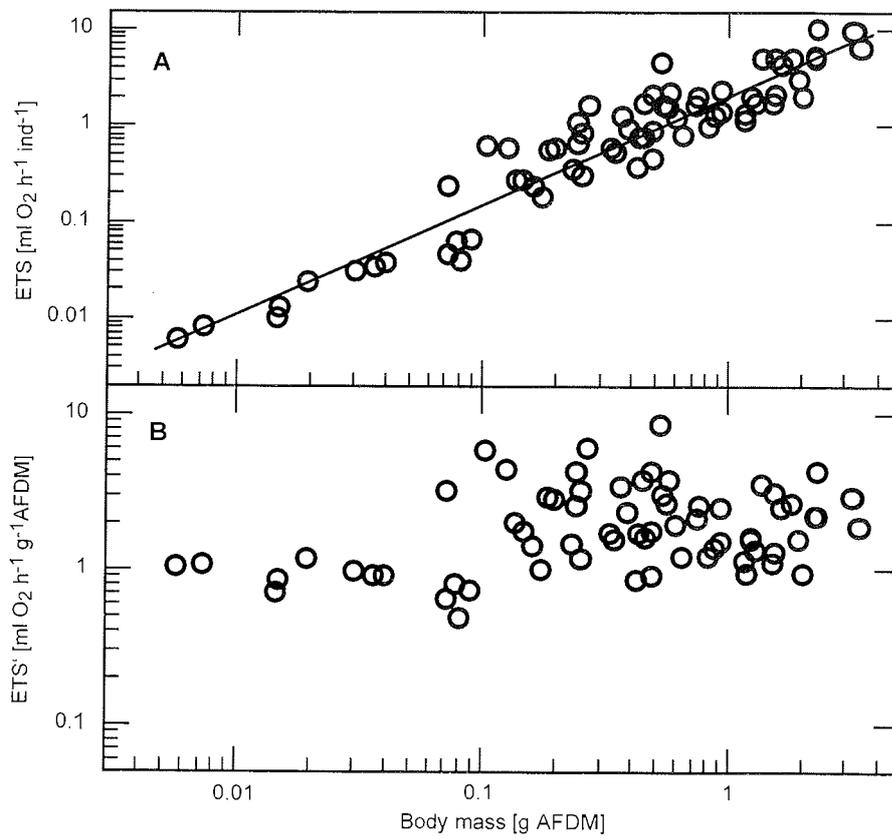
Figure 6 *Cinachyra antarctica*. Individual ETS (A) follows the regression log ETS = 0.318 + 1.136 × log
AFDM. Mass specific ETS' (B) does not show a trend with increasing body mass.
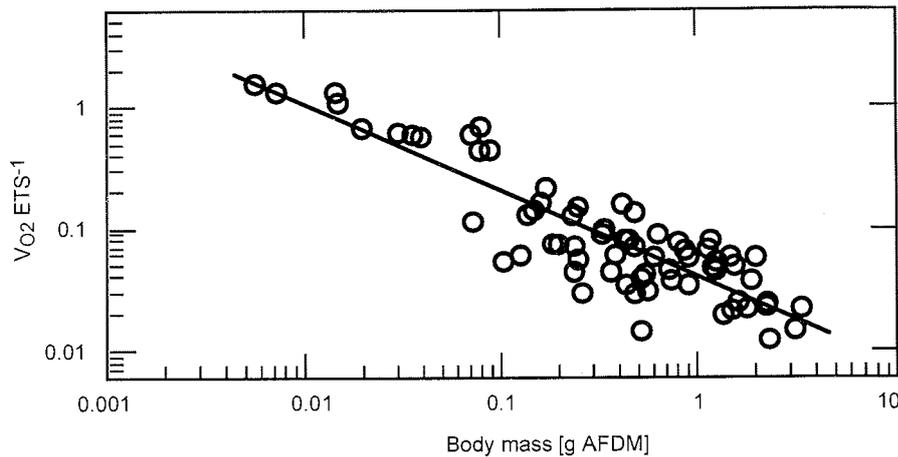
Figure 7 *Cinachyra antarctica.* Exponentially decreasing V_{O2}/ETS ratio follows the equation log $(V_{O2}$/ETS) $= -1.413 - 0.710 \times$ log AFDM (N= 68, $r^2 = 0.776$).

- Mass specific oxygen consumption rate of *Cinachyra antarctica* was described by the equation log $V'_{O2} = -1.095 - 0.547 \times$ log AFDM
- The activity of the electron transport system (ETS) increased exponentially with body mass: log ETS = 0.318 + 1.136 × log AFDM.
- The mass specific parameter ETS' was independent of body mass.
- The ratio of oxygen consumption over ETS decreased with body mass.

Modelling with AMIGO

Dayton et al. (1974) found *Cinachyra antarctica* of 41.2 gC in the Ross Sea, i. e. the boundary value for the $P_s/\Sigma R$ function thus was $P_s/\Sigma R = 0$ at $M_e = 2072$ kJ and

Equation 3 $\dfrac{P_s}{\Sigma R} = 0.242 - 0.0317 \times \log(M_e)$

where M_e is the energy equivalent of body mass. A detailed description of fitting of the $P_s/\Sigma R$ function is given in Publication III (pp 80-82). The growth curve for *C. antarctica* is shown in Figure 8.
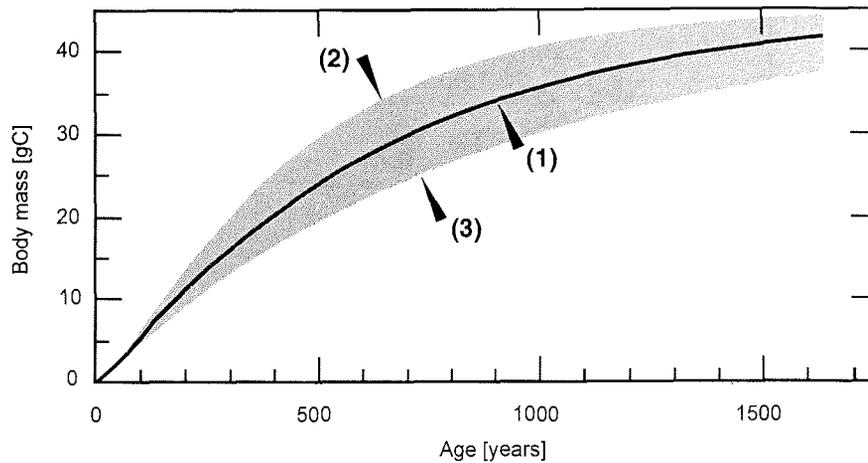
Figure 8 *Cinachyra antarctica*. Results of model output for mean (1), upper 95% (2), and lower 95% confidence limit of respiration data (3). Data points for each curve: N=493. The model was initialized with (log V'_{O2} = -1.095 - 0.574 × log AFDM) for curve (1), (log V'_{O2} = -1.095 - 0.473 × log AFDM) for curve (2), and (log V'_{O2} = -1.095 - 0.674 × log AFDM) for curve (3). Initial parameters equal for all three modelling runs were: log $P_s/\Sigma R$ = 0.242 - 0.032 × log M_e, step-size SS=1 day, initial body mass iniBM=0.001 gC. Parameters of the VBGF for curve (1) are: M_∞= 45.35 gC, k=0.0019, D=1.195, t_0=2.1, r^2=1.0.

- Averaged sized (this study) *Cinachyra antarctica* were **11 years** old (0.333 gC).
- Biggest *C. antarctica* (this study) were **35 years** old (1.56 gC).
- Average sized *C. antarctica* from the Ross Sea were **126 years** old (7.0 gC).
- Biggest *C. antarctica* from the Ross Sea were **1550 years** old (41.2 gC).
- Parameters of the von Bertalanffy growth function were:

  M_∞ = 45.35 gC, **k = 0.0019, D = 1.195**, t_0 = 2.1, r^2 = 1.0.

Population energy budget

To get a more reliable estimate of somatic production with regard to variation in time and space I merged all mass frequency data of *C. antarctica* sampled in the Weddell Sea (ANT XIII and ANT XV). Based on that merged MFD histogram somatic production amounted to 2.26 mgC m^{-2} y^{-1} in patches of average abundance (0.1 ind m^{-2}, Gutt & Starmans 1998). Results of the calculations regarding carbon requirements of *C. antarctica* are summarized in Table 2. Mean annual productivity (P_s/B) calculated from the modelling results was 0.077 (0.076 - 0.078).

	[mg C m^{-2} y^{-1}]
Consumption	**77** (74 - 80)
Assimilation	**28** (27 - 29)
Production	**2.26** (2.23 - 2.31)
Respiration	**26** (25 - 27)

Table 2 *Cinachyra antarctica.* Energy budget for mean abundance of 0.1 ind m^{-2} (Gutt & Starmans 1998). Values in brackets give an estimate of reliability of the calculation, they are calculated with error propagation from 95% confidence limit of the linear regression of oxygen consumption data.

Population energy budget – *Cinachyra antarctica*

- Average somatic production: **P$_s$ = 0.023 gC m^{-2} y^{-1}**.
- Average assimilation: **A = 0.028 gC m^{-2} y^{-1}**.
- Average consumption: **C = 0.077 gC m^{-2} y^{-1}**.
- Productivity: **P$_s$/B = 0.077**.
- Opal deposition: **0.01 gSiO$_2$ m^{-2} y^{-1}**.

3.3 *Rossella spp.*

Metabolic rate

Oxygen consumption data for hexactinellid sponges are not available on a large scale as most individuals found during ANT XV/3 and /4 were too large to fit into the largest respiration chambers (14 liters). To be nevertheless able to model growth for hexactinellid sponges I merged the available results for hexactinellid sponges with those for all Antarctic sponge species of this study and recalculated weighted linear least square regressions (Figure 9).

I did not determine ETS activity of hexactinellid sponges. The reasons are discussed in detail in section "4.2 Metabolic rate" (p 27).
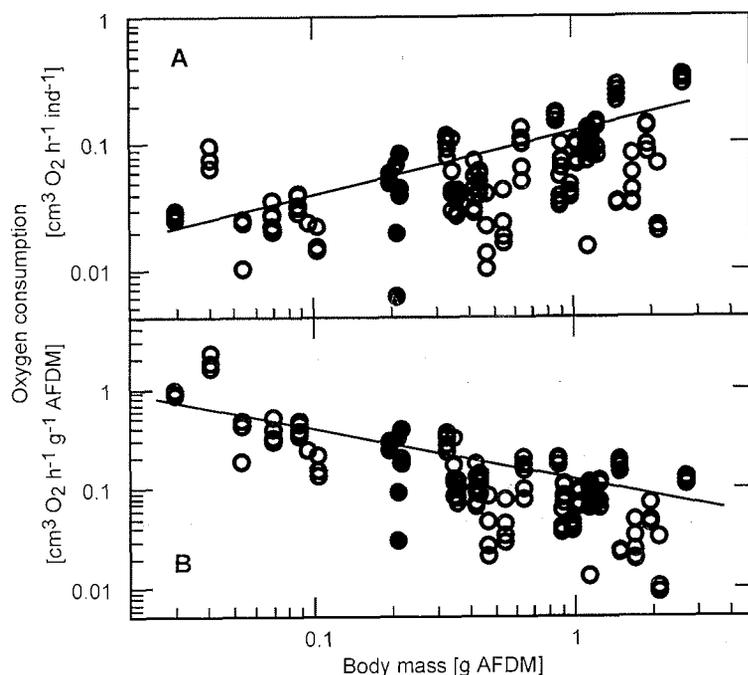
Figure 9 Antarctic sponges. Oxygen consumption data of determined in this study. Data for *Rossella spp.* are shown as dots, data for *Cinachyra antarctica* and *Stylocordyla borealis* are shown as circles. Regressions are weighted linear least square regressions. (A) Individual oxygen consumption rate: log V_{O2} = -0.908 + 0.499 × log AFDM, (N=147, R^2_{adj} = 0.665). (B) Mass specific oxygen consumption rate: log V'_{O2} =-0.908 - 0.501 × log AFDM (N= 147, R^2_{adj} = 0.667).

● A common relation between body mass and mass specific oxygen consumption rate was established from the three sponge taxa of this study (*Rossellidae spp.*, *Stylocordyla borealis* and *Cinachyra antarctica*): log V_{O2}' = -0.908 - 0.501 × log AFDM.

Modelling with AMIGO

The AMIGO model showed growth of hexactinellid sponges to be very slow (Figure 10). Results for hexactinellid sponges are summarized in Table 3. While averaged sized *Rossella spp.* in the Weddell Sea were 186 years old at body mass of 87.6 gC, largest individuals found in the Weddell Sea were 1515 years old at a body mass of 1681 gC. The often mentioned extremely large *Scolymastra joubini* found by

Dayton (1979) was 22719 years old. This result is discussed in detail in section "4.3 Modelling approach — Reliability of the AMIGO model." (pp 29-31).

	BM [gC]	Age [y]	Range [y]
smallest individual (WSS)	0.061	2.1	1.7 - 2.5
mean body mass (WSS)	87.64	186	150 - 232
largest individual (WSS)	1681	1515	1021 - 2266
largest individual (Ross Sea)	15605	22719	12878 - 40216

Table 3 *Rossella spp.* Examples of age [years] at size [gC] data according to the AMIGO model. "BM" indicates body mass, "Range" denotes limits of the results calculated with error propagation from the respiration experiments. It is an indication for the reliability of age estimates. "WSS" indicates 'Weddell Sea Shelf'.
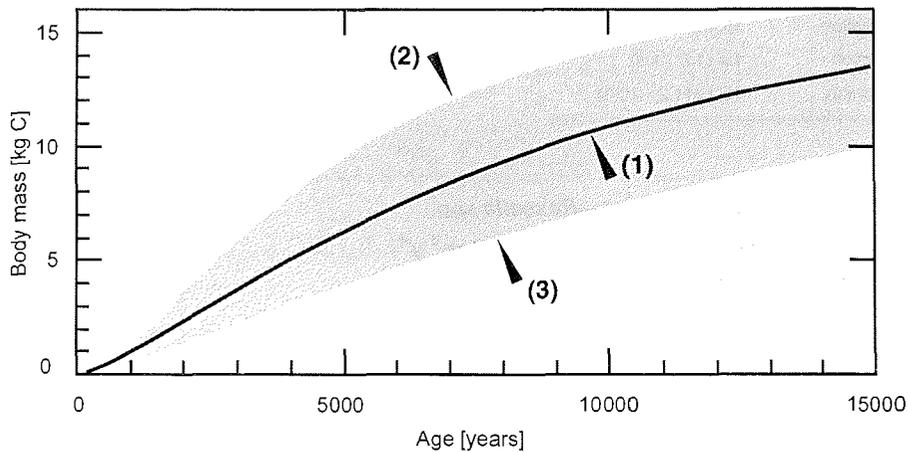
Figure 10 *Rossella spp.* Results of model output for mean (1), upper 95% (2), and lower 95% confidence limit of respiration data (3). Data points for each curve: N=5263. The model was initialized with log V'_{O2} = -0.908 - 0.501 × log AFDM for curve (1), log V'_{O2} = -0.908 - 444 × log AFDM for curve (2), and log V'_{O2} = -0.908 - 0.559 × log AFDM for curve (3). Initial parameters equal for all three modelling runs were: log $P_s/\Sigma R$ = 0.269 - 0.0198 × log M_e, step-size SS=1 day for body mass ≤140 g C and SS=10 days for body mass >140 gC, initial body mass iniBM=0.001 gC. It was not possible to fit a VBGF to the model results for hitherto unknown reasons (pers. com. T. Brey).

- Averaged sized *Rossella spp.* (175.2 g AFDM) were **186** years old.
- Biggest *Rossella spp.* (Weddell Sea) (3362 g AFDM) were **1515** years old.

Population energy budget

For calculation of the energy budget of *Rossella spp.* I used abundance and MFD data determined in an ongoing photographic study of N. Teixidó (unpubl. data). Photos were taken during ANT XIII and ANT XV of R/V Polarstern on the eastern WSS and cover a range of approximately 100-300 m water depth. Somatic production amounts to 1.4 gC m^{-2} y^{-1} in patches of average abundance (2.4 ind m^{-2}). Results of the calculations regarding carbon requirements of *Rossella spp.* are summarized in Table 4. Mean annual productivity (P$_s$/B) calculated from the modelling results was 0.006 (0.005 - 0.009).

	[g C m^{-2} y^{-1}]
Consumption	**45.3** (33.3 - 60.9)
Assimilation	**16.4** (12.2 - 22.1)
Production	**1.4** (1.0 - 1.8)
Respiration	**15.1** (11.2 - 20.3)

Table 4 *Rossella spp.* Energy budget for mean abundance (2.4 ind m^{-2} Teixidó, unpubl. data). Values in brackets give an estimate of reliability of the calculation, they are calculated with error propagation from 95% confidence limit of the linear regression of oxygen consumption data.

Population energy budget – *Rossella spp.*

● Average somatic production: **P$_s$ = 1.4 gC m^{-2} y^{-1}**.

● Average assimilation: **A = 16.4 gC m^{-2} y^{-1}**.

● Average consumption: **C = 45.3 gC m^{-2} y^{-1}**.

● Productivity: **P$_s$/B = 0.006**.

● Opal deposition: **9.57 gSiO$_2$ m^{-2} y^{-1}**.

3.4 "Average Antarctic shelf sponge"

Multibox corer samples taken on the eastern WSS give valuable estimates of the biomass contributed by different taxa (Gerdes et al. 1992, Brey & Gerdes 1997). It was, however, not possible to determine the sponge's species composition for such samples. To be able to calculate sponge population energy budgets without knowledge of the species composition it is therefore desirable to know energy budget parameters of an "average Antarctic shelf sponge" (AASS) which should show mean values for all components of the population energy budget. Such an AASS was derived as weighted mean from all above population energy budgets. An individual body mass of 1 gC was assigned to the AASS by division of the average energy budget parameters by the mean sponge biomass (70.6 gC). It is important to know that respiration of this AASS cannot be calculated with the equations given in the section "Metabolic rate" of each of

the studied sponge species. Instead respiration and all other parameters of the population energy budget have to be calculated from the individual energy budget of an AASS of 1 g C body mass (Table 5). As summing up abundance (from photographic studies) and mean biomass data (from this work) for the three studied sponge species yields a mean sponge biomass of 70.6 gC m^{-2} for the 100-300 m water depth horizon, "abundance" of the AASS was set to 70.6 ind m^{-2} for this depth horizon.

	AASS
Body mass	1 gC
"Abundance"	70.6 ind m^{-2}
Consumption	0.316 (0.246 - 0.407) gC ind^{-1} y^{-1}
Assimilation	0.115 (0.089 - 0.148 gC ind^{-1} y^{-1}
Production	0.007 (0.005-0.009) gC ind^{-1} y^{-1}
Respiration	0.108 (0.084 - 0.139) gC ind^{-1} y^{-1}
Opal deposition	0.052 (0.068 - 0.040) gSiO$_2$ ind^{-1} y^{-1}
Consumption	22.3 (17.4-28.7) gC m^{-2} y^{-1}
Assimilation	8.1 (6.3-10.4) gC m^{-2} y^{-1}
Production	0.5 (0.4-0.6) gC m^{-2} y^{-1}
Respiration	7.6 (6.0-9.8) gC m^{-2} y^{-1}
Opal deposition	3.66 (2.84 - 4.77) gSiO$_2$ m^{-2} y^{-1}

Table 5 Energy budget for the "average Antarctic shelf sponge" (AASS). "Abundance" refers to the 100-300m water depth horizon. Values in brackets give an estimate of reliability of the calculation, they were calculated with error propagation from 95% confidence limit of the linear regression of oxygen consumption data.

Sponge biomass peaks in the upper 400m water depth (Gerdes et al. in press, Figure 11). So carbon and silicon balances of the whole shelf area cannot be calculated by simple multiplication of area. Therefore the AASS was used as a basis for calculation of a weighted carbon and silicon budget for the eastern WSS. For the purpose of this calculation the area of the eastern WSS was defined as a rectangle of 30 km width between φ = 70°S λ = 007°W (Kapp Norvegia) and φ = 75°S, λ = 026°W (Halley Bay). Thus the eastern WSS has an area of 2.5×10^{10} m^{-2}. Mean sponge biomass between 100 and 700m water depth amounts to 45.3 gC m^{-2} (calculated from

Table 6 Energy budget for the sponge fauna on the eastern Weddell Sea shelf (WSS). Values in brackets were calculated with error propagation. Area of the eastern WSS was estimated with 2.5×10^{10} m^{-2}. Mean abundance of the average Antarctic shelf sponge (AASS) was set to 45.3 ind m^{-2} (calculated from Gerdes et al. in press).

	Weddell Sea Shelf sponge fauna
Body mass	1.13 Mt C
Opal mass	8.93 Mt SiO$_2$
Consumption	0.358 (0.279 - 0.461) Mt C y^{-1}
Assimilation	0.130 (0.101 - 0.167) Mt C y^{-1}
Production	0.007 (0.006 - 0.010) Mt C y^{-1}
Respiration	0.123 (0.095 - 0.158) Mt C y^{-1}
Opal deposition	1.03 (0.80 - 1.32) Mt SiO2 y-1

WM given in Gerdes et al. in press). As the AASS has a body mass of 1 gC, setting the "abundance" of the AASS to 45.3 ind m^{-2} yields the equivalent of the mean biomass per m^{-2} found by Gerdes et al. (in press). On this basis I calculated the energy budget of the sponges on the eastern WSS (Table 6). Calculations can not be extended further south towards the Filchner-Ronne Ice Shelf (Figure 2) or further west towards the Antarctic peninsula as Voß (1988) found sponges to be less abundant in areas other than the eastern WSS. Estimates of biomass for those areas are, however, not available.
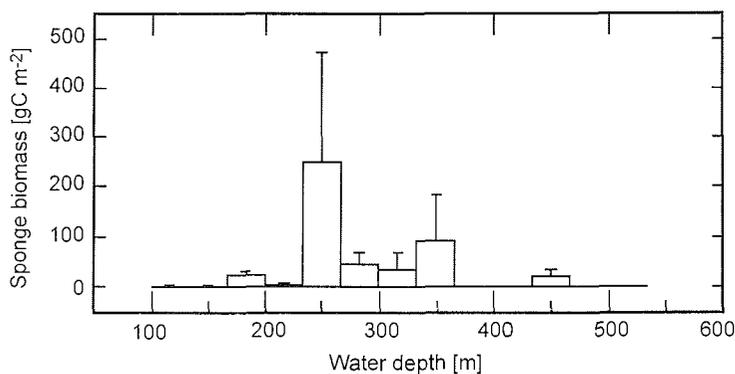
Figure 11 Sponge biomass on the eastern Weddell Sea shelf. Data [gC m^{-2}] are separated into depth horizons of 30m. Error bars are 1SE. Data were calculated from wet masses given in Gerdes et al. (in press).

Population energy budget – Average Antarctic shelf sponge (AASS)

- Body mass: **M = 1 gC**.
- Average somatic production: P_s = 7 mgC ind^{-1} y^{-1}.
- Average assimilation: **A = 0.115 gC ind^{-1} y^{-1}**.
- Average consumption: **C = 0.316 gC ind^{-1} y^{-1}**.
- Productivity: **P_s/B = 0.007**.
- Opal deposition: **52 mgSiO$_2$ ind^{-1} y^{-1}**.

4 Discussion

4.1 Sample treatment

Extensive descriptions of the problems involved in sponge life-maintenance are available in the literature (summarized in Osinga et al. 1999c). Interest in commercial applications of sponge culture methods is growing as sponges produce a variety of different bio-active compounds (Müller et al. 1999b). In spite of this growing interest in the culturing of sponges, progress in this subject since Kinne's review (1977) is limited. Osinga et al. (1999b) concluded that providing suitable alimentation is likely to be the single most important problem in sponge cultivation. My own experiments confirm this conclusion: Life maintenance of sponges was successful as long as ambient Antarctic water could be pumped through the aquaria but was more difficult and less successful when the water circulated in a closed system during the transition journey to South Africa. Upon collection specimens that are taken into an aquarium should be carefully selected avoiding individuals with injuries and those which can not be ridded completely of air (see section "2.2 How and where to catch a sponge and keep it alive" p 9).

- Life-maintenance of sponges is problematical but possible for intermediate periods of time (several weeks).
- Survival of sponges is greatly enhanced by constantly running ambient sea water.

4.2 Metabolic rate

Measurement of respiration at low temperatures has long been a major problem, as the drift of commonly used polarographic oxygen sensors is extremely large (see Publication I p 56). Oxygen microoptodes have the advantage of measurements with high resolution in time, high precision and accuracy as well as the possibility of online data registration. Hence, they are a very suitable tool for oxygen measurements in aquatic environments. Details of the methodology are discussed in Publication I (pp 52-53).

Figure 12 shows mass specific sponge oxygen consumption rates from different habitats (data compilation T. Brey). The data determined in this study are – together with those determined by Kowalke (2000), the lowest oxygen consumption rates hitherto documented for sponges. Nevertheless, it is worth noting that very small lollypop sponge individuals (*Stylocordyla borealis*) show the same mass specific oxygen consumption rates as sponges from warmer habitats. As high initial mass specific oxygen consumption rates are a basis for fast initial growth, lollypop sponges
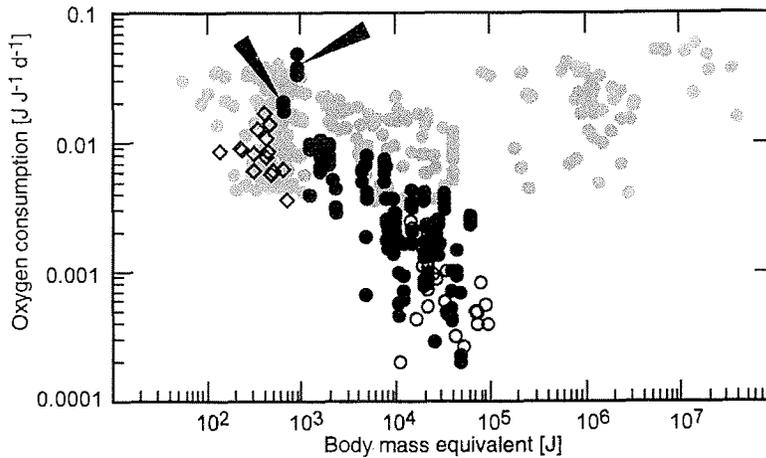
Figure 12 Mass specific oxygen consumption rates of sponges world-wide. Data of temperate and tropical sponges, shown as grey dots, are taken from Reiswig 1974, Cotter 1978, Barthel 1985, Ribes 1998. Data of polar sponges are shown in black (dots: this study, diamonds: Witte 1995, circles: Kowalke 2000). Results for small individuals of *S. borealis* are indicated with an arrow.

gain an advantage in competition for space during the recolonization process of iceberg scours.

Establishing correct metabolic rates was of paramount importance for the modelling approach. Laboratory respiration experiments, however, are known to be subject to artefacts. Transferring animals to respiration chambers can cause stress and subsequently elevated metabolic activity (Peck & Conway 2000). On the other hand it has been argued by Lampert (1984) that initially elevated metabolic activity may also reflect field conditions rather than the result of stress. Because of these uncertainties I chose to supplement respiration rate measurements with the determination of ETS. This parameter gives an approximation of the maximum amount of oxygen that can be processed at the mitochondrial and microsomal membranes (Lampert 1984). As the ETS assay is based on enzyme activity it is conservative for several hours before changes in the environment that cause quick changes in respiration rate are also reflected in ETS activity (Lampert 1984). Additionally, there was good evidence that the ratio of oxygen consumption rate over ETS (V_{O2}/ETS) was constant and independent of body mass of an individual (Ikeda 1989, Madon et al. 1998). Hence, after determination of respiration rate and ETS values for sponges spanning as much of the size spectrum as possible, I planned to establish the ratio V_{O2}/ETS for each studied species. Subsequently it would have been possible to calculate oxygen consumption data from ETS data for those individuals, which were too large for respiration experiments. This study was the first to establish ETS-data for sponges and I found the V_{O2}/ETS ratio not to be constant for *Cinachyra antarctica* or *Stylocordyla borealis*. As determination of ETS of several hundred individuals had shown that respiration experiments could not

be supplemented and far less be substituted in the planned way, ETS assays were not carried on for hexactinellid sponges.

- Oxygen microoptodes were a reliable new tool for measurements of low oxygen consumption rates specifically at low temperature.
- The activity of the electron transport system of Antarctic sponges can not be used as a substitute or supplement for respiration experiments

4.3 Modelling approach – Reliability of the AMIGO model

As pointed out in the introduction available methods for the determination of age or growth are not applicable for Antarctic sponges. Even though it is strongly desirable to determine such growth parameters as directly as possible to minimize errors sources, I had to choose the indirect approach of modelling growth from respiration data. Test runs of the AMIGO model with *Halichondria panicea* from the Baltic Sea (described in detail in Publication III pp 87-88) showed clearly that this approach yields valid results. Regarding Antarctic sponges there is at present only one indication for the reliability of the model which I describe below.

Dayton (1979) found that of marked 84 *Cinachyra antarctica* only 4 individuals showed measurable growth (approximately 2 cm in 10 years). He concluded that *C. antarctica* clearly was growing very slowly. Dayton's diameter measurements are not directly comparable to diameter measurements of this study as the former were taken underwater while the later were taken from drip dried sponges. *C. antarctica* contracts heavily when exposed to air (Barthel et al. 1991) thereby reducing the volume by a factor 2-3 (own observation). Taking these considerations into account an increase of 2 mm y^{-1} diameter as measured by Dayton (1979) corresponds to an accumulation of 4 - 29 mg C ind-1 y-1. According to my model only individuals with a body mass <1.2 gC (corresponding to D ≤ 40 mm, measured in the laboratory) show such rapid growth. Dayton (1979), however, rarely found such small individuals in the Ross Sea (Figure 4). Indirectly this can be regarded as a confirmation of the modelling results.

Mass frequency distribution data of the eastern Weddell Sea as found in this study confirmed results from the early expedition ANT XIII (Figure 4) while data of Dayton et al. (1974) showed a completely different picture for *Cinachyra antarctica* near McMurdo Station (Ross Sea). There, individuals were significantly bigger than individuals taken from the Weddell Sea (Figure 4). Reasons for such a marked difference have not yet been discussed at length in literature but the following aspects need to be kept in mind: the vicinity of McMurdo Station is to some extent protected from large grounding

icebergs (pers. comm. J. Gutt) and thus intervals between disturbance events may be considerably longer near McMurdo Station than they are on the eastern WSS. Beside the impact of disturbance intervals also food availability can affect growth and final size: the better and/or more an individual is fed the bigger it gets. On average PP on the Ross Sea shelf amounts to 142 gC m^{-2} y^{-1} (Nelson et al. 1996), while for the WSS 81 gC m^{-2} y^{-1} can be calculated from data given by v. Bröckel (1985). Compared with a PP of 16 - 100 gC m^{-2} y^{-1} in Antarctic waters in general (Grebmeier & Barry 1991) the Ross Sea sector of the Southern Ocean clearly shows elevated PP values. The higher average as well as maximum size of Ross Sea individuals may be caused by better alimentation. The effects of these differences between Ross Sea and Weddell Sea sponge individuals on the validity of modelling results are discussed below.

In contrast to Antarctic hexactinellids (Dayton et al. 1974, Dayton 1979) the rossellid sponge *Rhabdocalyptus dawsoni* in Saanich Inlet, B.C., Canada exhibits growth rates that can be measured directly (Leys & Lauzon 1998). In a three year study the authors found an average length increment of 1.98 cm y^{-1} with a maximum of up to 5.7 cm y^{-1}. Average sized individuals (32 cm length) were estimated to be 35 years old, while largest individuals (100 cm length) were 220 years old. Unfortunately no conversions to AFDM or carbon values are possible. The results presented by Leys & Lauzon are the only other report of growth rates of hexactinellid sponges. If hexactinellids in the temperate waters of British Columbia can reach an age of 220 years, the modelled age for *Rossella spp.* on the WSS appears to be in a plausible range.

The very large individual of *Scolymastra joubini* found in less than 50m water depth in the Ross Sea (Dayton et al. 1974, Dayton 1979) was ~23000 years old according to modelling results. Extrapolation of results into such long time scales typically leads to large errors (expressed here as the large age range of 13000 - 40000 years). One has to keep in mind that modelling was performed on the basis of a) far smaller sponge individuals, and b) on respiration rates observed in individuals from the Weddell Sea. As discussed above, food supply differs strongly between the two sectors of the Southern Ocean (Nelson et al. 1996) and hence metabolic activity of benthic invertebrates may be higher in the Ross Sea than in the Weddell Sea. If so, the AMIGO age estimate for the 2m high *S. joubini* individual from McMurdo would overestimate its age substantially. Additionally, operating on such times-scales one has to think not only of biological implications but also consider geological events. Fluctuations of the sea level associated with the last glacial maximum (LGM ~18000-22000 years ago) will probably have left the site of the 2m-*S. joubini* 'high and dry' as the sea level during the LGM was 105-130m lower than today (reviewed in Yokoyama et al. 2001). It can therefore be concluded that no marine invertebrate on the Ross Sea shelf can be older than ~15000 years. Clearly model results transferred from the Weddell Sea to the Ross Sea need to be interpreted with great care.

Nevertheless we have to conclude, that hexactinellid sponges in Antarctica are among the oldest if not the oldest living creatures on this planet. Even if the 2m high *S. joubini* in the Ross Sea was only half the age suggested by growth curve (2) (Figure 10) it would still be > 6000 years old and hence the oldest living creature not only in the ocean but also compared with terrestrial life (Table 7). Physiological and molecular foundations upon which such an old age can be realized indicate that Antarctic sponges can be interesting model organisms for age and aging research.

Table 7 Comparison of longevity of selected plants and animals from different habitats. Age refers to maximum individual age documented hitherto.

Species	Habitat & Type	Age [years]	Study
Stylocordyla borealis	marine non-colonial invertebrate	138-170	this study
Lamellibrachia spp	marine non-colonial invertebrate	170-250	Bergquist et al. 2000
Rhabdocalyptus dawsoni	marine non-colonial invertebrate	220	Leys & Lauzon 1998
Zostera marina	marine seagrass clone	1000	Reusch et al. 1999
Gerardia spp.	marine colonial invertebrate	1800±300	Druffel et al. 1995
Cinachyra antarctica	marine non-colonial invertebrate	1050-2300	this study
Welwitschia mirabilis	terrestrial gymnosperm	1500-2000	Cooper-Driver 1994
Pinus longaeva	terrestrial pine tree	4713	Lanner & Connor 2001
Rossella spp.	marine non-colonial invertebrate	13000-40000	this study

- Model output and field/aquarium observations for *Halichondria panicea* were in good correspondence regarding maximum size and age at which it is attained.
- Model output for *Cinachyra antarctica* was consistent with observations from Dayton's 10-year field study.
- Model results transferred from the Weddell Sea to the Ross Sea need to be interpreted cautiously.

4.4 Population energy budgets

All energy budgets calculated in this study are based on samples, abundances and biomass data refering to the 100 - 300m water depth range. Mean abundance from photographic studies combined with mean biomass data estimated from size frequency data and size mass relations of the three taxa investigated here, result in a sponge biomass estimate of 70.6 gC m^{-2}. This agrees quite well with sponge biomass estimate of 73.0 gC m^{-2} based on quantitative box corer samples (Gerdes et al. in press).

Jarre-Teichmann et al. (1997) modelled trophic flows on the eastern WSS. They concluded that sponges dominate community wet biomass, but are no longer important in terms of organic carbon. This view clearly has to be reconsidered on the basis of more recent findings. Not only do sponges dominate benthic communities on the eastern WSS (71 gC m^{-2}) but sponge biomass alone also exceeds standing stock values observed for whole benthic communities elsewhere: Piepenburg et al. (2002) found 10 - 15 gC m^{-2} south of King George Island, in the Bransfield Strait, Antarctic Peninsula and 5 - 40 gC m^{-2} in the Drake Passage, north of King George Island. In spite of the large standing stock, sponges on the eastern WSS are not contributing substantially to carbon flow. This is reflected in very low productivity (0.007) and low consumption to biomass ratio (0.32). In this respect the modelling approach of Jarre-Teichmann et al. (1997) was very accurate. According to their model benthic carbon flow is predominantly mediated by polychaetes and crustaceans, a view that was supported by Brey & Gerdes (1998) who concluded that polychaetes, echinoderms and crustaceans are the most important groups mediating carbon flow on the eastern WSS.

It is worth noting, however that not all sponge species confirm this general picture of a high standing stock combined with extremely low productivity. The lollypop sponge *Stylocordyla borealis* on average accounts for 1.3 gC m^{-2} and shows a P_s/B ratio of 0.106, remarkably higher than the average sponge. As discussed in section "4.2 Metabolic rate" (p 27) this can be seen in the light of resettlement processes of iceberg scour marks where *S. borealis* gains an advantage over species growing more slowly.

Gerdes et al. (in press) showed that on the WSS benthic community biomass in general and sponge biomass in particular was strongly correlated with water depth (see also Figure 11). Hence, the population energy budgets calculated for the 100 - 300m water depth range are not valid for the whole eastern WSS down to 700m. Nevertheless, based on weighted estimates (Table 6) sponges on the eastern WSS produce approximately 1 Mt of opal per year (2.4 g SiO$_2$ m^{-2} y^{-1} for water depths of 100 - 700 m). Literature data about opal from primary production (PP) that reaches the sea floor are scarce (Ragueneau et al. 2000). Opal of diatom origin exported from the water column to the bottom is reported to be 0.3 mg SiO$_2$ m^{-2} y^{-1} in the Weddell Sea seasonal ice zone (SIZ) and on the Ross Sea shelf 400 mg - 16.9 g SiO$_2$ m^{-2} y^{-1} (Tréguer & Jacques 1992). Opal export on the WSS is likely to be higher than in the Weddell Sea SIZ because deep mixing can always reach the water-sediment interface (Fahrbach et al. 1992), albeit not as high as on the Ross Sea shelf, as PP is lower in the Weddell Sea (see above). Hence, on the WSS annual opal export from the water column to the benthos is most likely in the range of a few hundred milligrams per square meter. The opal accumulation rate of sponges on the WSS (2.4 g SiO$_2$ m^{-2} y^{-1}) will thus hardly be reached by primary producers, so that sponges – where present – constitute the most significant pathway of opal flow in the WSS ecosystem. Also in the Baltic Sea the abundant breadcrumb sponge *Halichondria panicea* can be an important mediator in

the silicon-cycle (Reincke & Barthel 1997). Studying Si-uptake kinetics of the sponge, Reincke & Barthel (1997) concluded that sponge growth was silicon limited rather than food limited in shallow waters of the Baltic Sea. Silicate concentrations there do not exceed 30 µM (v. Bodungen 1975), commonly observed summer values are around 4.5 µM (Reincke & Barthel 1997). Substantially higher (100-150 µM, Fahrbach et al. 1999) silicate concentrations on the eastern WSS are likely to be one of the key factors for the high glass-sponge biomass values observed there.

Furthermore, not only silicate uptake and opal production have substantial influence on the silicate cycle, also dissolution of opal plays an important rôle. Nelson et al. (1995) reviewed that on average 60% of the opal produced in the euphotic zone is dissolved in the upper 50-100m of the water column. Ragueneau et al. (2000) conclude that changes in primary productivity do not cause a clear trend of increased or decreased recycling of the silicon. Spicules of Antarctic sponges, however, may not be recycled at all as they may not dissolve in situ (Kabir 1996). Thus the accumulated spicule mass is deposited in the sediment after death of the individual and builds spicule mats up to 1.5 m thick (Koltun 1970, Barthel 1992). Spicule depositions can be up to 9000 years old (Conway et al. 1991), indicating that once opal is deposited in the form of sponge spicules it is removed from biological cycling in the ocean for a very long time, if not permanently. Despite their substantial contribution to local Si-cycling, it has nevertheless to be concluded that on a global scale sponges contribute far less to Si-cycling than the ubiquitous phytoplankton.

- Sponges dominate many communities on the eastern Weddell Sea shelf not only in terms of wet mass but also with respect to carbon.
- Sponges can subsist with very high standing stocks.
- Contribution to carbon flow is very low.
- Locally the sponge community is the predominant pathway for silicon to opal.

4.8 Conclusions and perspectives

Concluding I refer to the initial hypotheses: "Large hexactinellid sponges on the eastern Weddell Sea shelf are up to ~500 years old" (Hypothesis 1) and "Sponges are of structural importance only and are no major component of the carbon or silicon flow patterns on the eastern Weddell Sea shelf" (Hypothesis 2).

Hypothesis 1 clearly has to be rejected as largest hexactinellid sponges on the eastern Weddell Sea shelf can be more than 1500 years old. Regarding Hypothesis 2 results are ambivalent. Even though standing stock of sponges can be high, production

and productivity are very low, i. e. sponges do not play a major rôle in carbon cycling on the eastern Weddell Sea shelf. Still, sponges are not only of structural importance as they are – where present – an important pathway from dissolved silicic acid to opal and thus a major component of silicon cycling.

Despite the well studied dynamics of the recolonization process after iceberg scouring, it was so far impossible to assign time scales to any but the first recolonization stages (Gutt & Starmans 2001). Based on the presented modelling approach it is now possible to assign a minimum age to different recolonization stages by assessing the age of the largest hexactinellid sponge of the respective study site. Disturbance by iceberg scouring can also serve as a model for other types of disturbance (e.g. human activity) and my results can contribute to assess the impact of various disturbance events.

This study was the first to assess growth rates of Antarctic sponges and modelling results can presently not be validated by other methods. Such a validation of my results is still very desirable. Validation may soon be possible with fission-track-dating. Charged particles (e. g. radium) travelling through solid material (e.g. a sponge spicule) leave tracks of damage, where energy is transferred from the particle to the sample. Radium is present in seawater and thus possibly also in sponge spicules. As the number of fission tracks is counted under a microscope, single sponge spicules can be analyzed an possibly aged. Originally developed in the early 1960's (Fleischer & Price 1964) this method had initially been considered unreliable. After recent modifications the technique is now commonly used in geology, and applications in archeology are pending. In cooperation with F. Lisker, University Bremen, first sponge spicules are presently being analyzed.

- Hypothesis 1 is rejected. Hexactinellid sponges on the eastern Weddell Sea shelf (WSS) can be more than 1500 years old.
- Hypothesis 2 is rejected partially. Sponges are not only of structural importance but are also an important pathway in silicon cycling on the eastern WSS.
- The presented results enable us to assign time scales to iceberg scour marks more accurately by calculating the age of the largest hexactinellid sponge of the study site.
- Independent validation of modelling results with the fission track aging method is ongoing.

5 Publications

The below listed publications are part of this thesis and my share of each publication is explained.

Publication I

Susanne Gatti, Thomas Brey, Werner E. G. Müller, Olaf Heilmayer, Gerhard Holst

Oxygen microoptodes: A new tool for oxygen measurements in aquatic animal ecology. Mar Biol 140(6), 2002, pp1075-1085

I developed the conceptual and methodological approach for the respiration experiments in close cooperation with the second author. The idea for measurements inside living sponge tissue was suggested and developed by myself and improved in cooperation with the third author. After performing all experimental work with sponges I wrote the first version of the manuscript which was then improved in cooperation with the co-authors. Experimental work with scallops was performed by the fourth author.

Publication II

Susanne Gatti, Thomas Brey, Núria Teixidó, Wolf E. Arntz

The Antarctic lollypop sponge *Stylocordyla borealis* (Lovén, 1868): 1. Morphometrics and reproduction.

I developed the idea for separate morphometric analysis of different body parts of the sponge, conducted all experimental and computational work and wrote the first version of the manuscript which I then revised in close cooperation with the co-authors. Analysis of photographic material to estimate abundance data was performed by the third author.

Publication III

Susanne Gatti, Thomas Brey

The Antarctic lollypop sponge *Stylocordyla borealis* (Lovén, 1868): 2. Energetics and growth rates.

The second author initiated the study and formulated the idea to use metabolic data to calculate age and growth rates. I conducted all experimental work, developed and improved the modelling routine and performed the modelling runs. The procedure for subsequent result analysis and my first version of the manuscript were refined in cooperation with the co-author.

Publication I

Oxygen microoptodes:
a new tool for oxygen measurements in aquatic animal ecology

S Gatti[1], T Brey[1], WEG Müller[2], O Heilmayer[1], G Holst[3]

[1] Alfred-Wegener-Institut für Polar- und Meeresforschung
Columbusstr.
27515 Bremerhaven
Germany
sgatti@awi-bremerhaven.de

[2] Institute for Physiological Chemistry, Dep. "Applied Molecular Biology",
Johannes Gutenberg University
Duesbergweg 6
55099 Mainz
Germany

[3] Max Planck Institute for Marine Microbiology
Celsiusstraße 1
28359 Bremen
Germany

Abstract

We describe two applications of a recently introduced system for very precise, continuous measurement of water oxygen saturation. Oxygen microooptodes (based on the dynamic fluorescence quenching principle) with a tip diameter of ~50µm, an 8-channel optode array, an intermittent flow system, and online data registration were used to perform two types of experiments. The metabolic activity of Antarctic invertebrates (sponges and scallops) was estimated in respiration experiments and, secondly, oxygen saturation inside living sponge tissue was determined in different flow regimes. Even in long-term experiments (several days) no drift was detectable in between calibrations. Data obtained were in excellent correspondence with control measurements performed with a modified Winkler method. Antarctic invertebrates in our study showed low oxygen consumption rates ranging from 0.03 - 0.19 cm^3O_2 h^{-1} ind^{-1}. Oxygen saturation inside living sponge specimens was affected by flow regime and culturing conditions of sponges. Our results suggest that oxygen optodes are a reliable tool for oxygen measurements beyond the methodological limits of traditional methods.

Introduction

Oxygen consumption rates have been measured with a variety of methods. In spite of the multitude of available methods there are still experimental conditions where oxygen measurements are very difficult if not impossible (Wilson et al. 1993). Consequently, efforts to develop new sensors and new methods are still ongoing. Today polarographic oxygen sensors (after Clark 1956; hereafter called POS) and chemical methods developed from the Winkler method (Winkler 1888) are most commonly applied to measure oxygen content in water. While suitable in many experimental situations, measurements at low temperatures, of low oxygen consumption rates, of sediment oxygen profiles with high spatial and/or temporal resolution and of oxygen saturation inside living invertebrates are often difficult to perform with these techniques. POS have often been used successfully in marine sciences primarily because of a high resolution in time caused by fast response times of the sensors, typically approx. 1 s for micro-POS (Revsbech et al. 1983). However, POS give rise to five major problems. (1) They tend to drift after calibration. The underlying assumption, that drift between two consecutive calibrations is linear may not be valid and may cause considerable errors especially in experiments lasting several hours to a few days. (2) POS are not suitable for measurements at low temperatures (i. e. near or below 0° C) because of prolonged response times and decreasing stability (Peck & Uglow 1990). (3) POS consume oxygen themselves, and can thus only be used in setups with constant stirring. Oxygen consumption by POS can moreover affect results substan-

tially, especially when oxygen consumption rates of the specimens themselves are very low. The problem of oxygen consumption by POS has to some extent been ameliorated by the introduction of micro-POS (Revsbech et al. 1983) and the pulsing technique (Langdon 1984). Both variations of the method reduce the amount of oxygen consumed by sensors. (4) Mechanical fragility of the sensor tip and the covering membrane severely impede use in sediments and inside living tissue. Finally (5), POS are subjected to an aging process: even if unused, they cannot be stored for long periods of time after manufacturing (e. g. storage time for MasCom micro-POS ≤ 6-8 month according to manufacturer's product information).

The original Winkler method (Winkler 1888) has been subjected to several modifications primarily aiming at higher precision (revised in Bryan et al. 1976). The equipment needed is inexpensive and it can be used in the field, where a stable power supply is available. However, analysis of samples is laborious (requiring 3-5 min per sample) and resolution in time is impeded by the necessity of regular sample taking (Roland et al. 1999). Options for further automation of the procedure are limited.

Problems concerning precision, applicability with low temperatures and mechanical fragility have also been overcome by couloximetry (Peck & Uglow 1990). Results are as accurate, precise, and independent of temperature as those obtained by the micro-Winkler method. Sample volume for one analysis is much smaller (25 mm^3 for couloximetry vs. 1 cm^3 for micro-Winkler) but the equipment needed is more expensive and more difficult to set up and handle. While being very precise, micro-Winkler technique and couloximetry have the common disadvantage of low resolution in time, as single samples have to be analyzed separately.

Oxygen microoptodes (measurements based on dynamic fluorescence quenching) were introduced to aquatic sciences by Klimant et al. (1995) who documented that microoptodes do not consume oxygen. Hence, a zone of oxygen depleted water around the tip cannot develop. So microoptodes can be used in experimental systems without stirring the medium (e. g. inside tissue samples). Drift is assumed to be negligible. The high mechanical stability of the luminophore matrix offers the possibility to insert optodes into sediment and also into living tissue (Stefansson et al. 1989). Data obtained by microoptodes have the same accuracy and precision as data obtained by mini- or micro-POS (Klimant et al. 1995, Glud et al. 1999). A microoptode array for parallel operation of eight optodes and suggestions for its potential applications were introduced by Holst et al. (1997). The array was further optimized by PreSens GmbH, Germany. Precision and reliability of oxygen microoptodes have been well documented in a number of papers (e. g. Wolfbeis 1991, Glud et al. 1999, Stokes & Somero 1999, and references therein). Whereas microoptodes have been successfully applied in the biomedical field, they have not yet been widely adopted in aquatic ecology. We present

here two examples of practical use of microoptodes in systems where measurements with the commonly used POS would have been impossible.

Polar invertebrates usually have low oxygen consumption rates (e. g. Clarke 1983, Chapelle et al. 1994, Chapelle & Peck 1995, Peck & Conway 2000, and references therein). When comparing sessile invertebrates with motile fauna we can expect a considerably lower metabolic activity and thus extremely low oxygen consumption rates. Hence, a method is required that is (a) very sensitive and which (b) does not exhibit any drift.

It is possible to grow primmorphs (well defined sponge cell aggregations surrounded by a dermal membrane) from cell aggregations of the sponge *Suberites domuncula* (see methods-section). However, growth becomes limited or ceases when primmorphs reach a diameter of 3-4 mm (Müller et al. 1999a). In spite of a variety of culturing methods applied, the reasons for recess of growth remain unknown. Pumping structures such as choanocyte chambers have not yet developed in small primmorphs. It is possible that diffusion through the tissue does not provide enough gas exchange and growth is inhibited by lack of oxygen supply. To test this hypothesis we measured the oxygen content inside primmorphs reared under a variety of conditions and inside adult sponges, utilizing the described features of stability and high temporal resolution of oxygen microoptodes.

Materials and methods

The system used for our experiments is summarized in Figure I-1. Technical details can be found in Holst et al. (1997) and Klimant et al. (1997). Oxygen acts as a dynamic fluorescence quencher of a luminophore, which is immobilized in a polymer matrix. Intensity, lifetime, and modulation of phase angle of the fluorescence signal are influenced by the number of oxygen molecules present and can be measured.

As fluorescence intensity is affected by several additional factors (e. g. length, bending and micro bending of the cable) phase angle modulation was used to calculate oxygen saturation in the water.

The sensor consists of a fiber optic cable supplied with a standard glass fiber plug to connect it to the optode array. Technical specifications of microoptodes as provided by the

Table I-1 Technical specifications of microoptodes used in our experiments (as provided by the manufacturer, PreSens, Germany).

Measuring range	0 - 672 hPa (0-150% air saturation)	
Accuracy	± 0.2 hPa	at 5 hPa
	± 0.5 hPa	at 50 hPa
	± 3.0 hPa	at 210 hPa
Tip diameter	30-50 µm	
Response time	2-3 seconds	

manufacturer are given in Table I-1. The sensor end of the cable can be tapered to various tip diameters and is then coated with a ruthenium-II-luminophore-complex (details of sensor tip mounting are shown in Figure I-2). Light is emitted from one common light source (blue light emitting diode) through an optical switch to each of the eight sensors subsequently. The resulting fluorescence signal is detected and enhanced by a photomultiplier.

Depending on the number of sensors connected to the array, each sensor performs a measurement every 1-2 minutes. All data (time, sensor number, phase angle, and oxygen saturation, control for background lighting) are transmitted directly to a computer for continuous data registration. Two-point calibrations were performed with all microoptodes connected to the same water reservoir. Nitrogen bubbling and air bubbling were used to calibrate the 0% and 100% air saturation points, respectively. After stabilization of the phase angle, measurements were continued for at least 10 minutes. Signal variation after stabilization of the calibration signal was documented to
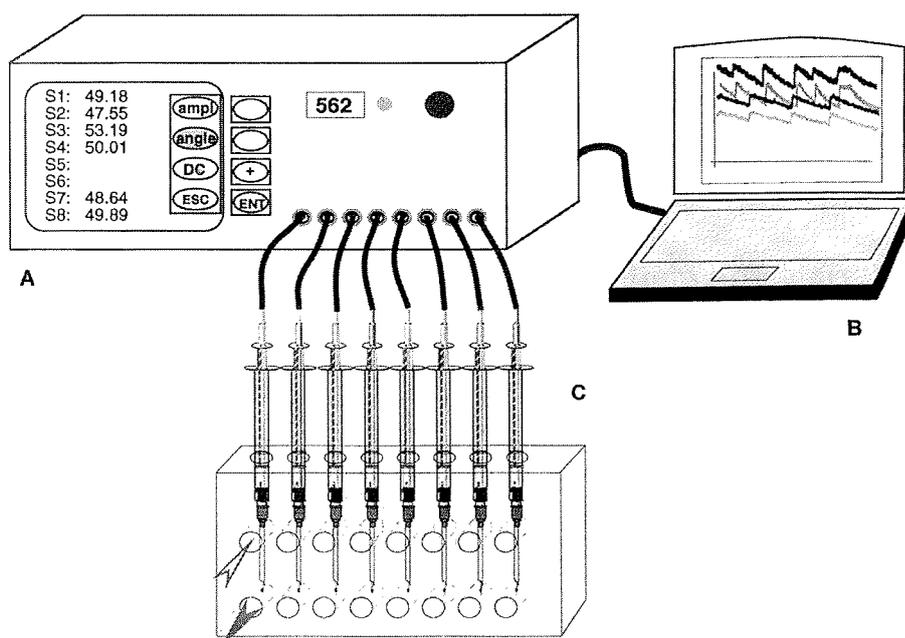
Figure I-1 Schematic diagram of the system used in both types of experiments. Optical cables are connected with standard glass fiber plugs to an eight-channel optode array (A). All data are transmitted directly to a computer (B) for continuous registration. For a better protection of sensor tips, sensors were kept in a sensor block (C) during the first set of experiments. Air and water tightness of syringes in the sensor block were ensured by double o-rings for every syringe (not shown). Arrows indicate direction of water flow (open arrow = from respiration chambers towards sensors; filled arrow = away from sensors to pumps). For the second set of experiments the sensors were inserted into the sponges directly instead of being kept in the sensor block. Details of sensor mounting in syringe are enlarged in Figure I-2.

optical cable

plunger rod

transport blocking
(removable)

safety block
(permanent)

sensor tip

(A)   (B)
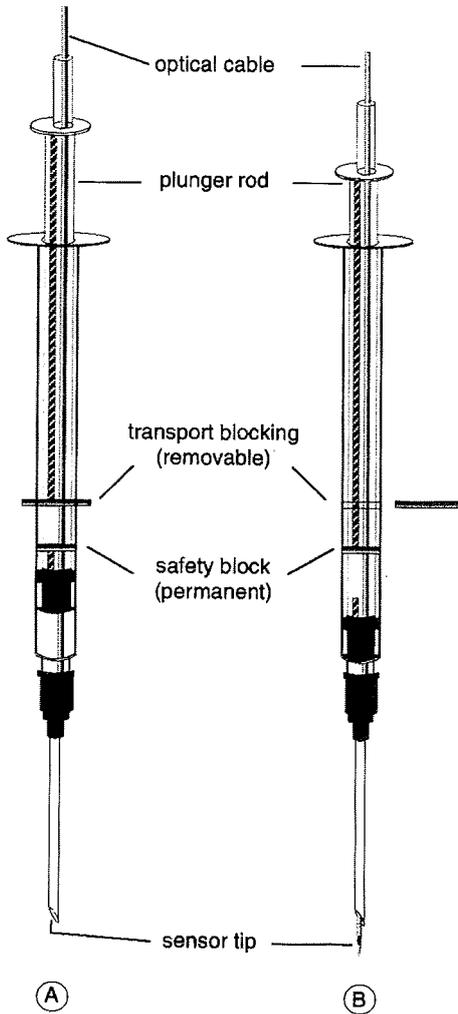
facilitate an estimate of drift during and in between experiments. Both calibration points were checked twice with a modified Winkler method (according to WOCE guidelines (Culberson 1991, Dickson 1996)). To estimate precision and accuracy of the method we compared 10 consecutive measurements as performed by each sensor using water of the calibration procedures (i.e. water with 0% and 100% air saturation). This was repeated prior to each experiment.

Two types of experiments were performed. (1) Respiration experiments: Oxygen consumption rates of Antarctic invertebrates (sponges: *Cinachyra antarctica* (Carter, 1872) and *Stylocordyla borealis* (Lovén, 1887), scallop: *Adamussium colbecki* (Smith, 1902)) were determined from decrease of oxygen saturation in an intermittent flow system. (2) Oxygen content inside living sponge tissue: Oxygen saturation inside living sponges *(Suberites domuncula* (Olivi, 1792)) was measured and compared to simultaneously measured oxygen saturation of the water surrounding the sponge.

Figure I-2 Schematic drawing of microoptode mounted in a standard 1 cm^3 syringe. The optical cable is permanently fixed to the plunger rod. By pushing or pulling the plunger rod the sensor tip is retracted into the needle tip ((A) protected position for transportation) or protruding from the needle tip ((B) measuring position). A gap in the stabilizing structure of the plunger rod (hatched bar) and a permanent safety block determine both end points of plunger rod movement and thus maximum retraction or protrusion of sensor tip. (n. b. the sensor will also be able to measure oxygen saturation when inside the needle. However, as water exchange within the needle is limited, results obtained from such measurements would be subject to prolonged response times and would not reflect the true oxygen content within surrounding water masses.)

Respiration experiments

All respiration experiments were performed on board RV "Polarstern" (during expeditions ANT XV/3 and XV/4 in 1998 to the Weddell Sea, Antarctica) in a temperature controlled room at near ambient water temperature (-0.5° to +0.5°C) and salinity (S=34). Respiration chambers were immersed in a larger volume of water (200 dm^3) to maintain temperature stable during periods of automated defrosting cycles in the temperature controlled room. Unfiltered seawater was used as pilot studies had shown that both sponge species (*C. antarctica* and *S. borealis*) had tightly closed oscula when kept in filtered seawater. As all specimens were taken from water depths below the euphotic zone, all experiments were carried out in the dark. One control
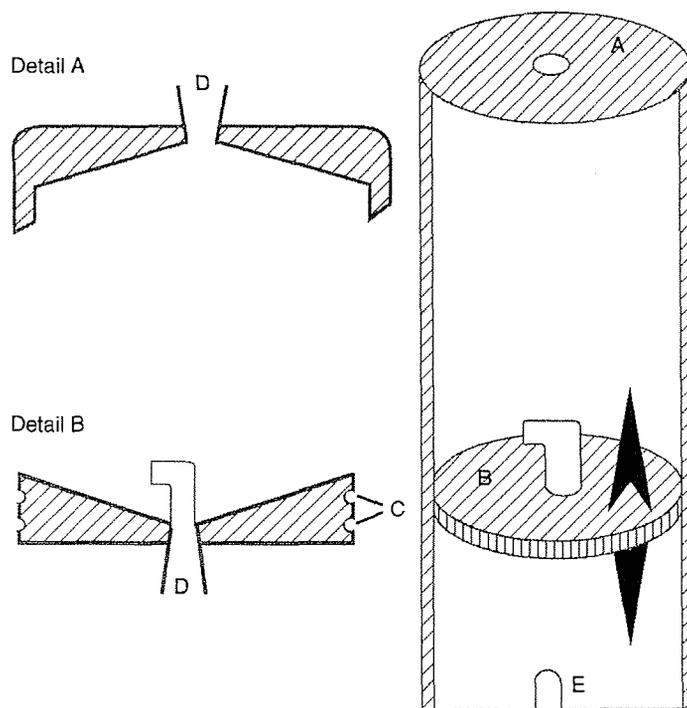
Figure I-3 Respiration chambers with variable volume. The top lid (A) of the chamber is fixed. Bottom lid (B) is movable inside the chamber to adjust chamber volume prior to an experiment. Air and water tightness are ensured by a set of two o-rings between bottom lid and chamber wall (within the two notches C). Inflow of water through the tube connector (D) of the bottom lid (A), outflow of water through the tube connector of the top lid (A). Notch (E) within the chamber wall allows the tubing to be passed to the pumps when the chamber is standing in an upright position. Please note: Both lids slope towards the central hole to avoid the trapping of air bubbles.

chamber (i. e. without animal) was run in parallel to each experiment. After the first initial calibration, calibration points were checked regularly at the beginning of a new experiment. Daily blank controls of the optode array (with all sensors disconnected) were performed to control for internal (i. e. inside the optode array) ambient light conditions (for de-tails see manual of 8-channel optode array, PreSens). We used vari-able volume chambers (Figure I-3) to be able to adjust chamber size to a wide variety of animal sizes. Chambers were equipped with a movable bottom lid, which could be pushed into the cylindrical respiration chambers to reduce the water volume around the animal. Air and water tightness was accomplished by double o-rings between the cylindrical chamber and the lid. Chamber volume was adjusted to specimen size once prior to each experiment and then kept constant for the duration of one experiment. Control chambers were adjusted to a similar volume as experimental chambers. Measurements started immediately after closing of the chambers without dedicating time for acclimation of the animals to chambers, as we wanted to compare initial oxygen consumption rates with those obtained in subsequent experimental cycles. To ensure a constant water flow through experimental chambers all chambers were connected to an intermittent flow system. Water was pumped from the respiration chamber to the sensor and back to the respiration chamber with two four-channel peristaltic pumps with a nominal maximum capacity of 1.7 dm^3 min^{-1} $channel^{-1}$ (Masterflex: precision pump, model 7520-47). Highest pumping rates were used for largest chamber sizes. A set of preliminary experiments with ink showed quick and even mixing inside all the various sizes of chambers we used.

Circulation through the chamber was opened for 100% saturated water when oxygen saturation fell below 80% inside the chambers and closed again, when saturation was back at 100%. Depending on availability of respiration chambers and of invertebrate specimens, every individual was allowed to go through 3-7 repeated cycles of opening and closing of the system. Cycles lasted 2-14 hours each. For calculation of total oxygen consumption in a respiration chamber, linear regressions of oxygen saturation versus time were calculated for all measurements in one cycle. Cycles shorter than three hours (i. e. less than 90 single measurements) were excluded from the analysis. Visual inspection of the data of cycles with a regression coefficient $r^2 < 0.9$ revealed unusual peaks and troughs in oxygen saturation data possibly caused by strong defrosting cycles in the cool room. So those cycles were also excluded from further analysis. Visual inspection of the remaining data sets (with a regression coefficient $r^2 > 0.9$) revealed no peaks or troughs, which would affect linear regression. After every experiment total water volume in each respiration chamber including adjacent tubing was determined by emptying the chamber contents into a measuring cylinder. Ammonia was measured in each chamber to control for waste products using a test kid by Merck (Merckoquant® for ammonium). After experiments on the ship were complete specimens were frozen (-30°C).

To determine wet mass (WM), dry mass (DM) and ash free dry mass (AFDM) sponges were weighed, oven dried for 24h at 100°C and ignited for 24h at 500°C (Paine 1964). Scallops were oven dried for 24h at 80°C and ignited for 12h at 500° C. Data for sponges' ash mass were corrected for water loss from spicule matrix during burning as documented by Dayton et al. (1974). Mass specific oxygen consumption rates (O_{2cons}) were calculated according to

Equation I-1 $$O_{2cons} = \frac{\frac{sat_{t=0} - sat_{t=60}}{100} \bullet O_{2sat} \bullet V - O_{2contr}}{bm}$$

where O_{2cons} = mass specific oxygen consumption rate [$cm^3 O_2\ h^{-1}\ g^{-1}$ AFDM]; O_{2sat} = oxygen content of seawater saturated with oxygen [$cm^3 O_2\ dm^{-3}$ seawater] computed according to Benson & Krause (1984); $sat_{t=0}$ = oxygen saturation [%] at beginning of experiment; $sat_{t=60}$ = oxygen saturation [%] after 60 minutes as calculated from linear regressions of each cycle; V = true water volume of respiration chamber and tubing [dm^3] (i. e. corrected for animal volume); bm = body mass of animal [AFDM]; O_{2contr} = oxygen consumption attributed to bacteria and microheterotrophs inside experimental chamber.

Oxygen consumption in control chambers was attributed to bacterial and microheterotrophic respiration. It can be assumed that growth of this size fraction of organisms was similar in control and experimental chambers. We further assume that such growth occurs both, along the walls of respiration chambers as well as in the water volume. To be able to include both types of growth we created an artificial factor VA (VA=V×A, where V = volume of respiration chamber and tubing [cm^3] and A = inner surface area of respiration chamber and adjacent tubing [cm^2]) to which oxygen consumption inside control chambers was fitted. Weighted linear regression (Draper & Smith 1980) showed that VA correlated well with oxygen consumption inside control chambers

Equation I-2 O_{2contr} [$cm^3\ O_2\ h^{-1}\ VA^{-1}$] = 2.38×10^{-3} + VA $\times\ 5.00 \times 10^{-8}$

(N=42, R^2_{adj}=0.71, p<0.001). Oxygen consumption of bacteria and heterotrophs inside experimental chambers (O_{2contr}) was calculated according to the fitted regression.

Oxygen content inside living sponge tissue

All experiments with *Suberites domuncula* were performed at the University of Mainz (Institute of Physiological Chemistry) in November 1999. Experiments were conducted with adult sponges (A) and three different types of primmorphs (P) (Table I-2). Adult sponges were taken from the Mediterranean Sea in 1997 and have since then been kept in aquaria. For cultivation of primmorphs some cells were taken from adult sponges and incubated separately in artificial seawater in petri dishes (ø 47 mm).

Table I-2 *Suberites domuncula.* Sponges and incubation conditions used in the second set of experiments. Primmorphs (P) are cell lumps of approx. 3 mm diameter which form after some weeks from tissue samples taken from adult (A) sponges. All sponges were kept in artificial seawater (S=40-42 and T=16-19°C).

Sponge	Type	Pressurized	Feeding	Antibiotics
P1	primmorph	no	beer wort	yes
P2	primmorph	no	no	yes
P3	primmorph	yes	no	yes
A1	adult	no	no	no
A2	adult	no	no	no

To avoid bacterial growth antibiotics were added. After some weeks the cells had rearranged and formed an irregular lump surrounded by a dermal membrane, the pinacoderm (Müller et al. 1999a). All primmorphs used in our experiments were of similar size (diameter approx. 3 mm). Type P1 was additionally fed with extra nutrients (beer wort). Type P1 and P2 primmorphs were incubated in stagnant water without flow, type P3 primmorphs were incubated in a pressurized chamber (1 atmosphere overpressure (Krasko et al. 1999)) at constant flow of approx. 80 cm/sec through the chamber. The number of available primmorphs was limited by the principle difficulties of cultivating well-defined primmorphs that had developed the pinacoderm (Müller et al. 1999a). We had to use primmorphs reared under a number of different conditions to achieve a maximum number of experiments.

Measurements were performed at T=19°C, S=40 and atmospheric pressure without any flow. Primmorphs were usually kept in the same petri dishes also used for cultivation; measurements of adults were performed in 2 dm^3 glass beakers. Additionally P3 was exposed to varying flow speed in an aquarium. One microoptode was inserted into the sponge specimen while a second sensor measured oxygen saturation of the surrounding water close to the sponge. Inserting the microoptode initially caused a contraction in adult sponges. After a recovery time of approximately 15 minutes, sponges appeared to be in their normal state of relaxation again. To compensate for a possible initial reaction of the sponge to insertion of the optode every experiment lasted for 20 - 45 minutes (i. e. at least 20 min. of which the sponges appeared in their normal state of relaxation). We assume that adult sponges recovered completely from our experiments as none of them died in the next two weeks. Primmorphs, however, died subsequently as had all other primmorphs after reaching maximum size of ca. 3 mm even when not subjected to experiments.

Results

For both types of experiments sensors and optode array worked reliably and without any problems. Precision and accuracy were high (Figure I-4), albeit slightly higher for water with 0% oxygen saturation (open symbols) than for 100% saturated water (filled symbols). Calibrations were easy to perform and in close correspondence with Winkler measurements (Figure I-5).
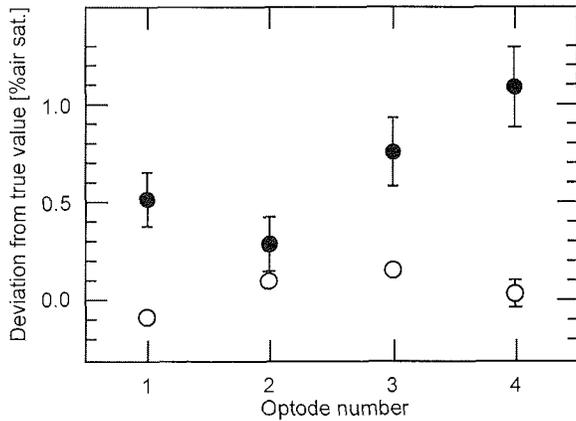
Figure I-4 Precision and accuracy of microoptodes. Precision is given as mean deviation from true oxygen saturation value [% air saturation] for water of 0% (open symbols) and 100% air saturation (filled symbols) for each of the four optodes used during our experiments (n=130 for each sensor and saturation level). Accuracy can be inferred from error bars (± 1SE). Were error bars are missing they are inside the symbol.
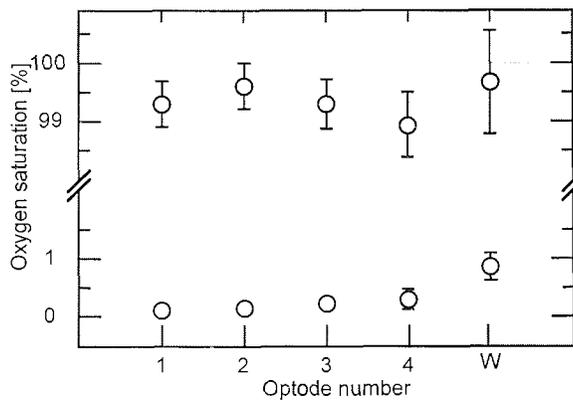
Figure I-5 Comparison microoptode with Winkler measurements. Oxygen saturation as measured by four optodes after approximately 15 minutes of nitrogen bubbling (for 0% calibration point) or air bubbling (for 100% calibration point). Displayed data are means ± 1 SE of experiments performed within a period of three months. W = mean of Winkler control measurements. Where the error bars are not shown, they are inside the symbol.

Microoptode		1	2	3	4
0% calibration	r_s	0.600	0.118	0.279	0.236
	p	0.025*	0.659	0.297	0.378
	n	15	15	15	15
	drift	+0.03%	n. s.	n. s.	n. s.
100% calibration	r_s	-0.574	-0.745	-0.679	-0.490
	p	*	0.007**	0.014*	0.077
	n	14	14	14	14
	drift	-2.95%	-3.38%	-3.36%	n. s.

Table I-3 Drift of microoptodes in between experiments. Means for each calibration process were Spearman rank correlated with time [days after first experiment]. Spearman rank correlation coefficients (r_s), p-values of significance (p), and number of experiments (n) are given for each of the four optodes used during respiration experiments. 'Drift' refers to the drift of each optode as calculated from all calibrations over a period of 93 days.

There was no significant difference between measurements of microoptodes and Winkler control measurements (ANOVA: 100% air saturation: n=64, p=0.83; 0% air saturation: n=64, p=0.15). Drift between calibrations was negligible (Table I-3). Of the four optodes used in respiration experiments only one optode showed significant drift of the 0% calibration point: +0.03% in 93 days. Drift of the 100% calibration point was slightly larger and significant for all but one optode: -3.0% to -3.4% in 93 days.

Respiration experiments

Exemplary typical raw data are presented for two individuals of *Stylocordyla borealis* (Figure I-6). While the circulation was closed (white blocks), decrease of oxygen content within respiration chambers was continuous and uniform. Variation around linear regressions was minimal for experimental chambers but higher for control chambers. Slope of decrease of oxygen saturation was uniform within single experiments i. e. there was no difference in slope detectable that could be attributed to acclimation of animals. After opening of the circulation, flushing of chambers was quick (grey blocks), optode-response instantaneous and usually oxygen levels were back to 100% air saturation after 10-15 minutes. For all species of Antarctic invertebrates we show the results of one typical experimental run (Figure I-7AB). Oxygen consumption rates of the Antarctic sponges ranged between 0.04 and 0.38 cm^3O_2 h^{-1} $g^{-1}AFDM$ and were generally lower than those of the scallop (0.15 to 0.35 cm^3O_2 h^{-1} $g^{-1}AFDM$) (Figure I-7B). For all species individual oxygen consumption increased with size of the specimen (increase 3.4fold for *C. antarctica*, 4.1fold for *S. borealis* and 5.8fold for *A. colbecki* over size range of 0.09 - 1.28 gAFDM (Figure I-7A)). Mass specific respiration rates, however, decreased with increasing specimen size for all species (Figure I-7B). Large *C. antarctica* used 24% of the amount of oxygen per g AFDM of small specimen, *S. borealis* used 33%, and *A. colbecki* 43%. At the end of each experiment ammonia concentrations in all respiration chambers were below detection limits. The complete sets of results covering the known size range of each species and ecological interpretations will be presented elsewhere.

Oxygen content inside living sponge tissue

Saturation around the sponges (control values) varied slightly between measurements (max. SE of control measurements: ±1.42 % air saturation), as there was no water flow or mixing within the petri dishes but sponges did consume oxygen. To facilitate direct comparison between different experiments all results were expressed as % oxygen saturation of the surrounding water. Oxygen saturation inside living sponge tissue varied markedly between individuals (Figure I-8). P3 reared in the
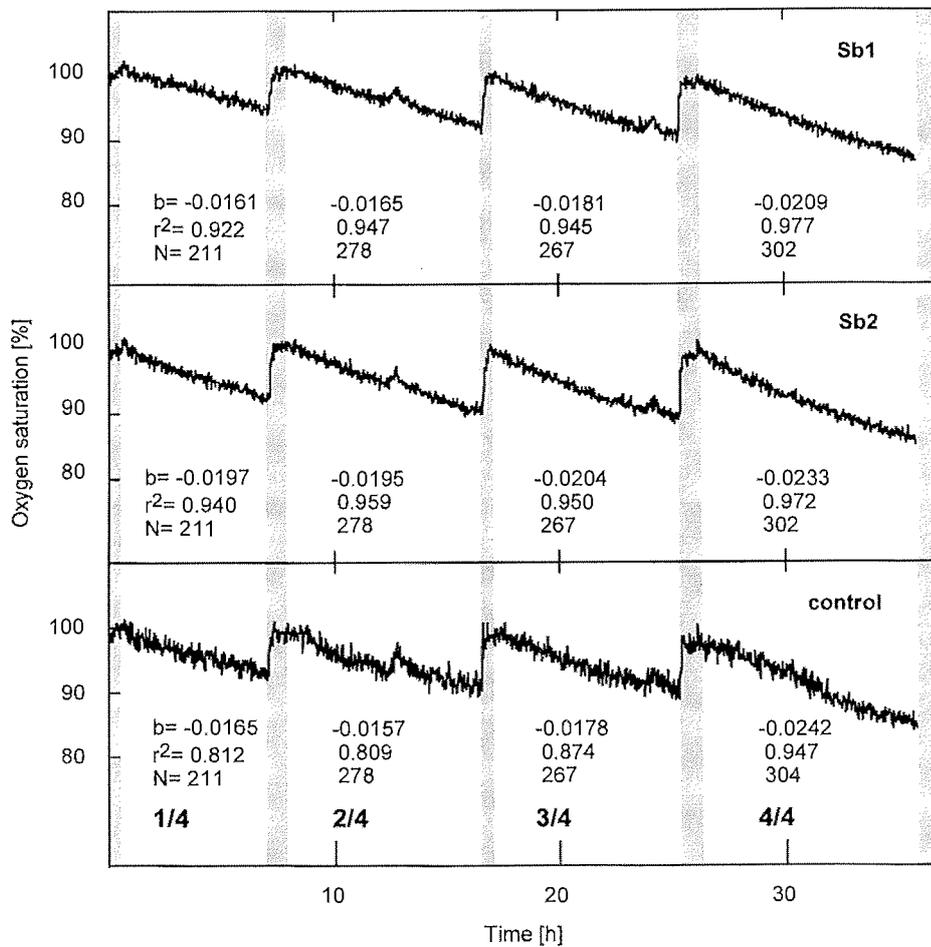
Figure I-6 *Stylocordyla borealis* Unprocessed data of respiration experiments of two individuals (Sb1 and Sb2) and one control run. Grey blocks: data were excluded from analysis e. g. when the system was opened for flushing; white blocks: measuring phase with closed system. Linear regressions were calculated for measuring phases with closed system only. For every cycle the slope (b) of linear regression, correlation coefficient (r^2), and the number of single measurements (N) included in the linear regression are given (in this order).
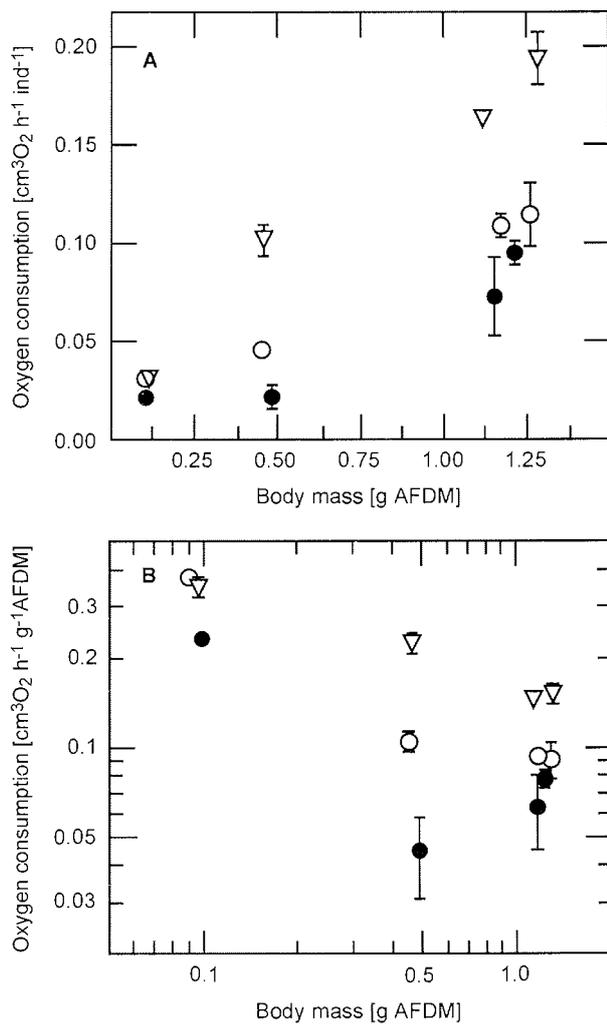
Figure I-7AB Antarctic invertebrates. Oxygen consumption rates versus body mass for *Adamussium colbecki* (open triangles), *Cinachyra antarctica* (dots) *Stylocordyla borealis* (circles) are shown as means ± 1 SE. Where error bars are not shown they are inside the symbol. (A) oxygen consumption rates of individuals [cm^3O_2 h^{-1} ind^{-1}] versus body mass [gAFDM]. (B) Mass specific oxygen consumption rates [cm^3O_2 h^{-1} g^{-1}AFDM] versus body mass [g AFDM]. Please note logarithmic scale of both axes.

pressurized flow environment and adult sponges showed highest oxygen saturation values when compared to the surrounding water (50.8 - 71.2%). P1 (no flow, fed with beer wort) showed the overall lowest oxygen saturation inside the tissue (mean oxygen saturation 2.3% of the surrounding water). P2 (no flow, or feeding) had a mean oxygen saturation of 15.0% of the surrounding oxygen saturation. Even though P3 had to be taken out of the flow and the pressurized chamber for measurements, mean oxygen saturation in this specimen was 30fold higher when compared with P1. Additionally P3 was tested in an aquarium with running seawater. Oxygen saturation inside the primmorph was initially 32.7% ± 0.49 of surrounding water (mean ± 1 SE). With the onset of increased flow speed also oxygen saturation inside the sponge increased (48.3% ± 0.62, mean ± 1 SE). When flow speed was reduced oxygen saturation inside the sponge dropped instantaneously to 12.9% ± 0.45.

Adult sponges typically showed low oxygen content in the beginning of each experiment but rising values for about 20 minutes thereafter. Oxygen content then stabilized between 50 and 60% of the surrounding water (Figure I-8).

Figure I-8 *Suberites domuncula.* Oxygen content inside living sponges. Data displayed are means ± 1 SE for 10-15 consecutive measurements. Open symbols: primmorphs, filled symbols: adult sponges (P1: fed; P2: not fed; P3: flow and pressure; A1 & A2 adult sponges). Where error bars are not shown they are inside the symbol. Please note the broken y-axis.
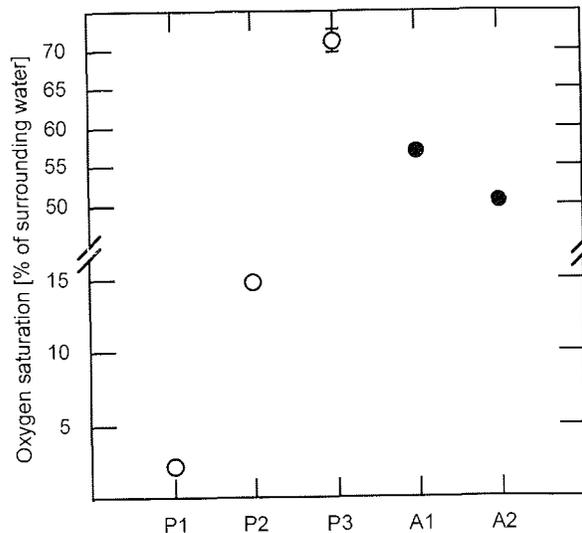
Discussion

Respiration experiments

We measured oxygen consumption rates of three species of Antarctic invertebrates in an intermittent flow system using microooptodes. For all three species, oxygen consumption rates were low (0.04 - 0.38 cm^3O_2 h^{-1} $g^{-1}AFDM$). These data are among the lowest oxygen consumption rates measured directly (Table I-4). Couloximetry is one of the methods that have successfully been used for oxygen measurements of polar invertebrates in several studies (e. g. Chapelle et al. 1994, Chapelle & Peck 1995, Schmid 1996, Brockington 2001, Peck & Veal 2001). The authors gained precision but lost high resolution in time by utilizing this method. High resolution in time is obtained with very precise microooptodes. In our experiments drift of the microooptodes at 0°C was negligible (maximum 3.38% over 93 days) and distinctly lower than in POS at any temperature (Figure I-9). Moreover, POS drift becomes larger and less predictable with decreasing temperatures making them rather unsuitable for measuring small changes in oxygen concentration at lower temperatures (Schmid 1996). Oxygen consumption rates of the Antarctic demosponges *Isodyctia kerguelensis* and *Mycale acerata* were measured in an open flow system equipped with POS (Kowalke 2000). Unfortunately it is not stated if or how the large drift was accounted for. In the light of the known large drift of POS at low temperatures it must be difficult to

(a) distinguish equilibrium from non-equilibrium states after only 3 hours of adjustment time, when theoretically (Propp et al. 1982) more than 9 hours are needed and (b) to measure oxygen consumption rates that are much lower than the drift.

Open flow systems are highly desirable for laboratory experiments with sponges because it has been well documented that sponges depend on flow for various biological functions (e. g. Hummel et al. 1988, Leichter & Witman 1997). Also, open flow systems ensure that specimens are exposed to constant oxygen saturation levels near 100%. However, special attention has to be paid to time required to attain equilibrium between inflow of water

Figure I-9 Drift of oxygen sensors. Data shown are means ± 1SE for two or three sensors used in up to 36 calibration procedures (each lasting for 20-30 minutes). Circles: POS (polarographic oxygen sensors) unpubl. data O Heilmayer and M Langenbuch, AWI, dot: POS, Baumgärtl and Lübbers (1983), x: microoptodes, maximum drift in our experiments).

with 100% oxygen saturation and outflow of water from the chamber. On the other hand small changes in oxygen concentration are easier to detect in closed bottle systems (e. g. Chapelle et al. 1994). Furthermore, no adjustment time is needed when operating a closed bottle system. We decided not to use an open flow system. Times needed for equilibrium adjustment would have been too long for the chamber size (0.2 - 14.7 dm^3) we used and the maximum flow speed available. To be able to nevertheless utilize the advantages of an open flow system (constant flow through respiration chambers) and a closed chamber system (very small oxygen consumption rates are easier to detect) we used an intermittent flow system. Regular opening of the chambers and flushing with water from a large reservoir (in our case 200 dm^3) did not only bring oxygen saturation back up to 100% but also flushed out waste products. Ammonia levels in our experiments were always below detection level.

We could not find a consistent increase or decrease of oxygen consumption rates within experiments, i. e. sponges did not need an acclimation time for adjustment to the respiration chambers. It has been argued, that transferring specimens into respiration chambers causes stress to the animals and temporarily elevated metabolic rates (Peck & Conway 2000). On the other hand Lampert (1984) argues, that it is not clear whether initially higher metabolic rates are an experimental artefact or reflect conditions in the

field. In the later case reduced flow speeds in respiration chambers, alterations in light regime or confinement to a respiration chamber itself could cause reductions in metabolism as observed in later phases of respiration experiments. Both arguments may be valid for certain groups of higher invertebrates and stress can certainly play an important role in respiration experiments with vertebrates. Our results suggest that sponges do not exhibit such alterations in metabolic rates due to transfer to respiration chambers as oxygen consumption did neither decrease nor increase systematically with duration of the experiments.

Table I-4 Oxygen consumption rates for cold water invertebrates. Data are minimum and maximum values of the respective study and are given as [cm^3O_2 h^{-1} $g^{-1}AFDM$] or when indicated by * as [cm^3O_2 h^{-1} $g^{-1}DFM$] (DFM= dry flesh mass). Methods (Meth.) for oxygen determination are abbreviated with C = couloximetry; P = POS (standard Clarke-type); M = microoptode; W = Winkler method, H = oxygen consumption rates calculated from heat production data. Abbreviations of incubation system (Syst) refer to the following methods: O = open flow system, C= closed bottle, I= intermittent flow.

Species	Min	Max	Temp [°C]	Meth.	Syst.	Study
Brachiopoda						
Liothyrella uva	0.031	0.103	1.0±0.5	C	C	Peck 1989
Crustacea						
Saduria entomon	0.050	0.117	0.0	C	C	Schmid 1996
Waldeckia obesa	0.042	0.071	0.0±0.1	C	C	Chapelle et al. 1994
Echinodermata						
Sterechinus neumayeri	0.023	0.084	-1.8/+0.5	C	C	Brockington & Peck 2001
Mollusca						
Adamussium colbecki	0.149	0.352	0.0±0.5	M	I	this study
Astarte montagui	0.004	0.039	0.0	C	C	Schmid 1996
Chlamys islandica	0.085	0.370	0.0	C	C	Schmid 1996
Clinocardium ciliatum	0.050	0.057	0.0	C	C	Schmid 1996
Laternula elliptica	0.085	0.222	0.5±0.3	W	C	Ahn & Shim 1998
Nacella concinna	0.039*	0.105*	1.0±0.5	C	C	Peck 1989
Nacella concinna	0.095*	0.242*	-0.7±0.1	C	C	Peck & Veal 2001
Porifera						
Cinachyra antarctica	0.091	0.380	0.0±0.5	M	I	this study
Isodyctia kerguelensis	0.027	0.041	1.0	P	O	Kowalke 2000
Mycale acerata	0.069	0.125	1.8	P	O	Kowalke 2000
Stylocordyla borealis	0.044	0.240	0.0±0.5	M	O	this study
Tetilla cranium	0.352	0.490	-0.5	-	H	Witte & Graf 1996
Thenea abyssorum	0.336	0.654	-0.5	-	H	Witte & Graf 1996
Thenea muricata	0.186	0.688	-0.5	-	H	Witte & Graf 1996

Data of oxygen consumption rates of polar sponges are rare. Apart from this study, Witte & Graf (1996) and Kowalke (2000) provide the sole oxygen consumption rates of polar sponges. Witte & Graf (1996) calculated oxygen consumption data from heat production measurements. Whenever anoxic metabolism can be ruled out (as in the case of polar sponges) heat production data reflect oxygen consumption as accurately and precisely as direct measurements of oxygen consumption (pers. com. U. Witte). We would have expected higher oxygen consumption rates for *M. acerata* and *I. kerguelensis* than for species used in our experiments for two reasons: Water temperature in the experiments with *M. acerata* and *I. kerguelensis* was up to 1.8°C higher than in our experiments and secondly, especially *M. acerata* is known to be one of the few fast growing species of Antarctic sponges (Dayton et al. 1974). However, oxygen consumption rates of *M. acerata* and *I. kerguelensis* are comparable to our results and 5-10fold lower than those for the Arctic deep-sea species *Thenea spp* and *T. cranium*. Due to the above-mentioned difficulties with the experimental setup, we think that the results for *M. acerata* and *I. kerguelensis* need to be interpreted with much caution.

Oxygen content inside living sponge tissue

In the second set of experiments oxygen saturation was measured inside sponge primmorphs and adult specimens. No oxygen consumption rates were determined in this experiment.

As shown in Figure I-8 oxygen saturation inside primmorphs incubated in constant flow (in a pressurized chamber) i. e. P3 and adult sponges, was much higher than in primmorphs held in stagnant water (P1, P2). It could also be shown that flow speed had a distinct effect on oxygen saturation inside P3 (initially: 32.7%; increased flow speed: 48.3%; reduced flow speed: 12.9%). This observation corresponds well to the fact that rearing primmorphs outside the chamber with flow (and pressure) is much more difficult and survival rates are lower than for those reared inside the pressurized chamber (Müller pers. obs.). However, pressure inside the chamber is generated with a constant flow of water. So far it is impossible to determine whether the differences in oxygen saturation are caused primarily by the water current, by pressure, or by a combination of both. As measurements with P3 were performed in an aquarium without extra pressure it seems likely that flow is the more important component of the two. To further elucidate the importance of all factors, it will be necessary to perform a series of parallel experiments with a larger number of primmorphs once difficulties in incubation of primmorphs have been overcome. Comparable oxygen saturation in P3 and adult sponges might indicate, that water flow which is usually generated by pumping structures can also be applied successfully from outside. Primmorphs that have not yet developed such structures clearly suffer from oxygen depletion inside their tissue when

reared without flow. Our experiments were aimed at detecting differences and testing the new method rather than carrying out a systematic investigation of flow, pressure and/or nutrients. It could be shown that microoptodes are a valuable tool to rapidly and reliably detect differences of oxygen saturation inside living sponges.

We presented two unprecedented practical examples of applications of a new, reliable method to determine oxygen saturation in water samples as well as inside living tissue. Oxygen optodes work particularly well at low temperatures because of increased oxygen fluorescence intensity at low temperatures (Wolfbeis 1991). In our experiments oxygen optodes were easy to use and gave precise, reproducible results. We used optodes successfully in experiments lasting several days. Drift over 93 days was negligible. With the eight-channel optode array several experiments can be run simultaneously. Initially encountered problems with breaking optodes due to shearing

Table I-5 Comparison of different methods for measurements of oxygen saturation (or oxygen content) of water samples. (+ feature is fully supported by method; ± feature is supported to some extent, e. g. depends on the precise handling of the method; - feature is not supported by method; ø not applicable; d discrete measurements; c continuous measurements). Please note: Only selected methods have been discussed in the text explicitly. A basic description of additional methods can be found in Lampert (1984) and references therein.

Features / Methods	Cartesian diver	Volumetric	POS	Micro-POS	Couloximetry	Winkler	Micro-Winkler	Optodes	Microoptodes
Clear signal = high sensitivity	±	±	±	+	+	±	±	+	+
Short response time	+	±	±	+	-	-	-	+	±
Precise reproducible results	+	±	±	+	+	±	+	+	+
High resolution in time	±	±	±	+	-	-	-	+	±
Continuous or discrete measurements	d	d	c	c	d	d	d	c	c
Mechanical robustness	ø	+	-	-	+	+	+	+	±
Drift negligible	+	+	-	-	±	ø	ø	+	+
Multichannel usage	+	+	±	±	+	+	+	+	+
Inexpensive	±	+	±	-	-	+	+	+	+
Portability	+	+	±	±	±	+	+	+	+
Ship board usage possible	±	-	±	±	±	+	+	+	+
Easy to use/maintain	±	+	-	±	-	±	±	+	+
Measurements inside tissue samples	-	-	-	±	+	±	±	±	+
For specimen of various size classes	-	+	+	+	+	+	+	+	+
Suitable for low temperatures	+	+	-	-	+	+	+	+	+
Applicable without stirring of medium	+	+	-	-	+	+	+	+	+
insensitive to autofluorescence of sample	+	+	+	+	+	+	+	±	±
Commonly applied method today	-	-	±	+	±	+	+	-	-

forces upon insertion into extremely tough sponge tissue were ameliorated by mounting optode tips movable in syringe needles (Figure I-2). The injection needle could then be inserted into the sponge tissue first and the optode could be pushed forward inside the injection needle and finally into the tissue itself. A comparison of the most commonly used methods to measure oxygen saturation in water samples is given in Table I-5. All methods mentioned show strong features as well as shortcomings.

Applicability of microoptodes is limited in experiments in which light plays an important role. On one hand photosynthesis can be enhanced by the light pulses of the optode array. On the other hand autofluorescent samples can cause an error when the fluorescence signal is detected. These problems can be overcome by optical shielding of the optode tip but the sensor tip will then be much bigger and resolution in space will be strongly reduced. Nevertheless, at present microoptodes provide the only means of precise measurements at low temperatures with high resolution in time. Furthermore, microoptodes are cheaper than POS, and easier to handle than couloximetry. These features may be utilized in the future for in situ measurements directly comparing in- and out-flowing water (e. g. of sponges, bivalves, and ascidians). It should be possible to conduct shallow water experiments with microoptodes by scuba diving. Moreover, optodes could also be deployed from submersibles for in situ study of metabolic rates of deep-sea fauna.

PUBLICATION II

The Antarctic lollypop sponge *Stylocordyla borealis* (Lovén, 1868): 1. Morphometrics and reproduction

S. Gatti, T. Brey, N. Teixidó, W. E. Arntz

Alfred-Wegener-Institut für Polar- und Meeresforschung
Columbusstr.
27515 Bremerhaven
Germany
sgatti@awi-bremerhaven.de

Abstract

Parts of the Weddell Sea shelf (Antarctica) are characterized by dense aggregations of the lollypop sponge *Stylocordyla borealis*. Regardless of its distinct appearance and its known importance for recolonisation processes after iceberg scouring *S. borealis* has not yet been the subject of detailed ecological research. Mean abundance of *S. borealis* as documented in this study was 3 ind m^{-2} (SE ± 0.2), densest aggregations were inhabited by 48 ind m^{-2}. We determined basic morphometric relationships and presence or absence of embryos relative to size and mass of individuals. Bodies and stalks showed marked differences in their composition with bodies containing 9.2 % organic matter (% of wet mass) while stalks showed the lowest organic matter content documented for sponges (2.3 % of wet mass). Bodies contained 88.5 % ± 0.8 (mean ± 1SE) of the organic matter of the individual and can thus be assumed to be the metabolically active part, whereas stalks are of structural importance. Of the examined individuals 29% carried macroscopically visible embryos. At present it is not known how the embryos are released from the adult sponge. Based on size frequency distributions we hypothesize that the bodies of some individuals can be completely lost upon release of large numbers of embryos and may be regenerated thereafter.

Introduction

The lollypop sponge *Stylocordyla borealis* (Lovén, 1868) (Demospongiae, Hadromerida) is a very conspicuous member of the Antarctic sponge fauna. From underwater video and photographic studies we know that this species usually occurs in patches of sometimes dense aggregations (Figure II-1) on the shelf of the eastern Weddell Sea (Barthel & Gutt 1992, Gutt et al. 1996). Single individuals of lollypop sponges have been encountered in the Ross Sea near the stations McMurdo and Terra Nova Bay (pers. comm. McClintock). According to Burton (1928) *S. borealis* also occurs throughout the northern and southern Atlantic Ocean. Research on the family Stylocordylidae hitherto comprises histological studies (e. g. Sarà et al. in press), evaluation of its taxonomic status (e. g. Bergquist 1972) and biogeographical descriptions (e. g. Koltun 1976). Ecological data of lollypop sponges and Antarctic sponges in general are scarce. From extensive underwater imaging studies Gutt et al. (1996) concluded that *S. borealis* plays an important role in early recolonisation processes in iceberg scour marks. Despite their abundance and known structural importance on the eastern Weddell Sea shelf we know next to nothing about basic morphometric relationships or life cycle strategies of lollypop sponges. Sarà et al. (in press) recently clarified the reproduction mode of *S. borealis*.
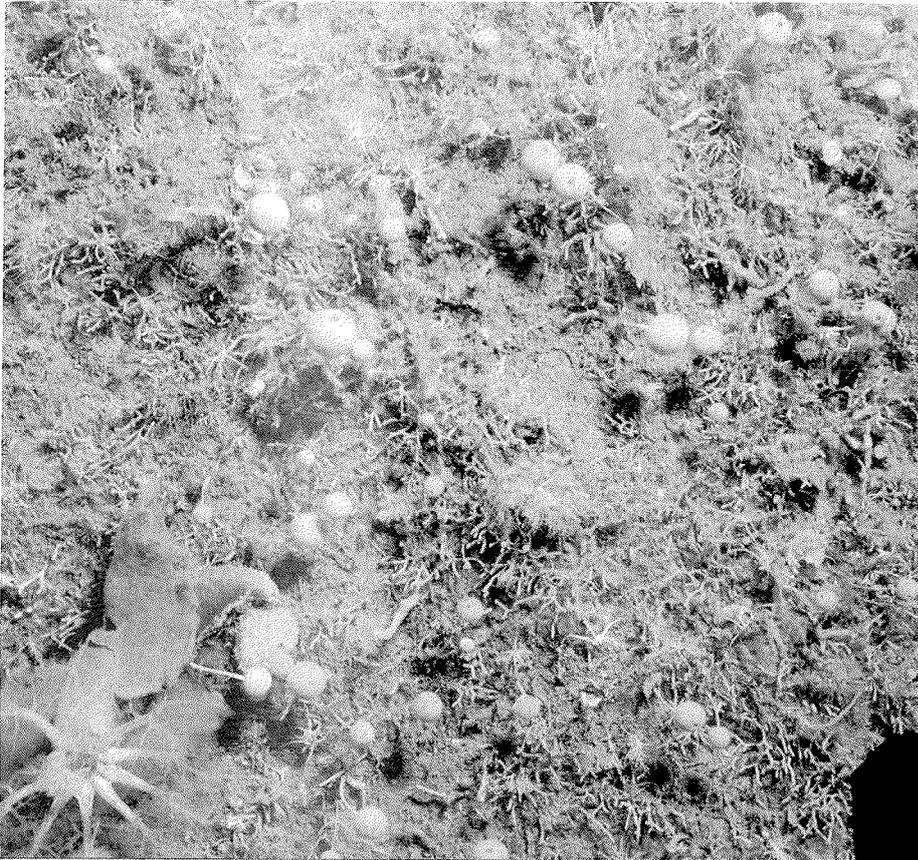
According to their study lollypop sponges reproduce sexually by generating embryos. The authors concluded that embryos fall from the adult sponge and settle in close vicinity of it, as they did not find any larvae. We established basic morphometric relationships, and assessed reproductive effort of individuals of different size. These data will serve as a basis for further modelling of the growth and energy budget of S. borealis (Gatti & Brey subm.).

Materials and methods

Samples were taken in 1998 during RV "Polarstern" cruise ANT XV/3 (EASIZ II) in the eastern Weddell Sea. A complete list of stations, water depths, and deployed gear is given in Arntz & Gutt (1999). To assess abundance of Stylocordyla borealis a 70-mm underwater camera (Photosea 70) was used at 12 stations (depth range: 159 - 279 m) on the continental shelf off Kapp Norvegia. At each station sequences of 80-100 perpendicular colour slides (Kodak Ektachrome 64), each covering approximately $1 m^2$ of the seabed, were taken at evenly spaced time intervals along a transect. The optical resolution was around 0.3 mm. A total of 1131 seafloor photographs was analysed representing an area of 1131 m^2. A detailed description of the camera system is given in Arntz and Gutt (1999). In each picture all specimens of S. borealis were counted and were related to one of the two categories of benthic structure according to Gutt & Starmans (2001): (i) recolonisation stage or (ii) undisturbed scenario.

Conversion factors of different units of mass and volume, as well as relationships between mass of stalk and mass of body were determined from all intact specimens sampled during the entire cruise. One station (PS 48-222) yielded a catch of approximately 400 individuals of S. borealis (120ft bottom trawl, water depth about 250m, trawling distance 931.3m) of which about 180 specimens were in a sufficiently good condition for morphometric examination. These specimens were also used to establish a mass frequency distribution.

Length (L) and diameter (D) measurements taken are illustrated in Figure II-2. Volume (V), wet mass (WM), dry mass (DM) and ash free dry mass (AFDM) were determined following common procedures (e. g. Gatti et al. in press). AFDM was corrected for water loss of spicule mass during ignition (Dayton et al. 1974).

Figure II-1 Stylocordyla borealis. Dense aggregation of individuals on the shelf of the eastern Weddell Sea (station: PS 48-242, depth: ~166m). Photo: Julian Gutt, AWI.

All measurements were recorded for body and stalk separately. The indices 'body', 'stalk', 'tot' indicate that the value refers to body or stalk only or to the complete individual. Indices 'Smax', 'Smin' and 'S10' refer to maximum, minimum of stalk diameter and to stalk diameter 10 cm from the top, respectively (see also Figure II-2).

Inside a number of individuals we found spherical corpuscles of approximately 0.2 - 2 mm diameter which were identified as embryos by Sarà et al. (in press).

D_{body} 35.5
4.5
21.8
0.48
175

Body

$AFDM_{body}$ 2.5
0.0041
0.8
173

L_{body} 39.4
4.5
23.7
175

D_{Smin}
5.2
0.9
2.8
176

$AFDM_{stalk}$ 0.8
0.0002
0.1
167

L_{stalk} 435.0
63.0
157.4
167

Stalk

$AFDM_{tot}$ Max 2.9
Min 0.018
Mean 0.8
N 155

Water
10.0
2.0
4.7
110 D_{S10}

Sediment
17.4
2.2
6.5 D_{Smax}
166
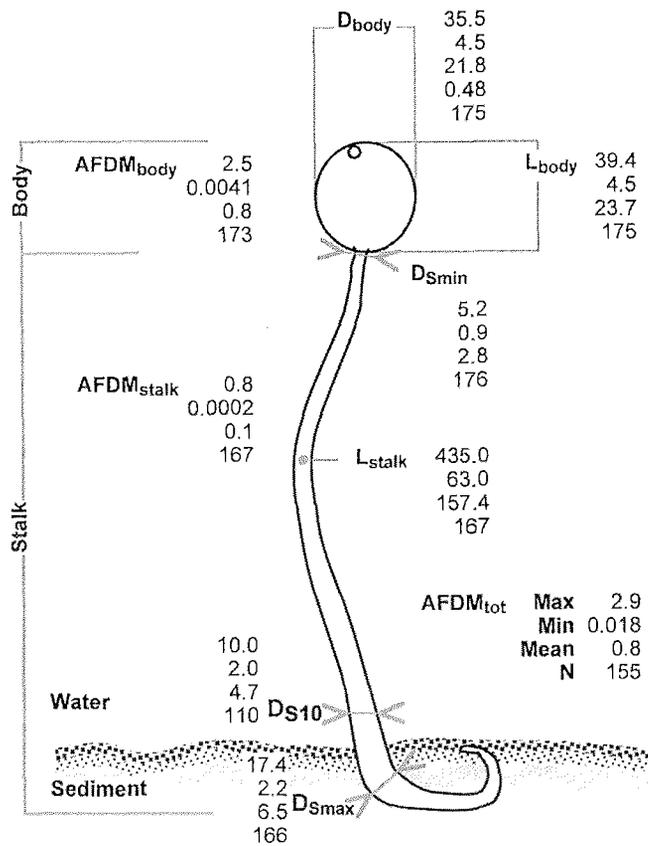
Figure II-2 *Stylocordyla borealis.* Average sized individual schematically drawn to scale. Measurements taken for morphometric analysis: L_{body} = body length (measured along stalk - osculum axis), D_{body} = body diameter (measured at a 90° angle to stalk-osculum axis), L_{stalk} = stalk length, D_{Smin} = stalk minimum diameter (usually directly below the body), D_{S10} stalk diameter 10 cm below the body (if applicable), and D_{Smax} = stalk maximum diameter (usually at a typical 90° sharp bend near basis of stalk). The column of data beside each measurement give maximum, minimum, mean values and number of individuals included in measurements in this order.

Table II-1 *Stylocordyla borealis*. Abundance in the eastern Weddell Sea during "Polarstern" cruise ANT XV/3. Data include mean ± SE, minimum, and maximum number of individuals per photo for each recolonisation stage and station. 'Total sum' refers the specimens counted within the photo sequences (n). Each photo covers an area of approximately 1 m².

Stat #	Area	Position Lat (S)	Long (W)	Depth [m]	Stage	N° photos [n]	Mean ± SE [ind m⁻²]	Min [ind m⁻²]	Max. [ind m⁻²]	Total [ind m⁻²]
73	N/KN	71° 07.2'	011°28.3'	276-278	U	56	1.9 ± 0.2	0	7	104
185	KN	71° 31.7'	014°22.9'	162-160	U	88	4.46 ± 0.4	0	17	393
					P	12	10.2 ± 1.4	6	20	122
					All	100	5.2 ± 0.4	0	20	515
192	KN	71° 13.6'	012°25.4'	253-244	U	31	0	0	0	0
					P	69	0.014 ± 0.01	0	1	1
					All	100	0.01 ± 0.01	0	1	1
200	KN	71° 15.4'	013°08.7'	154-157	U	83	1.6 ± 0.2	0	9	130
215	KN	71° 06.4'	011°31.9'	167-154	U	85	3.1 ± 0.5	0	21	266
					P	7	4.8 ± 2.7	0	21	34
					Scour	8	0	0	0	0
					All	100	3 ± 0.5	0	21	300
221	KN	70° 50.1'	010°35.6'	167-154	U	9	5.4 ± 1.7	0	16	49
					P	91	0.7 ± 0.2	0	9	64
					All	100	1.1 ± 0.3	0	16	133
226	KN	70° 50.4'	010°34.8'	249-259	P	62	1.2 ± 0.37	0	20	74
					Scour	37	0	0	0	0
					All	99	0.74 ± 0.24	0	20	74
229	KN	70° 50.7'	010°30.8'	223-228	U	97	0.04 ± 0.02	0	2	4
232	KN	70° 49.3'	010°29.0'	271-273	U	100	1.7 ± 0.2	0	9	174
239	KN	71° 06.2'	011°31.9'	190-227	U	42	3.2 ± 0.8	0	20	133
					P	55	3.6 ± 0.8	0	36	197
					All	97	3.4 ± 0.5	0	36	330
242	KN	71° 16.2'	012°19.8'	159-158	U	86	19.2 ± 1.4	0	48	1648
					P	13	2.6 ± 0.8	0	8	34
					All	99	17.0 ± 1.38	0	48	1682
278	N/KN	70° 53.4'	010°41.7'	279-273	U	100	0	0	0	0
All Stations						1131	3 ± 0.2	0	48	3427

As embryos could not be separated quantitatively from somatic tissue, counting of exact numbers of embryos per individual was impossible. Abundance of embryos within an individual was noted semi-quantitatively on a three-step scale (none, few, many) and was then correlated with parent size and mass.

Results

Table II-1 shows the abundance of *S. borealis* calculated from 1131 photos belonging to 12 stations. Abundance was highly variable among stations and indicates a patchy distribution pattern. Four photographic transects were selected to illustrate the spatial dispersion of *S. borealis* (Figure II-3).
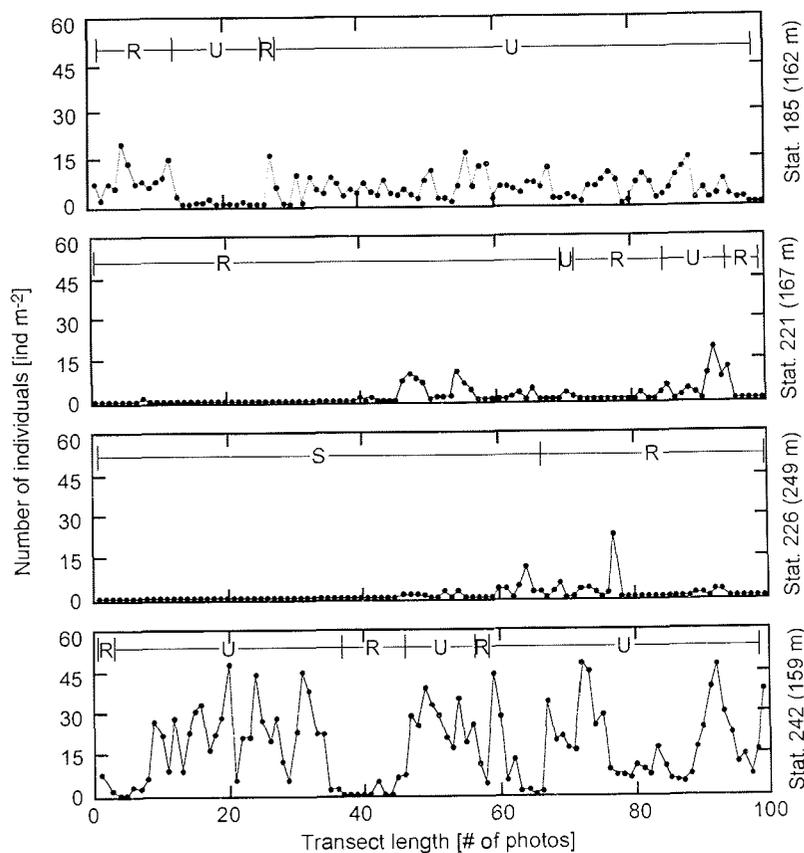
Figure II-3 *Stylocordyla borealis*. Spatial dispersion of along 4 photographic transects in Kapp Norvegia (Weddell Sea). Each point represents one photo analyzed. Different recolonisation stages are indicated by: R recolonisation stage (composed by initial recolonizing sessile species), U undisturbed, mature stage (consisting mainly of sessile suspension feeders), S scour mark (devoid of benthic fauna)

Mean abundance for all the stations was 3 ± 0.2 ind m^{-2} (mean $\pm$ SE). Three stations were characterized by the absence of *S. borealis* (279 photos). Five stations showed intermediate values (from 1.7 ± 0.2 to 5.2 ± 0.4 ind m^{-2}, 453 photos). Station 242 exhibited the highest mean value (17.0 ± 1.38, 99 photos) with a maximum of 48 ind m^{-2}. In undisturbed areas abundance of *S. borealis* was generally higher than within recolonization stages. Comparative abundance of this species revealed differences in densities within small spatial scale and benthic structure.

Most of the mass of an individual was found within the body rather than the stalk. Specifically, body mass was $67.4\% \pm 1.1$ of WM_{tot}, $55.1\% \pm 1.0$ of DM_{tot} and $88.5\% \pm 0.8$ of $AFDM_{tot}$ (all values mean $\pm$ 1 SE). Bodies consisted of $68.6\% \pm 0.62$ water, $21.8\% \pm 0.65$ spicule mass and $9.6\% \pm 0.18$ organic matter. Stalks consisted of $46.1\% \pm 0.63$ water, $51.6\% \pm 1.06$ spicule mass, and $2.3\% \pm 0.07$ organic matter. Maximum, minimum, and mean values of all length parameters and AFDM parameters are given in Figure II-2. Conversions between all mass and volume measurements are summarised in Table II-2.

Table II-2 *Stylocordyla borealis*. Relationship between the different mass and volume measurements given as slope (b) and intercept (a) of linear regression. Units: mass [g], volume [cm^3], length [mm].

X	Y	a	b	r^2
Vol	WM			
Vol_{tot}	WM_{tot}	0.9613	0.9749	0.926
Vol_{stalk}	WM_{stalk}	0.9240	0.7828	0.853
Vol_{body}	WM_{body}	0.9446	0.8675	0.898
Vol	DM			
Vol_{tot}	DM_{tot}	0.3395	0.2139	0.932
Vol_{stalk}	DM_{stalk}	0.4930	0.5633	0.866
Vol_{body}	DM_{body}	0.2616	0.2436	0.873
Vol	AFDM			
Vol_{tot}	$AFDM_{tot}$	0.0813	0.0655	0.932
Vol_{stalk}	$AFDM_{stalk}$	0.0281	0.0100	0.745
Vol_{body}	$AFDM_{body}$	0.1008	0.0942	0.879
WM	DM			
WM_{tot}	DM_{tot}	0.3509	0.3661	0.938
WM_{stalk}	DM_{stalk}	0.4554	0.2818	0.970
WM_{body}	DM_{body}	0.2740	0.2886	0.863
WM	AFDM			
WM_{tot}	$AFDM_{tot}$	0.0737	-0.0081	0.899
WM_{stalk}	$AFDM_{stalk}$	0.0252	-0.0052	0.869
WM_{body}	$AFDM_{body}$	0.1028	-0.0427	0.915
DM	AFDM			
DM_{tot}	$AFDM_{tot}$	0.1897	-0.0010	0.800
DM_{stalk}	$AFDM_{stalk}$	0.0547	-0.0191	0.872
DM_{body}	$AFDM_{body}$	0.3089	0.0077	0.719

Frequency distributions of $AFDM_{tot}$ and L_{tot} (Figure II-4 A and B, respectively) taken from the same set of individuals differed distinctly. No modes are distinguishable in L_{tot} frequency distribution while the $AFDM_{tot}$ distribution seems to comprise 5-6 modes.

Bodies were spherical or near spherical in shape (L_{body}/D_{body} = 1.1 ± 0.01). Some individuals had disproportional small bodies resulting in high L_{stalk}/L_{body} ratios (Figure II-5, circles). There were no disproportional large bodies, which would have caused much smaller L_{stalk}/L_{body} ratios (i. e. far below the regression line).
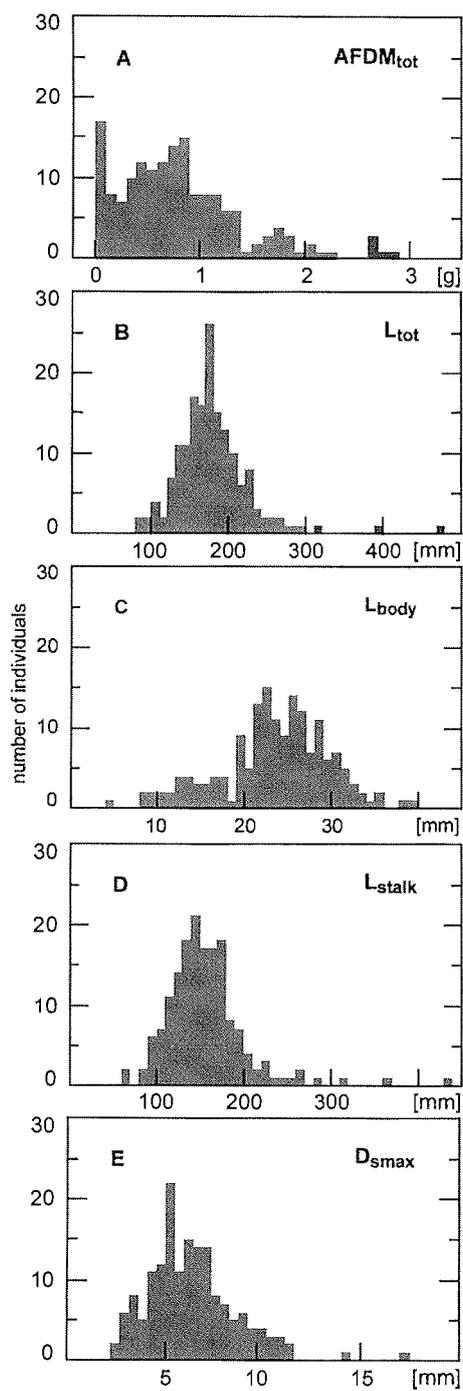
Figure II-4 *Stylocordyla borealis*. Frequency distributions of $AFDM_{tot}$ (A), L_{tot} (B), L_{body} (C), L_{stalk} (D), D_{Smax} (E). While L_{tot}, L_{stalk}, and D_{Smax} show typical distributions skewed to the left with one sharp peak, $AFDM_{tot}$ is much broader and L_{body} suggests division into two groups. Units for x-axes: (A): [g], (B)-(E): [mm].
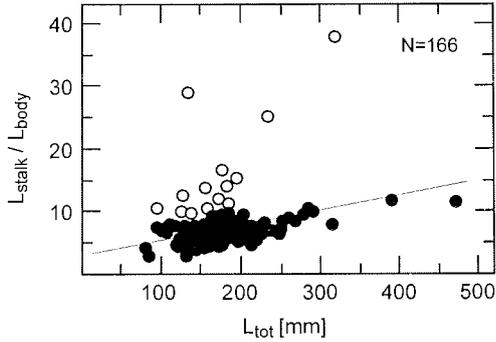
Figure II-5 *Stylocordyla borealis*. Regression plot of L_{stalk}/L_{body} vs. L_{tot}. Dots: typical individuals, circles: individuals with extraordinarily small body (large L_{stalk}/L_{body} ratio).

We found embryos in 29% of the individuals. All embryos were inside the body, none in the stalk of *S. borealis*. Within the body embryos appeared to be evenly distributed. Individuals of $L_{tot} \geq 120$ mm or $AFDM_{tot} \geq 0.2$ g carried embryos (Figure II-6). About half of the embryo carrying individuals had few embryos while the other half carried many embryos.
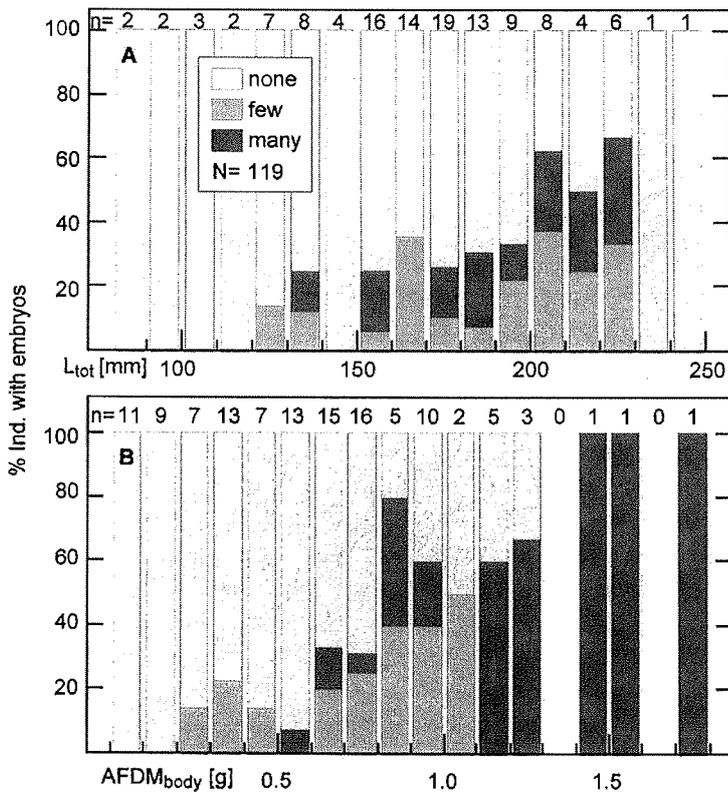
Figure II-6 *Stylocordyla borealis*. Percentage of population carrying embryos. Embryos inside the body were quantified on a three step semi-quantitative scale (none, few, many). For analysis individuals were grouped into L_{tot} classes of 10 mm (A) or $AFDM_{body}$ classes of 0.1 g (B). Numbers on top of each bar refer to number of individuals within the size (or mass) class.

Discussion

Evaluation of the photographic material (Table II-1, Figure II-3) revealed the variable abundance of *Stylocordyla borealis* within a small spatial scale (m^2) in different benthic assemblages over a relative large sampling area (1131 m^2). The low mean abundance of the photographic station 221 (identified mainly as a recolonization stage) contrasted with the bottom trawl at the nearby station 222, where around 400 specimens were found. An explanation of this difference is the patchy distribution of Antarctic fauna. Also other typical pioneer species (the gorgonians *Primnoisis antarctica*, *Primnoella sp.*) occurred in high densities dominated along the transect at station 221. Nevertheless, we can conclude that *S. borealis* is one of the most dominant species in the Kapp Norvegia area. Spatial distribution of Antarctic sponges is influenced by a number of biotic and abiotic factors (e. g. Barthel & Gutt 1992). The influence of reproduction on distribution patterns is discussed below.

Table II-3 Organic content of Antarctic sponges. Minimum value (Min), maximum value (Max), average value (Mean), standard error (SE) for AFDM as % of DM as found by the respective study as well as number of specimens (N) and number of species (Species) included in the study.

Min	Max	Mean	SE	N	Species	Study
13.8	72.0	30.4	3.7	66	16	Dayton et al. 1974
20.4	68.1	38.6	3.1	51	17	McClintock 1987
7.4	60.1	21.9	1.9	403	37	Barthel 1995
3.3	31.3	17.8	0.5	155	1 (total)	this study
0.04	8.4	4.0	0.1	167	1 (stalks)	this study
9.1	49.7	30.5	0.7	173	1 (bodies)	this study

Morphologically individuals of *S. borealis* are clearly divided into two parts: A spherical body on top of an elongated rather thin stalk. Bodies of *S. borealis* showed organic content values typical of Antarctic sponges (30.5 ± 0.7 $AFDM_{body}$ [% DM_{body}]) while stalks showed the lowest organic content values ($AFDM_{stalk}$ 4.0% $\pm$ 0.1 of DM_{stalk}) ever measured for sponges (Table II-3).

For the first time we documented a marked difference in organic content of different morphological parts of one sponge individual. Furthermore, the body contributed the largest portion of an individual (67.4 % of WM_{tot}, 55.1 % of DM_{tot}, 88.5 % of $AFDM_{tot}$). The high spicule content of the stalk (51.6 % of WM_{stalk}), its very low organic content (2.3 % of WM_{stalk}) and its comparatively low water content (46.1 % of WM_{stalk}) cause the stalk to be a rather dense and rigid structure. The body on the other hand consists of only 21.8 % (of WM_{body}) spicules, much more water (68.6 % of WM_{body}) and organic matter (9.6 % of WM_{body}). The body is thus less dense, much more porous and consequently more permeable for water. Such a clear division into morphologically, structurally and compositionally different parts suggests an equally clear division with regards to functional purposes. From the studies of Koehl et al. (2001) and Patterson et al. (1991) we know that nutrient availability, gas exchange and consequently metabolic activity of sessile invertebrates are positively correlated with

water flow speed. Moreover, the steepest gradient in increase of flow velocity is found within the first few centimetres above the bottom (Jumars & Nowell 1984). Principally sessile organisms can utilise various strategies to access more favourable higher layers of water: (1) Organs for prey capture as well as nutrient and gas exchange can be extended into higher water layers. Captured nutrients and exchanged gases need to be actively transported from the capture site down to the metabolically active body part (e. g. Crinoidea). (2) Assimilation can be performed in apical body parts and acquired energy equivalents serve as an energetic reservoir for maintenance of lower body parts (e. g. Sedentaria). In this case transportation of energy equivalents is necessary. And (3) the whole metabolically active part of an individual can be raised into the water column by a 'self-made' carrier which in itself does not cause high energetic costs for building or maintenance (e. g. Pennatulacea). Our results strongly suggest that *Stylocordyla borealis* belongs to the third group. A separation into a structural part (the stalk) lifting the complete metabolically active part of the individual (the body) up into more favourable water layers may even be energetically more efficient than transportation of energy equivalents or food particles. The general scarcity or absence of thinly encrusting sponge species from the Antarctic benthos (Barthel et al. 1997) may be related to the overall low food particle availability (Arntz et al. 1994). A separation into morphologically, structurally and compositionally different parts has hitherto not been documented for sponges and can be considered a special adaptation of a filter feeding organism to general food scarcity in the Antarctic environment.

Sponges, contrary to other metazoans, lack distinct tissues and have often been considered to be simple lumps of cells with little or no co-ordination between cells. This perception of sponges as simple organisms even led to explicit restriction in research (Schupp et al. 1999). While other erect sessile marine organisms were regularly examined for intra-individual gradients of secondary metabolites, sponges were subjected to such research only recently (Becerro et al. 1998). Physiological evidence is accumulating supporting the observed morphological and compositional differences. (1) Becerro et al. (1998) and Schupp et al. (1999) documented a gradient of levels of secondary metabolites within one individual. (2) A marked difference in organic content of stalks and bodies of *S. borealis* was found (this study). (3) Metabolic activity within individuals *S. borealis* differs strongly between stalk and body (Gatti & Brey, subm). (4) Reproduction products were concentrated within certain body parts and were absent from other body parts of *R. topsenti* (Ayling 1980) and for *S. borealis* in this study (see below). These results indicate that sponge biology may be a little more elaborate than has hitherto been assumed.

The smallest individual carrying embryos had a L_{tot} of 123 mm (i.e. 26% of maximum L_{tot}). Larger individuals tended to carry more embryos and also a larger proportion of individuals participated in reproduction (Figure II-6). Fell (1993) reviews that reproduction in sponges starts once a minimum size (or age) is attained. Jamaican

Mycale sp. produce eggs only when specimens have reached a volume of at least 8% of maximum individual volume (Reiswig 1973). *Raspailia topsenti* in northern New Zealand did not reproduce when an individual had less than 5% of maximum number of finger-like protrusions from the base (Ayling 1980). On the other hand do all individuals (i. e. also very small ones) of the Macedonian freshwater sponge *Ochridaspongia rotunda* and the Caribbean *Clathrina* contribute to reproduction (Gilbert & Hadzisce 1977, Johnson 1978, respectively). Also, all but the very small postlarval individuals of *Haliclona loosanoffi* (from the Cape Hatteras region) initiate gametes (Fell 1976). This evidence suggests that reproduction can start very early in the life history of many sponges. However, Witte (1995) found that individuals of *Thenea abyssorum* from the Greenland deep sea started reproducing only at a minimum diameter of 8 mm (i. e. 32% of maximum diameter). *S. borealis* in our study carried at least some embryos when they had reached 26% of maximum L_{tot}. Reproduction in the two studied species of polar sponges thus started comparatively late i. e. at a larger size than in tropical or temperate sponge species. Such a comparatively late onset of reproduction can also be observed in other polar marine invertebrates (e. g. Clarke 1982).

The body part is the sole site of reproduction, as we never found embryos in the stalk part of an individual. It has hitherto been assumed that reproductive products (eggs, sperm, embryos or developing larvae) were distributed evenly in all parts of a sponge individual (Simpson 1984). The only other report of a strict limitation of reproductive products to certain parts of a sponge refers to *Raspailia topsenti* where larvae are found in apical parts only (Ayling 1980). Upper parts of a sponge are usually exposed to a more favourable current regime supplying more food particles (see above). As oogenesis is a particularly energy consuming process (Fell 1983) an alignment of the sites of oogenesis and of enhanced food supply within one individual is plausible. Also, from a larvae, embryos, or gametes point of view it is advantageous to start dispersal from an elevated point utilizing stronger currents rather than starting close to the sediment surface where flow velocity is generally smaller (Jumars & Nowell 1984).

Approximately 8.4 % of the collected individuals carried a disproportional small body (Figure II-5 circles). For the majority of the individuals (91.6 %) $AFDM_{tot}$ depended to more than 82% on $AFDM_{body}$. As $AFDM_{body}$ has such a large influence on $AFDM_{tot}$ the frequency distribution of $AFDM_{tot}$ (Figure II-4A) reflects variations in body mass rather than consecutive age groups as typically caused by subsequent reproductive events. The conclusion that the modes do not represent age classes is substantiated by the fact that comparable modes could not be found in the frequency distributions of L_{tot}, L_{stalk}, or D_{Smax} (Figure II-4B-D).

To explain the presence of disproportional small bodies we propose the following hypothesis: an individual may loose its body and subsequently the body can be regrown on top of the stalk material left after body loss. If indeed only the body would

be affected by a mechanism of loss we would find a 'too small' body on top of a 'too large' stalk during the period of regrowth. Neither L_{stalk} nor D_{Smax} would be affected by such a loss of body and the described difference in frequency distribution plots would be plausible. Reasons for such a body loss could be (1) predation, (2) physical damage or (3) reproductive events. As lollypop sponges often occur in dense aggregations, predation (because of easy access to prey) and physical damage (e. g. iceberg scouring) should affect a larger number of individuals (i. e. more than 8.4 % of the population). To us the most likely explanation for loss of a body is a reproductive event. The body of some of the individuals containing 'many' embryos was densely packed with several hundred embryos and with very little tissue in between. Some of the larger embryos were more than 1.5 mm in diameter. If a large proportion or all of those embryos were released within a short period of time the body would virtually be an empty sphere. Furthermore the body wall would be ruptured several times to release many embryos at once. Release of reproductive products through the dermis has previously been reported for *Hemectyon ferox* (Fell 1983). Additionally, Maldonado & Uriz (1999) report that chances of establishing new populations are enhanced by the dispersal of larger fragments of sponge containing embryos. While according to Sara (pers. com.) and Maldonado and Uriz (1999) embryos alone are limited in their dispersal ability, larger sponge fragments containing embryos can travel rapidly over several kilometres (Maldonado & Uriz 1999). Following that argument, embryos of *S. borealis* could reach open patches some distance away when incorporated in body fragments but would stay within the same patch when released from the body without fragmentation. One body rupturing from its stalk and containing several hundred embryos would be able to initiate a new dense aggregation of lollypop sponges at considerable distance downstream. Even though we were never able to directly observe release of embryos, we hypothesise that occasional massive embryonic release and/or fragmentation from single individuals with subsequent regrowth of body material is the mechanism underlying the observed difference L_{stalk}/L_{body} ratios (Figure II-4). In the extremely fire-resistant and shade intolerant giant sequoia (Stephenson 1992) the simultaneous release of several million seeds (Hickman 1996) is event driven by fires around the tree trunk. At present it is unknown whether release of embryos in *S. borealis* is also event driven by some hitherto unknown mechanism or whether it follows an internal rhythm. A detailed study of genetic variation within and between aggregations of *Stylocordyla borealis* would further our knowledge about dispersal patterns of this species.

The findings of this paper will serve as a basis for a detailed study of metabolic activity of the different parts of *S. borealis*. Based on respiration rates we will model growth rates of this species and assess its contribution to carbon flow patterns on the Antarctic shelf.

PUBLICATION III

The Antarctic lollypop sponge *Stylocordyla borealis* (Lovén, 1868):
2. Energetics and growth rates

S. GATTI, T. BREY

Alfred-Wegener-Institut für Polar- und Meeresforschung
Columbusstr.
27515 Bremerhaven
Germany
sgatti@awi-bremerhaven.de

Abstract

At present it is impossible to assess growth or age of slow-growing Antarctic sponges with traditional methods. We introduce a new approach (AMIGO: Advanced Modelling of Invertebrate Growth from Oxygen consumption data) to model growth and age at size from oxygen consumption data. The model showed good agreement with field and laboratory data of the temperate *Halichondria panicea* except in very young individuals. AMIGO was then applied to estimate growth and age of the lollypop sponge *Stylocordyla borealis*, a known early settler in iceberg scour marks on the Antarctic shelf. Metabolic activity was inferred from mass specific respiration rates and the activity of the electron transport system (ETS) for individuals of 0.03-2.9 g $AFDM_{tot}$. Bodies of *S. borealis* showed a markedly higher ETS activity than did stalk parts. According to our model average sized *S. borealis* ($AFDM_{tot}$ = 0.8 g) were 10 years old while the largest individual ($AFDM_{tot}$ = 7.7 g) was 151 years old. Using data on abundance and size frequency distributions we calculated a P_s/B ratio of 0.106 for *S. borealis* on the eastern Weddell Sea shelf.

Introduction

The lollypop sponge *Stylocordyla borealis* (Lovén, 1868) (Demospongiae, Hadromerida) is a very conspicuous member of the Antarctic sponge fauna occurring in sometimes dense aggregations ($\leq$ 48 ind m^{-2} Gatti et al. subm). In spite of their abundance and their known significance for resettlement processes after iceberg scouring (Gutt 1996, Gutt & Starmans 2001), data about growth rates and population dynamic parameters of lollypop sponges are hitherto lacking. The main reason for this lack of such data on Antarctic sponges in general is the fundamental difficulty of measuring the very slow growth rates directly. Dayton (1979) found that only two sponge species (*Mycale acerata* and *Homaxinella sp.*) were growing comparatively fast. Nine species near McMurdo (Ross Sea, Antarctica), however, showed no measurable increase in size in 10 years. Sponges lack such structures that may serve as 'growth recorders' such as skeleton parts of molluscs, echinoderms or fish (Campana & Neilson 1985, Gage 1990a, b, Rodhouse 1991). Aging by the naturally occurring radionuclide [32]Si is not possible as single sponge spicules contain insufficient activity and larger samples would be a mixture of old and recent spicule material (pers. comm. M. Rutgers van der Loeff, AWI). Carbon content of spicules is too low (<0.2% of spicule mass Schwab & Shore 1971) to facilitate analysis of carbon isotope ratios.

In this study we determined mass specific respiration data and ETS data (activity of the electron transport system) for lollypop sponges and modelled growth rates from those data. Based on our modelling results, we calculated population dynamic

parameters of *S. borealis* and evaluated this species' contribution to energy flow patterns on the eastern Weddell Sea shelf. Our modelling results are the first estimate of growth rates of the Antarctic lollypop sponge and contribute to answering the following questions: (1) Is *S. borealis* only of structural importance for the resettlement process after iceberg scouring or does also play an important role in carbon and silicon cycling on the eastern Weddell Sea shelf? (2) Sponges are presently one of the main targets in the intensified search for bio-active compounds (Müller et al. 2000). Could *S. borealis* support a managed sustainable exploitation if e.g. it was of commercial interest owing to bio-active compounds?

Materials and methods

Study area: Samples were taken within the framework of the EASIZ II program (Ecology of the Antarctic Shelf Ice Zone) in austral summer 1998 during RV "Polarstern" cruise ANT XV/3 to the eastern Weddell Sea. A complete list of stations, water depths, and deployed gear is given in Arntz & Gutt (1999). Experiments (respiration and ETS assays) were performed during ANT XV/3 and XV/4 (Jan. - May 1998). Life maintenance of sponges at 0°C in natural unfiltered seawater was successful for the entire period of five month throughout which sponges appeared to be in a healthy physiological state (visual inspection).

1. Metabolic rate

Respiration rates were determined form decrease of oxygen saturation in an intermittent flow system, using unfiltered seawater. Oxygen saturation data were recorded continuously by oxygen microoptodes and recorded online by a laptop computer. Details of the experimental system are given in Gatti et al. (2002). Microoptodes do not consume oxygen and show hardly any drift at low temperatures (Gatti et al. 2002). They are thus a very suitable tool for measurements of low respiration rates in cold water. Oxygen consumption rates were calculated by

Equation III-1
$$V'_{O_2} = \frac{\dfrac{sat_{t=0} - sat_{t=60}}{100} \times O_{2sat} \times V - O_{2contr}}{M}$$

Where: V'_{O_2} = mass specific oxygen consumption rate [$cm^3\ O_2\ h^{-1}\ g^{-1}$ AFDM], O_{2sat} = oxygen content of seawater saturated with oxygen [$cm^3 O_2\ dm^{-3}$ seawater], $sat_{t=0}$ = oxygen saturation [%] at beginning of experiment, $sat_{t=60}$ = oxygen saturation [%] after 60 minutes as calculated from linear regressions of each cycle, V = true water volume of respiration chamber and tubing [dm^3] (i. e. corrected for animal volume), M = body

mass of animal [g AFDM], O_{2contr} = oxygen consumption attributed to bacteria and microheterotrophs inside experimental chamber, AFDM = ash free dry mass (after 24 hours of igniting at 500°C).

We used individuals of 0.03 g - 2.7 g AFDM in our respiration experiments. Influence of body mass on respiration rates was assessed by weighted least square linear regression (Draper & Smith 1980). Each group of data points (same body mass, different respiration rates) represents repeated measurements of the respiration of one individual. Variance between the repeated measurements is used as a measure of data reliability. Inverted variances are applied as weights to the regression thus assigning more weight to data with less variance. Using this technique we were able to compensate for the bias in data introduced by different quality of measurements. The upper and lower 95% confidence limits for the slope of the weighted regression were calculated according to Sachs (1999).

The activity of the electron transport system (ETS) was determined by the tetrazolium (INT) reduction technique introduced by Packard (1971). ETS data give an estimate of the maximum amount of oxygen that can be processed at the mitochondrial and microsomal membranes of an organism (Lampert 1984). Handling of samples and concentrations of the added chemicals followed the procedures given in Owens & King (1975) with the exception of the quenching solution. Because of its toxicity the quenching solution of Owens & King (50% formalin and 50% 1M H_3PO_4, pH 2.5) was substituted by fuming hydrochloric acid. A set of pilot studies had shown that this chemical stopped the reaction as quickly and completely as the Owens & King (1975) quenching solution. Marked differences in organic content of body and stalk part of an individual (Gatti et al. subm.) motivated determination of ETS activity for body and stalk parts, separately. Samples of approx. 0.2 mg WM were routinely taken from: (1) a quarter section of the stalk (approx. 1 cm long) and (2) the inner tissue of the body (i. e. excluding material from the dermal membrane). Absorbance of the sample and measurement of turbidity control were determined in separate readings as suggested by Packard & Williams (1981). Two abiotic controls (i. e. without sponge tissue) were run in parallel with every set of 10 assays to control for bacterial contamination of the chemicals. To calculate maximum oxygen consumption from ETS data we modified the equation given by Packard & Williams (1981) into

Equation III-2 $$ETS' = \frac{60 \times Q \times H \times (A_{assay} - A_{contr} - A_{turb})}{1.42 \times S \times M_{sample} \times T}$$

where: ETS' = mass specific activity of the electron transport system [$mm^3O_2\ h^{-1}\ g^{-1}AFDM$] or [$mm^3O_2\ h^{-1}\ g^{-1}WM$], H = crude homogenate volume (here: 3 cm^3 + sponge volume [cm^3]), Q = volume of quenched assay (here: 5 cm^3), A_{assay} = assay absorbance at 490nm, A_{contr} = absorbance of abiotic control at 490 nm, A_{turb} =

absorbance of turbidity control at 760 nm, S = volume of supernatant added (here: 1 cm^3), M_{sample} = mass of the sample [g AFDM] or [g WM], and T = incubation time [min].

ETS' data were corrected for differences between incubation temperature and *in situ* temperature following the Arrhenius equation. ETS_{tot} of an individual was calculated with

Equation III-3 $ETS_{tot}=ETS_{stalk}+ETS_{body}=ETS'_{stalk}\times M_{stalk}+ETS'_{body}\times M_{body}$

where: ETS_{tot} = ETS of the whole individual [cm^{3}O$_2$ h^{-1} ind^{-1}], ETS_{stalk} = ETS of the stalk part of an individual [cm^{3}O$_2$ h^{-1} ind^{-1}], ETS_{body} = ETS of the body part of an individual [cm^{3}O$_2$ h^{-1} ind^{-1}], ETS'_{body} = mass specific ETS activity of the body [cm^{3}O$_2$ h^{-1} g^{-1}AFDM] or [cm^{3}O$_2$ h^{-1} g^{-1}WM], ETS'_{stalk} = mass specific ETS activity of the stalk [cm^{3}O$_2$ h^{-1} g^{-1}AFDM] or [cm^{3}O$_2$ h^{-1} g^{-1}WM], M_{body} = mass of the body [g AFDM] or [g WM], and M_{stalk} = mass of the stalk [g AFDM] or [g WM].

2. Modelling

Clarke (1987) formulated the energy budget equation as

Equation III-4 $A=P_s+P_g+\Sigma R+U$

where A = assimilation, P_s = somatic production, P_g = production of gonad tissue, ΣR = sum of all respiratory costs (including basal metabolism, cost of locomotion, and costs of somatic and gonadic reproduction), and U is excretion. The sum of all respiratory costs (ΣR) is an equivalent of oxygen consumption (V_{O2}) and it is not possible to determine its different components by experiment (Clarke 1987). Nevertheless, if reliable measurements of oxygen consumption rates are available, accumulated production can be calculated from such data (Lampert 1984). One problem arises from these considerations: ΣR as well as the ratio $P_s/\Sigma R$ depend on the age and/or size of an individual. From data given by Thomassen & Riisgård (1995) it was possible to relate the $P_s/\Sigma R$ ratio to body mass of a sponge individual (demosponge *Halichondria panicea* from the Baltic Sea). As our knowledge about reproduction patterns of Antarctic sponges in general and *S. borealis* specifically is presently limited (Burton 1928, Gatti et al. subm., Sarà et al. in press), and we do not know how often this species reproduces, we did not explicitly include a term describing reproductive effort into our modelling approach. Neglecting reproduction events leads to an overestimation of somatic growth. Hence all growth rates ($G_t = \delta M \times \delta t^{-1}$, where M is body mass and t is time) derived from our model are maximum growth rate estimates and thus minimum age estimates.

The modelling routine AMIGO (Advanced Modelling of Invertebrate Growth from Oxygen consumption) was written for the software ME10 (Hewlett & Packard: Student

Addition of production from previous time interval to body mass

final body mass reached **?**

YES

End of calculations output of results

NO

Calculation of oxygen consumption per given body mass & time intervall

INPUT
e.g. starting body mass, step-size (time) etc.

Calculation of $P_s/\Sigma R$ ratio for given body mass

Conversion of oxygen consumption to energy equivalent

Conversion of energy equivalent to production (P_s)

Version 7.1). Computations of this study were performed with AMIGO 4.04. The model calculates somatic production from oxygen consumption data. Figure III-1 shows a flow chart of the modelling routine.

Figure III-1 Flow chart of the AMIGO modelling routine. Conversions between units of mass and oxygen consumption follow: C_{org} [mg] = 0.44 × O_2 [cm^3] (Lampert 1984), M_e [kJ] = 45.7 × C_{org} [g] (Salonen et al. 1976), C_{org} [g] = AFDM [g] × 0.5 (Barthel 1986).

Relationship of individual body mass and oxygen consumption was calculated with

Equation III-5 $\log V'_{O2} = a' + b' \times \log M$

where V'_{O2} = mass specific oxygen consumption [cm^{3}O$_2$ g^{-1}AFDM h^{-1}] and M = body mass [g AFDM] as determined in our respiration experiments.

The relationship between body mass and the ratio $P_s/\Sigma R$ was calculated with

Equation III-6 $\dfrac{P_s}{\Sigma R} = a'' + b'' \times \ln M_e$

where: P_s = somatic production, ΣR is oxygen consumption and M_e is the energy equivalent of body mass [kJ]. The boundary value for this function is given as $P_s/\Sigma R = 0$ at $M_e = M_{emax}$, where M_{emax} is defined as the energy equivalent of maximum body mass observed in the field increased by 10% to account for incomplete sampling of the population. To test the model we used oxygen consumption data and the $P_s/\Sigma R$ ratio of *Halichondria panicea* as derived from Thomassen & Riisgård (1995).

For estimation of growth rates of *Stylocordyla borealis* we performed three modelling runs: (1) with oxygen consumption data as described by the weighted least square linear regression, (2) and (3) with oxygen consumption data as described by the upper and lower 95% confidence limit for the estimation of slope of the weighted linear regression line, respectively.

3. Calculation of population energy budget

A von Bertalanffy growth function (VBGF) $M_t=M_\infty (1-e^{-k(t-t0)})^D$, where M_t is the body mass at given time t, M_∞ is the infinite body mass, k and D are constants defining shape of the growth curve, and t_0 is the theoretical age at which $M_t=0$, was fitted iteratively to mass at age data as obtained from the modelling output. Infinite body mass (M_∞) was set equal to M_{max} from the AMIGO model (= 4.38 gC) Using the average assimilation efficiency of 188 herbivorous suspension feeding species (36.3%, SD: 25.9 - 44.2%, Brey unpubl. data compilation) and model output data, we calculated carbon requirements of individual lollypop sponges. Applying a mean body mass of 0.414 gC, carbon requirements were calculated for average and high density patches of *S. borealis* (3.02 ind m^{-2} and 48 ind m^{-2}, respectively, Gatti et al. subm). Annual production to biomass ratio (P_s/B) was then calculated by the mass specific growth rate method (MSGRM) following Brey et al. (1996) and Brey (1999) using the automated spreadsheet computations for mass frequency distributions given in Brey (2001) and the mass frequency distribution for *S. borealis* shown in Figure III-2.
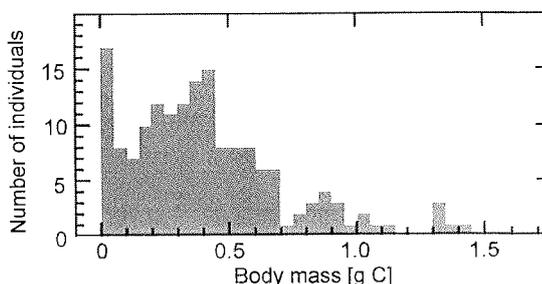
Figure III-2 *Stylocordyla borealis*. Mass frequency distribution (gC) of individuals (N=165) collected at station PS 48-222 during ANT XV/3. Graph is modified from Gatti et al. (subm).

Results

1. Metabolic rate

Relationship between body mass (AFDM) and oxygen consumption rates of *Stylocordyla borealis* is shown in Figure III-3AB. Individual oxygen consumption rate increased exponentially with body mass (Figure III-3A): log V_{O2} = -0.855+0.479×log M (R^2_{adj} = 0.690, N= 70, p≤0.001), whereas mass specific oxygen consumption rate decreased exponentially with increasing body mass (Figure III-3B): log V_{O2} = -0.855-0.521×log M (R^2_{adj} = 0.724, N= 70, p≤0.001).
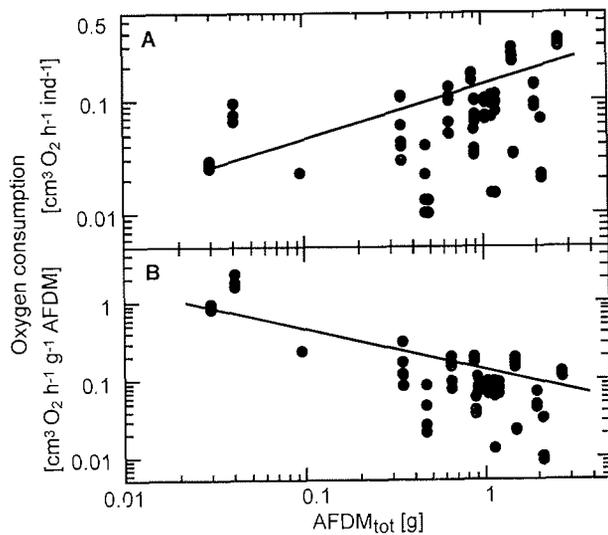
Figure III-3AB *Stylocordyla borealis*. Total individual (A) and mass specific (B) respiration rates. Regressions shown are weighted least square linear regressions: (A): log V_{O2} = -0.855+0.479×log M (R^2_{adj} = 0.690, N= 70, p≤0.001); (B): log V_{O2} = -0.855-0.521×log M (R^2_{adj} = 0.724, N= 70, p≤0.001). For discussion of regression technique see text.

Table III-1 *Stylocordyla borealis*. Comparison of ETS_{body} and ETS_{stalk} in terms of WM and AFDM. N=40 for all analyses; * indicates significantly higher values (p<0.001).

ETS'	$cm^3 h^{-1} g^{-1}$ WM		$cm^3 h^{-1} g^{-1}$ AFDM	
	Mean	SE	Mean	SE
Body	0.202*	0.010	1.965	0.098
Stalk	0.061	0.004	2.900*	0.190

Based on wet mass ETS'_{body} was significantly higher than ETS'_{stalk} (p<0.001), whereas based on AFDM ETS'_{body} was significantly lower than ETS'_{stalk} (p<0.001) (Table III-1). Individual ETS activity increased exponentially with body mass (Figure III-4A) but there was no significant relation between either one of the mass specific ETS' parameters and body mass (Figure III-4B). Oxygen consumption rate to individual ETS activity ratio (V_{O2}/ETS) decreased exponentially with body mass (Figure III-5). It decreased from 0.47 for small sponges (AFDM = 18 mg) to 0.043 for large individuals (AFDM = 2.9 g).

2. Modelling

A test run of our model with *Halichondria panicea* data of Thomassen & Riisgård (1995) showed good agreement between predicted and observed value of body mass (M_t) and growth rate (G_t) at time t (Figure III-6). The fit is almost perfect for M>2.36 g C (age ≥5.6 years), whereas systematic deviations are present in smaller and younger individuals.
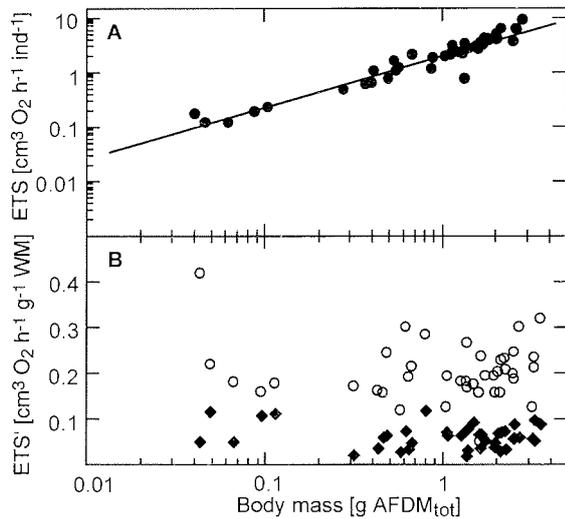
Figure III-4AB *Stylocordyla borealis.* Increasing individual ETS_{tot} activity (A): $\log ETS_{tot} = 0.289 + 0.948 \times \log M$ (N=70, $r^2 = 0.926$) and mass specific ETS' activity (B) separated for body (circles) and stalk (diamonds) parts of an individual showing no trend with increasing body mass.
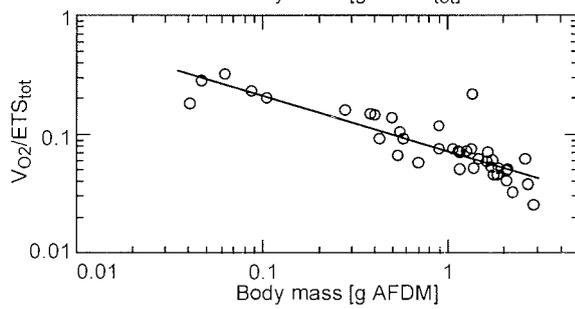
Figure III-5 *Stylocordyla borealis.* Exponentially decreasing ratio V_{O2} over ETS_{tot} activity vs. $AFDM_{tot}$. $\log VO2/ETS_{tot} = -1.143 - 0.469 \times \log AFDM_{tot}$ (n=70, $r^2 = 0.753$).
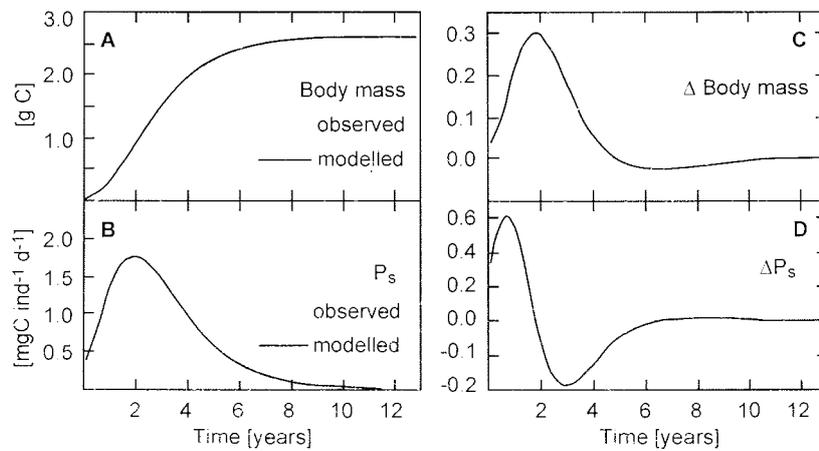
Figure III-6 *Halichondria panicea.* Comparison of model output with observed data for: body mass at time t (A), P_s at time t (B), difference between observed and modelled body mass at time t (C), and difference between observed and modelled P_s values at time t (D) (data points for each curve: N=202). The model was initialized with the following parameters: $\log V'_{O2} = 0.232 - 0.073 \times \log M$, $\log(P_s/\Sigma R) = 0.213 - 0.044 \times \log M_c$, stepsize SS=1 day, and initial body mass iniBM=0.03 gC.

According to the growth curve for *Stylocordyla borealis* as derived from the AMIGO model (Figure III-7) the smallest individual of our experiments ($AFDM_{tot}$ = 0.018 g) was 188 days (95% confidence interval:128-273 days) old, an averaged sized individual ($AFDM_{tot}$ = 0.828 g) was 10.4 (9.3-11.6) years old and the largest individual of this study ($AFDM_{tot}$ = 2.9 g) was 32.9 (32.9-33.2) years old. The largest individual found during ANT XIII/3 in 1996, weighted 7.7 g ($AFDM_{tot}$) corresponding to an age of 152.3 (137.6-169.5) years.
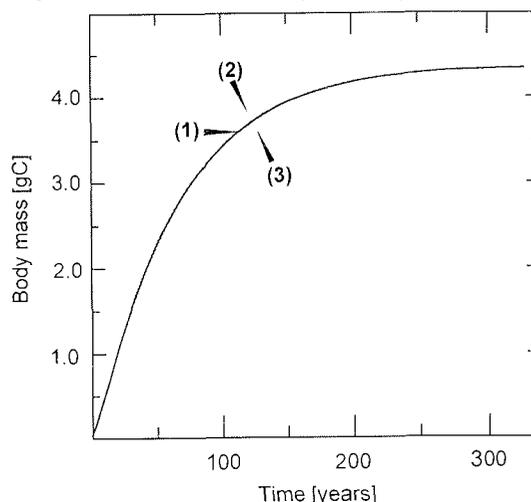
Figure III-7 *Stylocordyla borealis*. Results of model output for weighted linear least square regression (1) (log V_{O2} = -0.855 -0.521 × log M), upper 95% confidence limit of slope of weighted regression (2) (log V_{O2} = -0.855 - 0.444 × log M), lower 95% confidence limit of slope of weighted regression (3) (log V_{O2} =-0.855-0.597×log M). Data points for each curve: N=1201. The model was initialized with log($P_s/\Sigma R$)=0.219-0.041×log M_e, step-size SS=1 day, initial body mass iniBM=0.0001 gC. Parameters of the VBGF for curve (1) are: M_∞= 4.38 gC, k=0.015, D=1.185, t_0=0.0, r^2=1.0.

3. Population energy budget

The parameters of the computed general VBGF are M_∞ = 4.38 gC, k = 0.015, t_0 = 0.0 and D = 1.185. Somatic production of the population shown in Figure III-2 amounted to 0.133 gC y^{-1} m^{-2} in patches of average abundance (3.02 ind m^{-2}, Gatti et al. subm.). All results of the calculations regarding carbon requirements of lollypop sponges are summarized in Table III-2. Mean annual productivity calculated with the MSGRM was P_s/B = 0.106.

Patch	Mean density	Max. density
Abundance (ind m^{-2})	3.02	48
Biomass (gC m^{-2} y^{-1})	1.25	19.9
Consumption (gC m^{-2} y^{-1})	4.46	70.8
Assimilation (gC m^{-2} y^{-1})	1.62	25.7
Production (gC m^{-2} y^{-1})	0.133	2.11
Opal production (gSiO$_2$ m^{-2} y^{-1})	1.19	18.9
Respiration (gC m^{-2} y^{-1})	1.48	23.57

Table III-2 *Stylocordyla borealis*. Energy budget for patches with average and maximum abundance. Calculations are based on model results for weighted linear least square regression of respiration data, mean sponge biomass of 0.414 gC and a mean assimilation efficiency of 36.3% (see text for reference)

Discussion

1. Metabolic rate

Oxygen consumption rates of *Stylocordyla borealis* are low when compared with tropical or boreal invertebrates but within the range of oxygen consumption rates known for Antarctic invertebrates (Figure III-8).

During the respiration experiments we had to use unfiltered seawater as the sponges had tightly closed oscula when exposed to filtered seawater (Gatti et al. 2002). We conclude that sponges were feeding during our experiments and, since we were not able to measure true resting metabolism (i. e. that of fasting individuals) which should be somewhat lower than our data. Ideally the oxygen consumption

Figure III-8 Comparison of invertebrate oxygen consumption data worldwide. Data shown are residuals of the regression of mass specific oxygen consumption data vs. body mass. Grey dots: 19834 data points, 771 invertebrate species including 13 sponge species (unpublished data compilation T. Brey); black dots, oxygen consumption of *S. borealis* (N=70 data points).

measurements used for our AMIGO model should include year-round measurements. By measuring summer-metabolism only we possibly overestimate the annual oxygen consumption.

Our study is the first to determine ETS activities of a sponge species. Our results are in general agreement with data from other taxa (e.g. Båmstedt 1980). However, we found ETS'_{body} $g^{-1}WM$ > ETS'_{stalk} $g^{-1}WM$ (Figure III-4B) whereas ETS'_{body} $g^{-1}AFDM$ < ETS'_{stalk} $g^{-1}AFDM$ (Table III-1). Stalks contained very little organic matter (2.3±0.7% of WM_{stalk}, mean ± SE) and a rather large proportion of spicules (51.6±1.1% of WM_{stalk}) (Gatti et al. subm.). The higher ETS'_{stalk} activity per gram AFDM indicates that the few living cells of a stalk are potentially metabolically very active (pers comm. Packard). As spicule synthesis is an energy consuming process (Simpson 1984, Jones & Pearson 1990, Frøhlich & Barthel 1997) a high level of ETS activity in spicule making stalk-cells is necessary, particularly as only a small number of cells participate in the process.

ETS$_{tot}$ increased linearly with body mass (Figure III-4A), whereas V$_{O2}$ increased exponentially but with an exponent < 1 (Figure III-3A). Thus the ratio V$_{O2}$/ETS$_{tot}$ decreased with increasing body mass (Figure III-5). From this regression we can calculate a theoretical minimum body mass of AFDM$_{tot}$ = 3.62 mg at which V$_{O2}$/ETS$_{tot}$ = 1. For smaller individuals oxygen consumption rates would exceed ETS$_{tot}$ values, which is theoretically impossible. The smallest individual Gatti et al. (subm.) found had an AFDM$_{tot}$ of 18 mg. Body length of that individual [~2mm] was comparable to the biggest embryos that were found in the specimens (Gatti et al. subm). Thus it is very likely that body mass even of the smallest free-living lollypop sponge is well above the theoretical minimum of 3.62 g AFDM.

In the sponge *Stylocordyla borealis* V$_{O2}$/ETS$_{tot}$ declined exponentially with increasing body mass (Figure III-5). This observation is contradictory to results of Madon et al. (1998) and Ikeda (1989). Both found constant V$_{O2}$/ETS ratio spanning body masses of several orders of magnitude (Madon et al.: 0.06-0.07 for zebra mussels, Ikeda: 0.62 - 0.71 for different species of myctophid fish). The highest ratio (0.47) we measured in young *S. borealis* may indicate that these juveniles may be somewhat overexploiting their electron transport system, almost reaching ratios documented for fish. This may be one reason for the rapid growth of juvenile lollypop sponges (Figure III-7), which is typical for early colonizers.

2. Modelling

Growth rates of most Antarctic sponges are too slow to be measured directly (Dayton 1979). Hitherto inferring growth rate from metabolic rate seems to be the only feasible approach to growth of Antarctic sponges. Empirical data about the P$_s$/ΣR ratio are summarized in Humphreys (1979) and in Banse & Mosher (1980). These data collections comprise a wide variety of invertebrate species (marine and terrestrial) but do not include any sponge species. The discussion of fundamental differences between sponges and other invertebrates regarding their metabolism (Thomassen & Riisgård 1995) makes the use of existing empirical data problematical. Consequently, we based our model on findings of the latter paper. Nevertheless our model based on oxygen consumption data provokes some problems. As stated before, our respiration data are likely to overestimate true resting metabolism as well as annual oxygen consumption rate. Together these overestimations lead to a possible overestimation of growth rates thus making our age-at-size data somewhat conservative.

The trial run with *Halichondria panicea* data (Figure III-6) indicates that the fit of our model is less than ideal regarding the smaller individuals. Hence our model results for young *Stylocordyla borealis* are also likely to be biased to some extend. Initial trial runs with different P$_s$/ΣR fittings had shown that there is a trade-off between bias in results for small individuals on one hand and bias in results for large individuals on the

other hand. For our purposes of assessing the sponges' contribution to carbon and silicon cycling in the eastern Weddell Sea we used model settings providing the better fit in older and larger individuals.

3. Population energy budget

Based on our findings we can estimate components of the energy budget: C = P + R + E, where C is consumption, P is production, R is respiration and E is excretion (Table 2). Carbon requirements of *Stylocordyla borealis* were calculated with 4.5 gC m^{-2} y^{-1} and 71.5 gC m^{-2} y^{-1} for patches with average and maximum abundance, respectively. These calculations need to be interpreted in the light of two aspects: Firstly, at present our knowledge about feeding strategies of Antarctic sponges is less than fragmentary. Secondly, also our knowledge about the dynamics heterotrophic pico- and nanoplankton of the food web is limited.

On the basis of initial feeding experiments (Orejas, unpubl. data) it can be hypothezised that *S. borealis* may be feeding year round on microheterotrophs and nanoflagellats - the smaller planktonic fraction. Carbon from this fraction of the plankton is available in Antarctic waters throughout the whole year, albeit at lower levels when compared with microplankton summer blooms (Kang et al. 1997). Direct and indirect evidence points toward the utilization of this fraction by some filter-feeding taxa, such as cnidarians on the eastern Weddell Sea shelf (Orejas 2001) and the bryozoan *Arachnopusia inchoata* at Signy Island (Barnes & Clarke 1995). Additionally, sponges have been observed to take up dissolved nutrients in other latitudes (Reiswig 1981, Pile et al. 1996, Ribes et al. 1999). Primary production (PP) in Antarctic waters ranges from 16-100 gC m^{-2} y^{-1} (Grebmeier & Barry 1991). On the eastern Weddell Sea shelf PP in summer 1983 was 674 mgC m^{-2} d^{-1} (v. Bröckel 1985) corresponding to 81 gC m^{-2} y^{-1} (120 d y^{-1} of PP). Even though *S. borealis* does most probably not utilize PP directly, the above PP-figures indicate that carbon flow towards the heterotrophic planktonic food web and subsequently to the benthos is principally sufficient for *S. borealis'* requirements. This conclusion is also correct for patches of densest aggregations (48 ind m^{-2}), as hardly any other species can be found inside such dense patches of *S. borealis*.

Annual production of the *Stylocordyla borealis* population shown in our mass frequency distribution (Figure III-2) with a mean abundance of 3.02 ind m^{-2} (Gatti et al. subm.) amounts to 0.133 gC m^{-2} y^{-1}. This value is in the same order of magnitude as that of seastars near McMurdo Station (e.g. *Acodontaster conspicuus*: 0.187 gC m^{-2} y^{-1}, *Odontaster validus* 0.104 gC m^{-2} y^{-1}, Dayton et al. 1974), but distinctly lower than that of the pectinid *Adamussium colbecki* near McMurdo Sound (5.0-6.5 gC m^{-2} y^{-1}, Stockton 1984, Berkman 1990).

Lollypop sponges showed low annual P_s/B values (~0.106 y^{-1}) albeit not as low as was expected prior to this study (P_{tot}/B=0.03, Jarre-Teichmann et al. 1997). Our results are in the same range as those for the bivalve *Yoldia eightsi* at Signy Island: 0.117 (Rabarts 1970 fidem Brey & Clarke 1993), the seastars at McMurdo Station: *Odontaster validus*: 0.036 - 0.045 (Dayton et al. 1974, McClintock et al. 1988) and *Acodontaster conspicuus*: 0.069 (Dayton et al. 1974) and the sea urchin *Sterechinus antarcticus* on the Southern Weddell Sea shelf: 0.065 (Brey1991) (all data compiled in Brey & Clarke 1993). Lollypop sponges are thus most likely not contributing substantially to carbon flow patterns on the eastern Weddell Sea shelf. Somatic production of 0.133 gC m^{-2} y^{-1} corresponds to a deposition of 1.19 g m^{-2} y^{-1} of opal (biogenic SiO_2) in the form of spicules within the lollypop sponges (Gatti et al., subm.). Opal from PP that reaches the sea floor has not yet been determined with certainty for the eastern Weddell Sea shelf (Ragueneau et al. 2000). In the seasonal ice zone of the Weddell Sea it amounts to few mg SiO_2 m^{-2} y^{-1} (Tréguer & Jacques 1992). Compared with these existing figures it can be concluded, that lollypop sponges can locally be the predominant pathway of silicate to opal. Sponge spicules of Antarctic sponges may not dissolve *in situ* (Kabir 1996) and the accumulated spicule mass is deposited in the sediment after the death of the individual creating spicule mats up to 1.5 m thick (Koltun 1970, Barthel 1992). Spicule depositions can be up to 9000 years old (Conway et al. 1991), indicating that once opal is deposited in the form of sponge spicules it leaves biological cycling in the ocean.

Interest in population dynamic parameters of sponges has hitherto been limited, as sponges rarely contribute substantially to benthic biomass and have not, apart from bath sponge species (e. g. *Hippospongia lachne*), been used commercially. Thus production and productivity data for sponges are scarce. Hitherto commercial exploitation of Antarctic sponges has not been a topic of any interest. However, the intense search for bio-active compounds has also reached Antarctic waters. Based on the rather low annual estimates of P_s/B ratio (0.106) the low standing stock (1.3 gC m^{-2} y^{-1}) of *S. borealis* we conclude that there is an extremely low potential for extra mortality and commercial exploitation of this sponge species would be ecologically and economically unsustainable.

Conclusions

Stylocordyla borealis is a slow-growing Antarctic sponge reaching a maximum age of 150 years. Production and growth rates of this species as calculated by our model are possible on the basis of the known carbon input to the benthic system. From the low annual P_s/B ratio (0.106) and production (0.133 gC m^{-2} y^{-1}) we must conclude, that *S. borealis* does not contribute substantially to carbon flow on the Antarctic shelf. Nevertheless it is an important mediator in permanent burial of opal.

Based on AMIGO this is the first estimate of growth rates of a slow-growing sponge species. AMIGO is a valuable tool in assessing growth rates and age of species which can otherwise not be dated. In ongoing studies we will establish growth rates also for the large hexactinellid sponge species which characterize undisturbed areas on the Antarctic shelf.

Acknowledgements

6 References

Ahn I-Y & Shim JH (1998) Summer metabolism of the Antarctic clam, *Laternula elliptica* (King & Broderip) in Maxwell Bay, King George Island and its implications. J Exp Mar Biol Ecol 224:253-264

Arntz WE & Gutt J (1999) The expedition ANTARKTIS XV/3 (EASIZ II) of "Polarstern" in 1998. Ber Polarforsch 301:1-229

Arntz WE, Brey T & Gallardo VA (1994) Antarctic zoobenthos. Oceangr Mar Biol Ann Rev 32:241-304

Atkinson D & Sibly RM (1997) Why are organisms usually bigger in colder environments? Making sense of a life history puzzle. TREE 12:235-239

Ayling AL (1980) Patterns of sexuality, asexual reproduction and recruitment in some subtidal marine Demospongiae. Biol Bull 158(3):271-282

Ayling AL (1983) Growth and regeneration rates in thinly encrusting Demospongiae from temperate waters. Biol Bull 165:343-352

Baker BJ, Yoshida WY & McClintock JB (1994) Chemical constituents of four Antarctic sponges in McMurdo Sound, Antarctica. Antarct J US 29(5):153-155

Banse K & Mosher S (1980) Adult body mass and annual production/biomass relationship of field populations. Ecol Monogr 50(3):355-379

Barnes DKA & Clarke A (1995) Seasonality of feeding activity in Antarctic suspension feeders. Polar Biol 15:335-340

Barthel D (1986) On the ecophysiology of the sponge *Halichondria panicea* in Kiel Bight. I. substrate specificity, growth and reproduction. Mar Ecol Prog Ser 32:291-298

Barthel D (1992) Do hexactinellids structure Antarctic sponge associations? Ophelia 36(2):111-118

Barthel D (1995) Tissue composition of sponges from the Weddell Sea, Antarctica: not much meat on the bones. Mar Ecol Prog Ser 123:149-153

Barthel D (1997) Fish eggs and pentacrinoids in Weddell Sea hexactinellids. Polar Biol 17(1):91-94

Barthel D & Gutt J (1992) Sponge associations in the eastern Weddell Sea. Antarct Sci 4(2):137-150

Barthel D & Tendal OS (1994) Synopses of the Antarctic Benthos, Vol 6: Antarctic Hexactinellida. Koeltz Scientific books, Königsstein

Barthel D, Tendal OS & Panzer K (1990) Ecology and taxonomy of sponges in the eastern Weddell Sea shelf and slope communities. Ber Polarforsch 68:120-130

Barthel D, Gutt J & Tendal OS (1991) New information on the biology of Antarctic deep-water sponges derived from underwater photography. Mar Ecol Prog Ser 69:303-307

Barthel D, Tendal OS, Gatti S (1997) The sponge fauna of the Weddell Sea and its integration in benthic processes In: WE Arntz & J Gutt (ed.) The Expedition ANTARKTIS XIII/3 (EASIZ I) of "Polarstern" to the eastern Weddell Sea in 1996. Ber Polarforsch (249), Bremerhaven, pp 44-52

Baumgärtl H, Lübbers DW (1983) Microcoaxial needle sensor for polarographic measurement of local O_2 pressure in the cellular range of living tissue. Its construction and properties In: Gnaiger, E & Forstner, H (ed) Polarographic oxygen sensors: Aquatic and physiological applications. Springer, Berlin, pp 37-65

Bavestrello G, Cattaneo-Vietti R, Cerrano C & Sarà M (1996) Spicule dissolution in living *Tethya omanensis* (Porifera: Demospongiae) from a tropical cave. Bull Mar Sci 258(2):598-601

Becerro MA, Paul VJ & Starmer J (1998) Intracolonial variation in chemical defenses of the sponge *Cacospongia sp.* and its consequences on generalist fish predators and the specialist nudibranch predator *Glossodoris pallida*. Mar Ecol Prog Ser 168:187-196

Beliaev GM & Ushakov PV (1957) Certain regularities in the quantitative distribution of the bottom fauna in Antarctic waters. Am Inst Biol Sci 112:116-119

Benson BB, Krause D Jr (1984) The concentration and isotopic fractionation of oxygen dissolved in freshwater and seawater in equilibrium with the atmosphere. Limnol Oceanogr 29:620-362

Bergquist DC, Williams FM & Fisher CR (2000) Longevity record for deep-sea invertebrate. Nature 403:499-500

Bergquist PR (1972) Deep water Demospongiae from New Zealand. Micronesica 8(1-2):125-136

Bluhm BA & Brey T (2001) Age determination in the Antarctic shrimp *Notocrangon antarcticus* (Crustacea: Decapoda), using the autofluorescent pigment lipofuscin. Mar Biol 138:247-257

Bluhm BA, Piepenburg D & Juterzenka von K (1998) Distribution, standing stock, growth, mortality and production of *Strongylocentrotus pallidus* (Echinodermata: Echinoidea) in the northern Barents Sea. Polar Biol 20:325-334

Bluhm BA, Brey T & Klages M (2001) The autofluorescent age pigment lipofuscin: key to age, growth and productivity of the Antarctic amphipod *Waldeckia obesa* (Chevreux, 1905). J Exp Mar Biol Ecol 258:215-235

Brey T (1991) Population dynamics of *Sterechinus antarcticus* (Echinodermata: Echinoidea) on the Weddell Sea shelf and slope, Antarctica. Antarct Sci 3:251-256

Brey T (1999) Growth performance and mortality in aquatic macrobenthic invertebrates. Adv Mar Biol 35:153-243

Brey T (2001) Population Dynamics in Benthic Invertebrates. A Virtual Handbook. Version 01.2. Alfred Wegener Institute for Polar & Marine Research, Germany, http://www.awi-bremerhaven.de/Benthic/Ecosystem/Food Web/Handbook/main.html

Brey T & Clarke A (1993) Population dynamics of marine benthic invertebrates in Antarctic and subantarctic environments: are there unique adaptations? Antarct Sci 5(3):253-266

Brey T & Gerdes D (1997) Is Antarctic benthic biomass really higher than elsewhere? Antarct Sci 9(3):266-267

Brey T & Gerdes D (1998) High Antarctic macrobenthic community production. J Exp Mar Biol Ecol 231:191-200

Brey T, Pearse JS, Basch L & McClintock JB (1995a) Growth and production of *Sterechinus neumayeri* (Echinoidea: Echinodermata) in McMurdo Sound, Antarctica. Mar Biol 124:279-292

Brey T, Peck LS, Gutt J, Hain S & Arntz WE (1995b) Population dynamics of *Magellania fragilis*, a brachiopod dominating a mixed-bottom macrobenthic assemblage on the Antarctic shelf. J Mar Biol Ass UK 75(4):857-869

Brey T, Jarre-Teichmann A & Borlich O (1996) Artificial neural network versus multiple linear regression: predicting P/B ratios from empirical data. Mar Ecol Prog Ser 140:251-256

Bröckel von K (1985) Primary production data from the South-Eastern Weddell Sea. Polar Biol 4:75-80

Brockington S (2001) The seasonal energetics of the Antarctic bivalve *Laternula elliptica* (King and Broderip) at Rothera Point, Adelaide Island. Polar Biol 24:523-530

Brockington S & Clarke A (2001) The relative influence of temperature and food on the metabolism of a marine invertebrate. J Exp Mar Biol Ecol 258:87-99

Brockington S, Peck LS (2001) Seasonality of respiration and ammonium excretion in the Antarctic echinoid *Sterechinus neumayeri*. Mar Ecol Prog Ser 219:159-168

Brockington S, Clarke A & Chapman ALG (2001) Seasonality of feeding and nutritional status during the austral winter in the Antarctic sea urchin *Sterechinus neumayeri*. Mar Biol 139(1):127-138

Bryan JR, Riley JP, Williams PJL (1976) A Winkler procedure for making precise measurements of oxygen concentrations for productivity and related studies. J Exp Mar Biol Ecol 21:191-197

Burton M (1928) A comparative study of the characteristics of shallow-water and deep-sea sponges, with notes on their external form and reproduction. J Quekett Microsc Club 16:49-70

Campana SE & Neilson JD (1985) Microstructure of fish otoliths. Can J Fish Aquat Sci 42:1014-1032

Chapelle G, Peck LS (1995) The influence of acclimation and substratum on the metabolism of the Antarctic amphipods *Waldeckia obesa* (Chevreux 1905) and *Bovallia gigantea* (Pfeffer 1808). Polar Biol 15:225-232

Chapelle G & Peck LS (1999) Polar gigantism dictated by oxygen availability. Nature 399:114-115

Chapelle G, Peck LS, Clarke A (1994) Effects of feeding and starvation on the metabolic rate of necrophagous Antarctic amphipod *Waldeckia obesa* (Chevreux, 1905). J Exp Mar Biol Ecol 183:63-76

Clark LC Jr (1956) Monitor and control of blood and tissue oxygen tensions. Trans Am Soc Artificial Internal Organs 2:41-46

Clarke A (1982) Temperature and embryonic development in polar marine invertebrates. Int J Invertebr Reprod 5(2):71-82

Clarke A (1983) Life in cold water: the physiological ecology of polar marine ectotherms. Oceangr Mar Biol Ann Rev 21:341-453

Clarke A (1985) Food webs and interactions: an overview of the Antarctic ecosystem In: Bonner, W.N., Walton, D.W.H. (ed.) Key Environments: Antarctica. Pergamon Press, Oxford, pp 329-350

Clarke A (1987) Temperature, latitude and reproductive effort. Mar Ecol Prog Ser 38:89-99

Clarke A (1988) Seasonality in the Antarctic marine environment. Comp Biochem Physiol B 90(3):461-473

Clausen HB (1973) Dating of polar ice by ^{32}Si. J Glaciol 12(66):411-417

Coma R, Ribes M, Gili J-M & Zabala M (2002) Seasonality of in situ respiration rate in three temperate benthic suspension feeders. Limnol Oceanogr 47(1):324-331

Comiso JC & Gordon AL (1998) Interannual variability in summer sea ice minimum, coastal polynyas, and bottom water formation in the Weddell Sea In: Jeffries, M. O. (ed.) Antarctic Sea Ice: Physical Processes, Interactions and Variability (Antarc. Res. Ser. 74). AGU, pp 293-315

Conway KW, Barrie JV, Austin WC & Luternauer JL (1991) Holocene sponge bioherms on the western Canadian continental shelf. Cont Shelf Res 11(8-10):771-790

Cooper-Driver, GA (1994) *Welwitschia mirabilis*: a dream come true. Arnoldia 54(2): 2-10

Culberson CH (1991) Dissolved oxygen. WOCE Operations manual 3 (Section 3.1 Hydrographic Programme): Woods Hole, Mass. ,USA http://whpo.ucsd.edu/manuals.htm

Dahm C (1996) Ökologie und Populationsdynamik antarktischer Ophiuriden (Echinodermata). Ber Polarforsch 194:1-289

Dayton PK (1979) Observations on growth, dispersal and population dynamics of some sponges in McMurdo Sound, Antarctica In: Levi, C., Boury-Esnault, N. (ed.) Biologie des Spongiaires. Colloq. Internat. C.N.R.S. Paris, pp 271-282

Dayton PK, Robilliard GA, Paine RT (1970) Benthic faunal zonation as a result of anchor ice at McMurdo Sound, Antarctica In: Holdgate, M. (ed.) Antarctic Ecology Vol.1. Academic Press, London, pp 244-258

Dayton PK, Robilliard GA, Paine RT & Dayton LB (1974) Biological accommodation in the benthic community at McMurdo Sound, Antarctica. Ecol Monogr 44(1):105-128

Dearborn JH, Hendler G & Edwards KC (1996) The diet of *Ophiosparte gigas* (Echinodermata: Ophiuroidea) along the Antarctic Peninsula, with comments on its taxonomic status. Polar Biol 16(5): 309-320

DeMaster DJ (1980) The half-life of ^{32}Si determined from a varved Gulf of California sediment core. Earth Planet Sci Lett 48:209-217

Dickson (1996) Determination of dissolved oxygen in seawater by Winkler titration. WOCE Operations manual 3 (Section 3.1 Hydrographic Programme): Woods Hole, Mass., USA
http://whpo.ucsd.edu/manuals.htm

Draper NR, Smith H (1980) Applied Regression Analysis. John Wiley and Sons, New York

Druffel ERM, Griffin S, Witter A, Nelson E, Southon J, Kashgarian M & Vogel J (1995) Gerardia: Bristlecone pine of the deep-sea? Geochim Cosmochim Acta 59(23):5021-5036

Engelmann MD (1966) Energetics, terrestrial field studies and animal productivity. Adv Ecol Res 3:73-115

Fahrbach E, Rohardt G & Krause G (1992) The Antarctic coastal current in the southwestern Weddell Sea. Polar Biol 12:171-182

Fahrbach E, Frenzel M, Harms S, Härter Fetter A, Iaremchouck A, Langredder J, Loske S, Meissner K, Casanovas CM, Monsees M, Pereira A, Rohardt G, Schröter M, Wisotzki A, Witte H (1999) Deep and bottom water formation in the Weddell Sea In: Eberhard Fahrbach (ed.) The Expedition ANTARKTIS XV/4 of the Research Vessel "Polarstern" in 1998. Ber Polarforsch, pp 69-74

Faure G (1986) Cosmogenic radionuclides (Chapter 23) Principles of isotope geology. John Wiley & Sons, New York, pp 405-426

Fell PE (1976) The reproduction of *Haliclona loosanoffi* and its apparent relationship to water temperature. Biol Bull 150:200-210

Fell PE (1983) Porifera In: K. G. Adiyodi & R. G. Adiyodi (ed.) Reproductive Biology of Invertebrates (Vol. 1 Oogenesis, Oviposition and Oosorption). John Wiley & Sons Ltd., Bath, pp 1-29

Fell PE (1993) Porifera In: K. G. Adiyodi & R. G. Adiyodi (ed.) Reproductive Biology of Invertebrates (Vol. 6 Asexual Propagation and Reproductive Strategies). John Wiley & Sons Ltd., Bath, pp 1-44

Fisher CR, Urcuyo IA, Simpkins MA & Nix E (1997) Life in the slow lane: Growth and longevity of cold-seep vestimentiferans. Mar Ecol 18(1):83-94

Fleischer RL & Price PB (1964) Glass dating by fission fragment tracks. J Geophys Res 69(2):331-339

Frøhlich H & Barthel D (1997) Silica uptake of the marine sponge *Halichondria panicea* in Kiel Bight. Mar Biol 128(1):115-125

Gage JD (1990a) Skeletal growth markers in the deep-sea brittle stars *Ophiura ljungmani* and *Ophiomusium lymani*. Mar Biol 104:427-435

Gage JD (1990b) Skeletal growth bands in brittle stars: microstructure and significance as age markers. J Mar Biol Ass UK 70:209-224

Gage JD (1991) Skeletal growth zones as age-markers in the sea urchin *Psammechinus miliaris*. Mar Biol 110:217-228

Gatti S & Brey T (subm) The Antarctic lollypop sponge *Stylocordyla borealis* (Lovén, 1868): 2. Energetics and growth. Mar Ecol Prog Ser

Gatti S, Brey T, Müller WEG, Heilmayer O & Holst G (2002) Oxygen microoptodes: a new tool for oxygen measurements in aquatic animal ecology. Mar Biol 140(6): 1075-1085:

Gatti S, Brey T, Teixido N & Arntz WE (subm) The Antarctic lollypop sponge Stylocordyla borealis (Lovén, 1868): 1. Morphometrics and reproduction. Mar Ecol Prog Ser

Gerdes D, Klages M, Arntz WE, Herman RL, Galéron J & Hain S (1992) Quantitative investigations on macrobenthos communities of the southeastern Weddell Sea shelf based on multibox corer samples. Polar Biol 12:291-301

Gerdes D, Hilbig B & Montiel A (in press) Impact of iceberg scouring on benthic communities in the high Antarctic Weddell Sea. Polar Biol

Gilbert JJ & Hadzisce S (1977) Life cycle of the freshwater sponge *Ochridaspongia rotunda* Arndt. Arch Hydrobiol 79(3):285-318

Glud RN, Klimant I, Holst G, Kohls O, Meyer V, Kühl M, Gundersen JK (1999) Adaptation, test and in situ measurements with O_2 microopt(r)odes on benthic landers. Deep-Sea Res I 46:171-183

Graça Md, Melão G & Rocha O (1999) Biomass and productivity of the freshwater sponge *Metania spinata* (Carter, 1881) (Demospongiae: Metaniidae) in a Brazilian reservoir. Hydrobiologia 390(1-3):1-10

Grebmeier JM & Barry JP (1991) The influence of oceanographic processes on pelagic-benthic coupling in polar regions: A benthic perspective. J Mar Syst 2:495-518

Gutt J (1996) The 'multistoried' habitat on the Antarctic sea floor. A biodiversity study. Annu Rep AWI Polar Mar Res 1994-1995:26-28

Gutt J, Starmans A & Dieckmann G (1996) Impact of iceberg scouring on polar benthic habitats. Mar Ecol Prog Ser 137(1-3):311-316

Gutt J & Starmans A (1998) Structure and biodiversity of megabenthos in the Weddell and Lazarev seas (Antarctica: Ecological role of physical parameters and biological interactions. Polar Biol 20(4):229-247

Gutt J & Starmans A (2001) Quantification of iceberg impact and benthic recolonisation patterns in the Weddell Sea (Antarctica). Polar Biol 24(8):615-619

Hellmer HH & Bersch M (1985) The Southern Ocean. A survey of oceanographic and marine meteorological research work. Ber Polarforsch 26:1-115

Heygster G, Pedersen L, Turner J, Thomas CH, Hunewinkel T, Schottmüller H & Viehoff T (1996) PELICON: Project for estimation of long-term variability of ice concentration. European Community Tech. Report Contract EV5V-CT93-0268(DG 12 DTEE)

Hickman (1996) The Jepsen manual: Higher plants of California. University of California Press, Los Angeles

Holst G, Glud RN, Kühl M, Klimant I (1997) A microoptode array for fine-scale measurement of oxygen distribution. Sensors and Actuators B 38-39:122-129

Hummel H, Sepers ABJ, de Wolf L, Melissen FW (1988) Bacterial growth on the marine sponge *Halichondria panicea* induced by reduced waterflow rate. Mar Ecol Prog Ser 42:195-198

Humphreys WF (1979) Production and respiration in animal populations. J Anim Ecol 48:427-453

Ikeda T (1989) Estimated respiration rate of mytophid fish from the enzyme activity of the eletron-transport-system. J Oceanogr Soc Japan 45:167-173

Jarre-Teichmann A, Brey T, Bathmann UV, Dahm C, Dieckmann GS, Gorny M, Klages M, Pagés F, Plötz J, Schnack-Schiel S, Stiller M, Arntz WE (1997) Trophic flows in the benthic shelf community of the eastern Weddell Sea, Antarctica In: B Battaglia, J Valencia & DWH Walton (ed.) Antarctic Communities: Species, Structure, and Survival. University Press, Cambridge, pp 118-134

Johnson MF (1978) Studies on the reproductive cycles of the calcareous sponges *Clathrina coriacea* and *Clathrina blanca* from Santa Catalina Island, California. Bull South Calif Acad Sci 50(8):73-79

Jones WC & Pearson JJR (1990) Effects of Metabolic inhibitors and nutrients on spicule formation in juveniles of *Sycon ciliatum* and *Grantia compressa* In: Rützler, Klaus (ed.) New Perspectives in Sponge Biology. Smithonian Institution Press, Washington D.C., pp 211-220

Jumars PA & Nowell ARM (1984) Fluid and sediment dynamic effects on marine benthic community structure. Amer Zool 24:45-55

Kaandorp JA (1991) Modelling growth forms of the sponge *Haliclona oculta* (Porifera, Demospongiae) using fractal techniques. Mar Biol 110:203-215

Kabir R (1996) Die chemische Loesung silikatischer Skelettelemente von Poriferen im Meerwasser. unpubl masters thesis University Kiel:1-111

Kang JS, Kang SH, Lee JH & Chung KH (1997) Antarctic micro- and nano-sized phytoplankton assemblages in the surface water of Maxwell Bay during the 1997 Austral Summer. Korean J Polar Res 8:35-45

Kim D (2001) Seasonality of marine algae and grazers of an Antarctic rocky intertidal, with emphasis on the role of the limpet *Nacella concinna* Strebel (Gastropoda: Patellidae). Ber Polarforsch 397:1-120

Kinne O (1977) Cultivation of animals - research cultivation, 3: Porifera In: Kinne, O. (ed.) Marine Ecology , Vol III (Cultivation), part 2. Wiley Interscience, London, pp 5.1:627-364

Klimant I, Meyer V, Kühl M (1995) Fiber-optic oxygen microsensors, a new tool in aquatic biology. Limnol Oceanogr 40:1159-1165

Klimant I, Kühl M, Glud RN, Holst G (1997) Optical measurement of oxygen and temperature in microscale: strategies and biological implications. Sensors and Actuators B 38:29-37

Koehl MAR, Carpenter R, Helmuth B (2001) The physical environment: Growing and flowing In: Jaap A. Kaandorp & Janet E. Kübler (ed.) The Algorithmic Beauty of Seaweeds, Sponges, and Corals. Springer, Berlin Heidelberg New York, pp 15-30

Koltun VM (1968) Spicules of sponges as an element of bottom sediments of the Antarctic In: Currie, R.I. (ed.) Symposium on Antarctic Oceanography, Santiago de Chile 1966. Scott Polar Research Institute, Cambridge, pp 121-123

Koltun VM (1970) Sponges of the Arctic and Antarctic: a faunistic review. Symp zool Soc Lond 25:285-297

Koltun VM (1976) Porifera-Part I: Antarctic sponges. BANZ Antarctic research expedition Reports, Series B IX(Part 4):147-198

Konecki JT & Targett TE (1989) Eggs and larvae of *Nototheniops larseni* from the spongocoel of a hexactinellid sponge near Hugo Island, Antarctic Peninsula. Polar Biol 10:197-198

Kowalke J (2000) Ecology and energetics of two Antarctic sponges. J Exp Mar Biol Ecol 247:85-97

Krasko A, Schröder HC, Perovic S, Steffen R, Kruse M, Reichert W, Müller IM, Wüller WEG (1999) Ethylen modulates gene expression in cells of the marine sponge *Suberites domuncula* and reduces the degree of apoptosis. J Biol Chem 274: 311524-31530

Kunzmann K (1996) Die mit ausgewählten Schwämmen (Hexactinellida und Demospongiae) aus dem Weddellmeer, Antarktis, vergesellschaftete Fauna. Ber Polarforsch 210:1-93

Lal D & Somayajulu BLK (1980) Possible application of cosmogenic ^{32}Si for studying mixing in near-coastal waters In: Goldberg, Horibe & Soruhashi (eds) (ed.) Isotope marine chemistry. Uchida Rokakuho, Tokyo, pp 145-156

Lal D, Nijampurkar VN & Somayajulu BLK (1970) Concentrations of cosmogenic Si^{32} in deep Pacific and Indian waters based on study of Galathea deep sea siliceous sponges. Galathea Rep 11:247-256

Lal D, Nijampurkar VN, Somayajulu BLK, Koide M & Goldberg ED (1976) Silicon-32 specific activities in coastal waters of the world oceans. Limnol Oceanogr 21:285-293

Lampert W (1984) The measurement of respiration In: Downing, JA & Rigler, FH (ed.) A Manual for the Assessment of Secondary Production in Fresh Waters IBP handbook 17. Blackwell, Oxford, pp 413-468

Langdon C (1984) Dissolved oxygen monitoring system using a pulsed electrode: Design, performance, and evaluation. Deep-Sea Res 31:1357-1367

Lanner RM & Connor KF (2001) Does bristlecone pine senesce? Exp Gerontol 36:675-685

Laudien J, Brey T & Arntz WE (subm) Population structure, growth and production of the surf clam Donax serra (Bivalvia, Donacidae) on two Namibian sandy beaches. Estuarine Coastal Shelf Sci

Leichter JJ, Witman JD (1997) Water flow over subtidal rock walls: Relation to distributions and growth rates of sessile suspension feeders in the Gulf of Maine. Water flow and growth rates. J Exp Mar Biol Ecol 209:293-307

Leys SP & Lauzon NRJ (1998) Hexactinellid sponge ecology: growth rates. and seasonality in deep water sponges. J Exp Mar Biol Ecol 230:111-129

MacMillan SM (1996) Starting a successful commercial sponge aquaculture farm. Center for Tropical and Subtropical Aquaculture Waimanalo, Hawai Publication Number 120

Madon SP, Schneider DW & Stoeckel JA (1998) In situ estimation of zebra mussel metabolic rates using the electron transport system (ETS) assay. J Shellfish Res 17(1):195-203

Maldonado M & Uriz MJ (1999) Sexual propagation by sponge fragments. Nature 398:476

Marliave JB (1992) Environmental monitoring through natural history research. Can Tech Rep Fish Aquat Sci 1879:199-209

MasCom, Analysegeräte Service, Norderoog1, 28259 Bremen, Germany http://www.mascom-ms.de

McClintock JB (1987) Investigation of the relationship between invertebrate predation and biochemical composition, energy content, spicule armament and toxicity of benthic sponges at McMurdo Sound, Antarctica. Mar Biol 94(3):479-487

McClintock JB, Pearse JS & Bosch I (1988) Population structure and energetics of the shallow-water Antarctic sea star Odontaster validus in contrasting habitats. Mar Biol 99:235-246

McNeil S & Lawton JH (1970) Annual production and respiration in animal populations. Nature 225:472-474

Moreno C (1980) Observations on food and reproduction in Trematomus bernacchii (Pisces: Nothothenoiidae) from the Palmer Archipelago, Antarctica. Copeia 1 (171-173)

Müller WEG, Wiens M, Batel R, Steffen R, Schröder HC, Borojevic R, Custodio MR (1999a) Establishment of a primary cell culture from a sponge: primmorphs from Suberites domuncula. Mar Ecol Prog Ser 178:205-219

Müller WEG, Wimmer W, Schatton W, Böhm M, Batel R & Filic Z (1999b) Initiation of an aquaculture of sponges from the sustainable production of bioactive metabolites in open systems: example, Geodia cydonium. Mar Biotechnol 1(6):569-579

Müller WEG, Böhm M, Batel R, De Rosa S, Tommonaro G., Müller IM & Schröder HC (2000) Application of cell culture for the production of bioactive compounds from sponges: synthesis of avarol by primmorphs from Dysidea avara. J Nat Prod 63:1077-10

Nelson DM, DeMaster DJ, Dunbar RB & Smith Jr. WO (1996) Cycling of organic carbon and biogenic silica in the Southern Ocean: Estimates of water-column and sedimentary fluxes on the Ross Sea continental shelf. J Geophys Res 101C(8):18519-18532

Orejas C (2001) Role of benthic cnidarians in energy transfer processes in the Southern Ocean marine ecosystem (Antarctica). Ber Polarforsch 395:1-186

Osinga R, De Beukelaer PB, Meijer EM, Tramper J & Wijffels RH (1999a) Growth of the sponge *Pseudosuberites (aff.) andrewsi* in a closed system. J Biotechnol 70(1-3):155-161

Osinga R, Redeker D, De Beukelaer PB & Wijffels RH (1999b) Measurement of sponge growth by projected body area and underwater weight. Mem Queensl Mus 44:419-426

Osinga R, Tramper J & Wijffels RH (1999c) Cultivation of marine sponges. Mar Biotechnol 1:509-532

Owens TG & King FD (1975) The measurement of respiratory electron-transport-system activity in marine zooplankton. Mar Biol 30:27-36

Packard TT & Williams PJl (1981) Rates of respiratory oxygen consumption and electron transport in surface seawater from the northwest Atlantic. Oceanol Acta 4(3):351-358

Packard TT (1971) The measurement of respiratory electron-transport activity in marine phytoplankton. J Mar Res 29(3):235-244

Paine RT (1964) Ash and calorie determinations of sponge and opisthobranch tissues. Ecology 45:384-387

Patterson MR, Sebens KP & Olson RR (1991) In situ measurements of flow effects on primary production and dark respiration in reef corals. Limnol Oceanogr 36(5):936-948

Peck LS (1989) Temperature and basal metabolism in two Antarctic marine herbivores. J. exp. mar. Biol. Ecol. 127(1):1-12

Peck LS, Uglow RF (1990) Two methods for the assessment of the oxygen content of small volumes of seawater. J Exp Mar Biol Ecol 141:53-62

Peck LS & Conway LZ (2000) The myth of metabolic cold adaptation: oxygen consumption in stenothermal Antarctic bivalves In: Harper, E., Taylor, J. D. & Crame, A.J. (ed.) The evolutionary ecology of bivalve molluscs Geological Society, London, Special Publications, 177. London Geological Society, London, pp 441-450

Peck LS, Veal R (2001) Feeding, metabolism and growth in the Antarctic limpet, *Nacella concinna* (Strebel 1908). Mar Biol 138:553-560

Peck LS, Brockington S & Brey T (1997) Growth and metabolism in the Antarctic brachiopod *Liothyrella uva*. Phil Trans R Soc Lond B 352(1355):851-858

Piepenburg D & Schmid MK (1996) Brittle star fauna (Echinodermata: Ophiuroidea) of the Arctic northwest Barents Sea: composition, abundance, biomass and spatial distribution. Polar Biol 16:383-392

Piepenburg D, Schmid MK & Gerdes D (2002) The benthos off King George Island (South Shetland Islands, Antarctica): further evidence for a lack of a latitudinal biomass cline in the Southern Ocean. Polar Biol 25:146-158

Pile AJ, Patterson MR & Witman JD (1996) In situ grazing on plankton < 10 µm by the boreal sponge *Mycale lingua*. Mar Ecol Prog Ser 141:95-102

PreSens Precision Sensing GmbH, Spitalplatz C 191, 86633 Neuburg a.d. Donau, Germany (http://www.presens.de)

Propp MV, Garber MR, Ryabuscko VI (1982) Unstable processes in the metabolic rate measurement in flow-through systems. Mar Biol 67:47-49

Rabarts IW (1970) Physiological aspects of the ecology of some Antarctic lamellibranchs. British Antarctic Survey Report AD6/2H/1970/N9(unpublished):1-5

Ragueneau O, Tréguer P, Leynaert A, Anderson RF, Brzezinski MA, DeMaster DJ, Dugdale RC, Dymond J, Fischer G, François R, Heinze C, Maier-Reimer E, Martin-Jézéquel V, Nelson DM & Quéguiner B (2000) A review of the Si cycle in the modern ocean: recent progress and missing gaps in the application of biogenic opal as a paleoproductivity proxy. Global and Planetary Change 26(4):317-365

Reincke T & Barthel D (1997) Silica uptake kinetics of *Halichondria panicea* (Pallas, 1766) in Kiel Bight. Mar Biol 129:591-593

Reiswig HM (1973) Population dynamics of three Jamaican demospongiae. Bull Mar Sci 23(2):191-226

Reiswig HM (1981) Partial carbon and energy budgets of the bacteriosponge *Verongia fistularis* (Porifera: Demospongiae) in Barbados. Mar Ecol 2(4):273-293

Reusch TBH, Boström C, Stam WT & Olsen JL (1999) An ancient eelgrass clone in the Baltic . Mar Ecol Prog Ser 183:301-304

Revsbech NP, Jørgensen BB, Blackburn HT, Cohen Y (1983) Microelectrode studies of the photosynthesis and O_2, H_2S and pH profiles of a microbial mat. Limnol Oceanogr 28:1062-1074

Ribes M, Coma R & Gili J-M (1999) Natural diet and grazing rate of the temperate sponge *Dysidea avara* (Demospongiae, Dendroceratida) throughout an annual cycle. Mar Ecol Prog Ser 176:179-190

Rodhouse PG (1991) Population structure of *Martialia hyades* (Cephalopoda: Ommastrephidae) at the Antarctic polar front and the Patagonian shelf, South Atlantic. Bull Mar Sci 49:404-418

Roland F, Caraco NF, Cole JJ, Giorgio Pd (1999) Rapid and precise determination of dissolved oxygen by spectrophotometry: Evaluation of interference from color and turbidity. Limnol Oceanogr 44:1148-1154

Sachs L (1999) Angewandte Statistik. Springer, Berlin Heidelberg New York

Salonen K, Sarvala J, Hakala I & Viljanen M-L (1976) The relation of energy and organic carbon in aquatic invertebrates. Limnol Oceanogr 21(5):724-730

Sarà A, Cerrano C & Sarà M (2002) Viviparous development in the Antarctic sponge *Stylocordyla borealis* Lovén, 1868. Polar Biol 25(6):425-431

Schalk PH (1988) Respiratory electron transport system (ETS) activities in zooplankton an micronekton of the Indo-Pacific region. Mar Ecol Prog Ser 44:25-23

Schmid MK (1996) Zur Verbreitung und Respiration ökologisch wichtiger Bodentiere in den Gewässern um Svålbard (Arktis). Ber Polarforsch 202:1-93

Schupp P, Eder C, Paul V & Proksch P (1999) Distribution of secondary metabolites in the sponge *Oceanapia sp.* and its ecological implications. Mar Biol 135:573-580

Schwab DW & Shore RE (1971a) Fine structure and composition of a siliceous sponge spicule. Biol Bull 140:125-136

Schwab DW & Shore RE (1971b) Mechanism of internal stratification of siliceous sponge spicules. Nature 232:501-502

Simpson (1984) The Cell Biology of Sponges. Springer, New York Berlin Heidelberg Tokyo

Stefansson E, Peterson JI, Wang YH (1989) Intraocular oxygen tension measured with a fiber-optic sensor in normal and diabetic dogs. Am J Physiol 256:H1127-1133

Stephenson N (1992) Long term dynamics of giant sequoia populations: Implications for managing a pioneer species. Proceedings of the Symposium of Giant Sequoias: Their place in the Ecosystem and Society.

Stokes MD, Somero GN (1999) An optical oxygen sensor and reaction vessel for high-pressure applications. Limnol Oceanogr 44:189-195

Tanaka K (2002) Growth dynamics and mortality of the intertidal encrusting sponge *Halichondria okadai* (Demospongiae, Halchondria). Mar Biol 140:383-389

Thomassen S & Riisgård HU (1995) Growth and energetics of the sponge *Halichondria panicea*. Mar Ecol Prog Ser 128 (1-3):239-246

Tréguer P & Jacques G (1992) Dynamics of nutrients and phytoplankton, and fluxes of carbon, nitrogen and silicon in the Antarctic Ocean. Polar Biol 12:149-162

Turon X, Tarjuelo I & Uriz MJ (1998) Growth dynamics and mortality of the encrusting sponge *Crambe crambe* (Poecilosclerida) in contrasting habitats: correlation with population structure and investment in defence. Funct Ecol 12(4):631-639

Bodungen B von (1975) Der Jahresgang der Nährsalze und der Primärproduktion in der Kieler Bucht unter Berücksichtigung der Hydrographie. unpubl phD thesis Christian-Albrechts-Universität Kiel

Voß J (1988) Zoogeography and community analysis of macrozoobenthos of the Weddell Sea (Antarctica). Ber Polarforsch 45:1-144

Wägele H (1988) Riesenwuchs contra spektakuläre Farbenpracht - Nudibranchia der Antarktis. Natur u Museum 118:46-53

Wilson TRS, Cussen H, Braithwaite AC (1993) An improved electrode for pore water oxygen measurement in ocean sediments. Sci Total Environ 135:115-121

Winkler LW (1888) The determination of dissolved oxygen in water. Ber Deut Chem Ges 21:2843-2846

Witte U (1995) Reproduktion, Energiestoffwechsel und Biodepositionsleistung dominanter Porifera aus der Tiefsee des Europäischen Nordmeeres. Ber SFB 313 University Kiel 53:99p

Witte U, Graf G (1996) Metabolism of deep-sea sponges in the Greenland-Norwegian Sea. J Exp Mar Biol Ecol 198:223-235

Wolfbeis OS (1991) Oxygen sensors In: Wolfbeis, OS (ed) Fiber optic chemical sensors. CRC Press, Boca Ranton, pp 19-5

Yokoyama Y, Deckker PD, Lambeck K, Johnston P & Fifield LK (2001) Sea-level at the Last Glacial Maximum: evidence from northwestern Australia to constrain ice volumes for oxygen isotope stage 2. Paleogeogr Paleoclimatol Paleoecol 165:281-297

7 Appendix

7.1 List of selected abbreviations

Abbreviation	Unit in parentheses
AASS	Average Antarctic shelf sponge (see section 3.4 p 24)
AFDM	Ash free dry mass [g] or [mg]
AMIGO	Advanced Modelling of Invertebrate Growth from Oxygen consumption data
C	Organic carbon [g] or [mg]
D	Diameter [mm]
d^{-1}	Per day
DM	Dry mass [g]
EASIZ	Ecology of the Antarctic Sea Ice Zone
ETS	Activity of the Electron Transport System [$cm^3O_2\ ind^{-1}\ h^{-1}$]
ETS'	Mass specific ETS [$cm^3O_2\ g^{-1}AFDM\ h^{-1}$]
ind	Individual
k	Growth parameter of the von Bertalanffy growth function
L	Length [mm]
SFD	Size-frequency-distribution
MHV	Masse-Häufigkeits-Verteilung
m	Meter
m^{-2}	Per square meter
M	Body mass [gWM], [gDM], [gAFDM], [gC]
M_e	Energy equivalent of body mass [kJ]
M_{max}	Maximum body mass at which the parameter $P_s/\Sigma R=0$
M_{emax}	Energy equivalent of maximum body mass
M_∞	Infinite body mass of the VBGF
MFD	Mass-frequency-distribution
P_s/B	Somatic production to biomass ratio
P_s	Somatic Production
PP	Primary production
ΣR	Sum of all respiratory processes (=oxygen consumption)
SD	Step-size for one step of result-writing to output-file (Step Display) [day]
SE	Standard error
SiO_2	Silica
SS	Step-Size for one step of modelling calculations [day]
SSE	Number of days after which modelling should stop
S_∞	Asymptotic maximum body size

List of Abbreviations (con't)

Abbreviation	Unit in parentheses
V	Volume [mm^3] or [cm^3]
VBGF	Von Bertalanffy growth function
VBWF	Von Bertalanffy Wachstumsfunktion
WM	Wet mass [g]
WSS	Weddell Sea shelf
y^{-1}	Per year

Indices	
body	Indexed measurement refers to body part of a *S. borealis*
S10	Diameter of a *S. borealis* stalk measured 10 cm below body
Smax	Maximum diameter of a *S. borealis* stalk [mm]
Smin	Minimum diameter of a *S. borealis* stalk [mm]
stalk	Indexed measurement refers to stalk part of a *S. borealis*
tot	Indexed measurement refers to complete *S. borealis*

7.2 Initial parameters for modelling

Table A1 *Stylocordyla borealis*. Parameters used for initializing the model. 'Mean' refers to the mean slope of the regression of respiration data. 'Upper 95%' and 'Lower 95%' refer to the upper and lower 95% confidence limit of the slope of the same regression. Data are used for error propagation.

Stylocordyla borealis		mean	upper 95%	lower 95%
method:		ln	ln	ln
for Ps/R vs body mass [kJ]	a=	0.2193497	0.2193497	0.2193497
for Ps/R vs body mass [kJ]	b=	-0.0413999	-0.0413999	-0.0413999
for Ps/R vs body mass [kJ]	a2=	1	1	1
for Ps/R vs body mass [kJ]	b2=	-0.2	-0.2	-0.2
critical BM [gC]	crit BM=	1	1	1
for: log msp rr = a+b*log M	a=	-0.85548	-0.85548	-0.85548
for: log msp rr = a+b*log M	b=	-0.52053	-0.44366	-0.5974
initial body mass [gC]	iniBM=	0.001	0.001	0.001
max. body mass [gC]	=	4.5	4.5	4.5
stepsize [days]	SS=	1	1	1
stepsize display [days]	SSD=	100	100	100
stepsize end [days]	SSE=	120000	120000	120000
AFDM -> C [g->g or mg->mg]	=	0.5	0.5	0.5
mg C-> gAFDM	=	0.002	0.002	0.002
gC->kJ	=	45.7	45.7	45.7
mlO2->gC	=	0.00044	0.00044	0.00044
mgO2->J	=	14.1	14.1	14.1
mgO2->mgC	=	0.309	0.309	0.309
WM->DM	=	0.186	0.186	0.186
DM->AFDM	=	0.372	0.372	0.372
WM->AFDM	=	0.075	0.075	0.075
Filename:		Sb_200_ln1b	Sb_200_ln3b	Sb_200_ln4b

RESULTS		[years]	[years]	[years]
min body mass (0.009 gC)	after	0.514	0.748	0.351
mean body mass (0.414 gC)	after	10.366	11.630	9.309
max body mass (1.445 gC)	after	32.906	33.196	32.892
ANT XIII max mass (3.85 gC)	after	152.318	137.584	169.477

Table A2 *Cinachyra antarctica*. Parameters used for initializing the model. 'Mean' refers to the mean slope of the regression of respiration data. 'Upper 95%' and 'Lower 95%' refer to the upper and lower 95% confidence limit of the slope of the same regression. Data are used for error propagation.

Cinachyra antarctica		mean	upper 95%	lower 95%
method:		ln	ln	ln
for Ps/R vs body mass [kJ]	a=	0.2417737	0.2417737	0.2417737
for Ps/R vs body mass [kJ]	b=	-0.031661	-0.031661	-0.031661
for Ps/R vs body mass [kJ]	a2=	1	1	1
for Ps/R vs body mass [kJ]	b2=	-0.2	-0.2	-0.2
critical BM [gC]	crit BM=	1	1	1
for: log msp rr = a+b*log M	a=	-1.09483	-1.09483	-1.09483
for: log msp rr = a+b*log M	b=	-0.57362	-0.473011	-0.674229
initial body mass [gC]	iniBM=	0.01	0.01	0.01
max. body mass [gC]	=	50	50	50
stepsize [days]	SS=	1	1	1
stepsize display [days]	SSD=	100	100	100
stepsize end [days]	SSE=	2000000	2000000	2000000
AFDM -> C [g->g or mg->mg]	=	0.4561	0.4561	0.4561
mg C-> gAFDM	=	0.0021925	0.0021925	0.0021925
gC->kJ	=	45.7	45.7	45.7
mlO2->gC	=	0.00044	0.00044	0.00044
mgO2->J	=	14.1	14.1	14.1
mgO2->mgC	=	0.309	0.309	0.309
WM->DM	=	0.186	0.186	0.186
DM->AFDM	=	0.372	0.372	0.372
WM->AFDM	=	0.075	0.075	0.075
Filename:		Ca_2072_In1	Ca_2072_In3	Ca_2072_In4

RESULTS		[years]	[years]	[years]
min body mass (0.0034 gC)	after	0.400	0.734	0.219
mean body mass (0.333 gC)	after	10.652	12.753	9.064
max body mass (1.561 gC)	after	34.868	35.533	34.854
Dayton's mean (6.965 gC)	after	125.990	109.331	148.096
Dayton's max (41.23 gC)	after	1550.671	1051.251	2305.843

Table A3 *Rossellidae spp.* Parameters used for initializing the model. 'Mean' refers to the mean slope of the regression of respiration data. 'Upper 95%' and 'Lower 95%' refer to the upper and lower 95% confidence limit of the slope of the same regression. Data are used for error propagation. Modelling of *Rossellidae spp.* growth rates was divided into two runs: the first from body mass 0.001 - 140 gC and the second from 140gC onwards. Where parameters differ between the two runs, those of the second run are given in parentheses.

Rossellidae spp.		mean	upper 95%	lower 95%
method:		ln	ln	ln
for Ps/R vs body mass [kJ]	a=	0.2690352	0.2690352	0.2690352
for Ps/R vs body mass [kJ]	b=	-0.019822	-0.019822	-0.019822
for Ps/R vs body mass [kJ]	a2=	1	1	1
for Ps/R vs body mass [kJ]	b2=	-0.2	-0.2	-0.2
critical BM [gC]	crit BM=	1	1	1
for: log msp rr = a+b*log M	a=	-0.90759	-0.90759	-0.90759
for: log msp rr = a+b*log M	b=	-0.5014	-0.443731	-0.559069
initial body mass [gC]	iniBM=	0.001 (140)	0.001 (140)	0.001 (140)
max. body mass [gC]	=	15605	15605	15605
stepsize [days]	SS=	1 (100)	1 (100)	1 (100)
stepsize display [days]	SSD=	100 (1000)	100 (1000)	100 (1000)
stepsize end [days]	SSE=	10000000	10000000	15000000
AFDM -> C [g->g or mg->mg]	=	0.4141	0.4141	0.4141
mg C-> gAFDM	=	0.0024149	0.0024149	0.0024149
gC->kJ	=	45.7	45.7	45.7
mlO2->gC	=	0.00044	0.00044	0.00044
mgO2->J	=	14.1	14.1	14.1
mgO2->mgC	=	0.309	0.309	0.309
WM->DM	=	0.186	0.186	0.186
DM->AFDM	=	0.372	0.372	0.372
WM->AFDM	=	0.075	0.075	0.075
Filename:		hex_ln1	hex_ln3	hex_ln4
RESULTS		[years]	[years]	[years]
min body mass (0.061 gC)	after	2.104	2.540	1.749
mean WSS (87.64 g C)	after	185.932	150.269	232.031
140 gC	after	253.289	199.032	325.077
max WSS (1681 gC)	after	1515.133	1020.567	2266.027
Dayton's max (15605 gC)	after	22718	12877	40215

7.3 AMIGO 4.04 source code

```
{***** GROWTH.MAC 4.04***********************************************************************************}

DEFINE SUSO1
RGB_COLOR 1 0.84 0
END_DEFINE
DEFINE SUSO2
RGB_COLOR 0.5 0 1
END_DEFINE
DEFINE SUSO3
RGB_COLOR 0.6 1 0
END_DEFINE
DEFINE SUSO4
RGB_COLOR 1 1 0.5
END_DEFINE
DEFINE
RGB_COLOR 0.7 1
END_DEFINE
DEFINE
DELETE ALL CONFIRM
END_DEFINE
DEFINE WF
WINDOW FIT
END_DEFINE
{***********************************************}
         DEFINE graph_schalter
         IF (WACHE1 = 1)
         READ STRING 'if "end M:(gC)" or "step end" new, do not change new graph! ' DEFAULT 'confirm
with enter' AAA
         ELSE_IF      (GRAPH = 0)
         LET KEEPGR (1)
         LET GRAPH  (1) SM_GROWTH
         ELSE_IF (GRAPH = 1)
         LET KEEPGR (0)
         LET GRAPH  (0) SM_GROWTH
         END_IF
         END_DEFINE
{***********************************************}
         DEFINE startbild
         DELETE ALL CONFIRM
         LET P1 0,0    LET P2 0,15
         kopf_drucken
         END
         WINDOW FIT
         END_DEFINE
{*************** READ NUMBER fuer confidence aendern ************}
DEFINE IN_CONF_T
         READ NUMBER
         'Please enter t from table: t = ' conf_t
         SM_CONFIDENCE
   END_DEFINE
   DEFINE IN_CONF_N
         READ NUMBER
         'Please enter number of observations: n = ' conf_n
         SM_CONFIDENCE
   END_DEFINE
   DEFINE IN_CONF_STDV
         READ NUMBER
         'Please enter standard deviation of x: stdv = ' conf_stdv
         SM_CONFIDENCE
   END_DEFINE
```

```
      DEFINE IN_CONF_XMEAN
            READ NUMBER
            'Please enter mean of x: xmean  = ' conf_xmean
            SM_CONFIDENCE
      END_DEFINE
      DEFINE IN_CONF_SUM
            READ NUMBER
            'Please enter sum of squares: (x - xmean)^2  = ' conf_sum
            SM_CONFIDENCE
      END_DEFINE
{*********************************************************}
      DEFINE IN_PSRA
            READ NUMBER
            'for M in [kJ] and log[Ps/R]= a+b*log[M] or Ps/R = a+b*lnM or Ps/R =a+b*M  enter a= ' PSRA
            SM_GROWTH
      END_DEFINE
      DEFINE IN_PSRB
            READ NUMBER
            'for M in [kJ] and log[Ps/R]= a+b*log[M] or Ps/R = a+b*lnM or Ps/R =a+b*M enter b= ' PSRB
            SM_GROWTH
      END_DEFINE
      DEFINE IN_PSRA2
            READ NUMBER
            'for M in [kJ] and Ps/R =a2+b2*M  enter a2= ' PSRA2
            SM_GROWTH
      END_DEFINE
     DEFINE IN_PSRB2
            READ NUMBER
            'for M in [kJ] and Ps/R =a2+b2*M  enter b2= ' PSRB2
            SM_GROWTH
      END_DEFINE
DEFINE IN_critBM
            READ NUMBER
            'critical bodymass [gC] for change of method into linear;   enter critBM=' critBM
            SM_GROWTH
      END_DEFINE
DEFINE IN_MSPA
            READ NUMBER
            'for M in {g AFDM] and log msp rr = a+b*log M  enter a= ' MSPA
            SM_GROWTH
      END_DEFINE
DEFINE IN_MSPB
            READ NUMBER
            'for M in {g AFDM] log msp rr = a+b*log M  enter b= ' MSPB
            SM_GROWTH
      END_DEFINE
DEFINE IN_IM
            READ NUMBER
            'enter initial body mass [gC] = ' IM
            SM_GROWTH
      END_DEFINE
DEFINE IN_BMEXIT
            READ NUMBER
            'enter max. body mass [gC] = ' BMEXIT
            LET KEEPGR (0)
            LET WACHE1 (1)
            LET GRAPH  (0)
            SM_GROWTH
      END_DEFINE
DEFINE IN_SS
            READ NUMBER
            'enter stepsize [days] = ' SS
            SM_GROWTH
```

```
        END_DEFINE
DEFINE IN_SSD
        READ NUMBER
        'enter stepsize display [days] = ' SSD
        SM_GROWTH
    END_DEFINE
DEFINE IN_SSE
        READ NUMBER
        'enter stepsize end [days] = ' SSE
        LET KEEPGR (0)
        LET WACHE1 (1)
        LET GRAPH  (0)
        SM_GROWTH
    END_DEFINE
DEFINE IN_AFDMC
        READ NUMBER
        'AFDM -> C [g->g or mg->mg] = ' AFDMC
        SM_CONVERSION
    END_DEFINE
DEFINE IN_MGCG
        READ NUMBER
        'mg C-> gAFDM = ' MGCG
        SM_CONVERSION
    END_DEFINE
DEFINE IN_GCKJ
        READ NUMBER
        'gC->kJ = ' GCKJ
        SM_CONVERSION
    END_DEFINE
DEFINE IN_MLOG
        READ NUMBER
        'mlO2->gC = ' MLOG
        SM_CONVERSION
    END_DEFINE
DEFINE IN_MGOJ
        READ NUMBER
        'mgO2->J = ' MGOJ
        SM_CONVERSION
    END_DEFINE
DEFINE IN_MGOM
        READ NUMBER
        'mgO2->mgC = ' MGOM
        SM_CONVERSION
    END_DEFINE
DEFINE IN_WMD
        READ NUMBER
        'WM->DM = ' WMD
        SM_CONVERSION
    END_DEFINE
DEFINE IN_DMA
        READ NUMBER
        'DM->AFDM = ' DMA
        SM_CONVERSION
    END_DEFINE
DEFINE IN_WMA
        READ NUMBER
        'WM->AFDM = ' WMA
        SM_CONVERSION
    END_DEFINE
DEFINE IN_OUTFILE
        READ STRING
        "Enter name for OUTFILE in " " DEFAULT ("+STR OUTFILE) OUTFILE
        SM_GROWTH
```

```
        END_DEFINE
DEFINE IN_FAKBM
        READ NUMBER
        "Enter factor for scaling BM - axis" FAKBM
        SM_GROWTH
    END_DEFINE
DEFINE IN_FAKDAY
        READ NUMBER
        "Enter factor for scaling day - axis" FAKDAY
        SM_GROWTH
    END_DEFINE
{*************************************************************************************************}

{***** GROWTH.QEL  4.04 *************************************************************************}
DEFINE methode
LOOP
    LET meth ((meth) +(1))
    EXIT_IF (meth = 1)
    EXIT_IF (meth = 2)
    EXIT_IF (meth = 3)
    EXIT_IF (meth = 4)
    EXIT_IF (meth = 5)
    LET meth (0)
    END_LOOP
SM_GROWTH
 END_DEFINE
{*********************************************************}
DEFINE regression
LOOP
    LET regr ((regr) +(1))
    EXIT_IF (regr = 1)
    EXIT_IF (regr = 2)
    EXIT_IF (regr = 3)
    LET regr (0)
    END_LOOP
SM_GROWTH
END_DEFINE
{*********************************************************}
DEFINE calculate
IF (GRAPH = 0)
  EDIT_PART '/' DELETE ALL CONFIRM END
  END_iF
LET P1  (0,0)
    LET P2  (0,15)
    LET P3  (0,25)
    LET P4  (0,35)
    LET P5  (0,50)
CURRENT_DIRECTORY 'c:/ARCHIV/ME10/GROWTH/RESULT'
  kopf_schreiben                { kopf_drucken  }
LET DAY (0)
    LET BMC (IM)
    LET MUE (0)
    LET BMJ (BMC*GCKJ)
    LET BMAF (BMC/AFDMC)
    LET CONF_LIM (10^(conf_t*conf_stdv*SQRT((1/(conf_n))+((LG (BMAF)-conf_xmean)^2)/conf_sum)))
IF (regr = 1)                {fitted weighted linear regression}
  LET RGC ((10^(MSPA+MSPB*LG (BMAF)))*BMAF*24*SS*MLOG) {respiration rate [gC / (SS * ind)] }
END_IF
IF (regr =2)     {upper 95% confidence limit}
  LET RGC ((CONF_LIM+10^(MSPA+MSPB*LG (BMAF)))*BMAF*24*SS*MLOG) {respiration rate [gC/(SS*ind)]}
END_IF

IF (regr = 3)     {lower 95% confidence limit}
```

```
    LET RGC ((-CONF_LIM+10^(MSPA+MSPB*LG (BMAF)))*BMAF*24*SS*MLOG) {respiration rate [gC/(SS*ind)]}
  END_IF
  LET RGCD (RGC/SS)                    {respiration rate per day [ml O2/ind] }
  LET RKJ (RGC*GCKJ)                   {respiration rate [kJ / (SS*ind)]}
  LET RKJD (RKJ/SS)                    {respiration rate per day [kJ/ind] }
  IF (meth = 1)              {log}
    LET PSR (10^(PSRA+PSRB*LG(BMJ)))   {dimensionless ratio}
  END_IF
  IF (meth = 2)              {linear}
    LET PSR (PSRA+PSRB*BMJ)            {dimensionless ratio}
  END_IF
  IF (meth = 3)             {exponential}
    LET PSR (PSRA*EXP(PSRB*BMJ))       {dimensionless ratio}
  END_IF
  IF (meth = 4)             {natural ln}
    LET PSR (PSRA+PSRB*LN(BMJ))        {dimensionless ratio}
  END_IF
  IF (meth=5)               {changing from natural ln to linear at critical bodymass}
    LET PSR (PSRA+PSRB*LN(BMJ))        {dimensionless ratio}
  END_IF
  LET PSKJ (RKJ*PSR)                   {somatic production [kJ / SS*ind]}
  LET PSKJD (PSKJ/SS)                  {somatic production [kJ /ind*day] }
  LET PSBM (PSKJ/BMJ)                  {somatic production [kJ / kJ*SS] }
  LET PSBMD (PSBM/SS)                  {somatic production [kJ / kJ*day] }
  LET P1 (P1+PNT_XY 0 -5)
    zeilen_druck
    END
beginn_plot
LOOP
    LET BMGC (BMAF*AFDMC+PSKJ/GCKJ)  {new body mass for next step of calculation [kJ] }
  LET MUE (LN (BMGC/BMC)/SS)          {specific growth rate }
  LET BMJ (BMJ+PSKJ)
  LET BMC  (BMJ/GCKJ)
  LET BMAF  (BMC/AFDMC)
  LET CONF_LIM (conf_t*conf_stdv*SQRT((1/(conf_n))+((LG (BMAF)-conf_xmean)^2)/conf_sum))
  IF (regr = 1)                        {fitted weighted linear regression}
    LET RGC ((10^(MSPA+MSPB*LG (BMAF)))*BMAF*24*SS*MLOG) {respiration rate [gC / (SS * ind)] }
  END_IF
  IF (regr =2)                  {upper 95% confidence limit}
    LET RGC ((CONF_LIM+10^(MSPA+MSPB*LG (BMAF)))*BMAF*24*SS*MLOG) {respiration rate [gC / (SS * ind)]}
  END_IF
  IF (regr = 3)                 {lower 95% confidence limit}
    LET RGC ((-CONF_LIM+10^(MSPA+MSPB*LG (BMAF)))*BMAF*24*SS*MLOG) {respiration rate [gC/(SS*ind)]}
  END_IF
  LET RGCD (RGC/SS)              {respiration rate per day [gC/(ind*day)] }
  ...LET RKJ (RGC*GCKJ)          {respiration rate [kJ / (SS*ind)]  }
  ...LET RKJD (RKJ/SS)           {respiration rate per day [kJ/(ind*day)] }
  IF (meth = 1)
    LET PSR (10^(PSRA+PSRB*LG(BMJ)))            {dimensionless ratio }
  END_IF
  IF (meth = 2)
    LET PSR (PSRA+PSRB*BMJ)            {dimensionless ratio}}
  END_IF
  IF (meth = 3)      {exponential}
    LET PSR (PSRA*EXP(PSRB*BMJ))       {dimensionless ratio }
  END_IF
  IF (meth = 4)
    LET PSR (PSRA+PSRB*LN(BMJ))        {dimensionless ratio }
  END_IF
  IF ( (meth=5) AND (BMC >= critBM)  )
  ...LET PSR (PSRA2+PSRB2*BMJ)
  ELSE_IF ( (meth=5) AND (BMC < critBM)  )
  ...LET PSR (PSRA+PSRB*LN(BMJ))
```

```
END_IF
LET PSKJ (RKJ*PSR)              {somatic production [kJ / ind*SS] }
LET PSKJD (PSKJ/SS)            {somatic production [kJ /ind*day] }
LET PSBM (PSKJ/BMJ)           {somatic production [kJ / kJ*SS] }
LET PSBMD (PSBM/SS)          {somatic production [kJ/kJ*d]}
IF (DAY >= DAYD)
LET BMC_ALT (BMC)
  zeilen_druck
LET DAYD (DAYD +SSD)
    LET P1 (P1+PNT_XY 0 -5)
 END_IF
EXIT_IF (BMC >= BMEXIT)
EXIT_IF ( DAY >= (SSE))
LET DAY (DAY + SS)
END_LOOP
IF ((DAY < (DAYD)) and (BMC <> BMC_ALT))
 zeilen_druck
END_IF
endergebnis
{ WINDOW FIT  }
END_DEFINE
{***********************************************************************************************}

{***** IN_OUT.QEL  4.04 **********************************************************************}
DEFINE endergebnis
LET MUE_D   ((INT (MUE  *10000000000+.5))/10000000000)
  LET BM_D   ((INT (BMC   *1000000   +.5))/1000000)
  LET BMJ_D   ((INT (BMJ  *1000000   +.5))/1000000)
  LET RKJD_D   ((INT (RKJD *1000000   +.5))/1000000)
  LET PSKJD_D  ((INT (PSKJD *1000000   +.5))/1000000)
  LET PSBMD_D  ((INT (PSBMD *10000000000+.5))/10000000000)
IF (GRAPH = 0)
   TEXT_SIZE 3.5
LET P3 (P3+PNT_XY 0 1)
TEXT ' day     MUE       BMC        BM[kJ]   R[kJ*ind-1*d-1]  Ps[kJ*ind-1*d-1]  Ps/BM[kJ*kJ-1*d-1]' P4
   END
LET P1 (P3+PNT_XY 0 -6)
LET DAY_P DAY
   TEXT   (' '+STR (INT(DAY_P +.5)) +'  '+STR (MUE_D) +'  '+STR (BM_D) +'  '+STR (BMJ_D) +'
'+STR (RKJD_D) +'   '+STR (PSKJD_D) +'        '+STR (PSBMD_D)) P1
   END
{TEXT ('day/365.242199='+STR DAY +'/365.242199='+STR ((INT(DAY/365.242199*10+.5))/10)+'Jahre') P4 END}
    TEXT ('result from : '+STR OUTFILE) P3
    LINE SOLID HORIZONTAL 0,19  270  END
    LET WACHE1 (0)
  END_IF
IF (GRAPH = 1)
  IF (KEEPGR = 1)
    LET P1 (P4+PNT_XY 0 -25)
    TEXT_SIZE 3.5
    TEXT ('result from : '+STR OUTFILE) P1
    LET P1 (P4+PNT_XY 0 -30)
    LINE SOLID HORIZONTAL 0,4  270  END
    LET KEEPGR (2)
  ELSE_IF (KEEPGR = 2)
    LET P1 (P4+PNT_XY 0 -40)
    TEXT_SIZE 3.5
    TEXT ('result from : '+STR OUTFILE) P1
    LET P1 (P4+PNT_XY 0 -45)
    LINE SOLID HORIZONTAL 0,-11 270  END
    LET KEEPGR (3)
  ELSE_IF (KEEPGR = 3)
    LET P1 (P4+PNT_XY 0 -55)
```

```
    TEXT_SIZE 3.5
    TEXT ('result from : '+STR OUTFILE) P1
    LET P1 (P4+PNT_XY 0 -60)
    LINE SOLID HORIZONTAL 0,-26 270  END
    LET KEEPGR (4)
  ELSE_IF (KEEPGR = 4)
    LET P1 (P4+PNT_XY 0 -70)
    TEXT_SIZE 3.5
    TEXT ('result from : '+STR OUTFILE) P1
    LET P1 (P4+PNT_XY 0 -75)
    LINE SOLID HORIZONTAL 0,-41 270  END
    LET KEEPGR (5)
  ELSE_IF (KEEPGR = 5)
    LET P1 (P4+PNT_XY 0 -85)
    TEXT_SIZE 3.5
    TEXT ('result from : '+STR OUTFILE) P1
    LET P1 (P4+PNT_XY 0 -90)
    LINE SOLID HORIZONTAL 0,-56 270  END
    LET KEEPGR (6)
ELSE_IF (KEEPGR = 6)
    LET P1 (P4+PNT_XY 0 -100)
    TEXT_SIZE 3.5
    TEXT ('result from : '+STR OUTFILE) P1
    LET P1 (P4+PNT_XY 0 -105)
    LINE SOLID HORIZONTAL 0,-71 270  END
    LET KEEPGR (7)
ELSE_IF (KEEPGR = 7)
    LET P1 (P4+PNT_XY 0 -115)
    TEXT_SIZE 3.5
    TEXT ('result from : '+STR OUTFILE) P1
    LET P1 (P4+PNT_XY 0 -120)
    LINE SOLID HORIZONTAL 0,-86 270  END
    LET KEEPGR (8)
ELSE_IF (KEEPGR = 8)
    LET P1 (P4+PNT_XY 0 -130)
    TEXT_SIZE 3.5
    TEXT ('result from : '+STR OUTFILE) P1
    LET P1 (P4+PNT_XY 0 -135)
    LINE SOLID HORIZONTAL 0,-101 270  END
    LET KEEPGR (9)
ELSE
    LET P1 (P4+PNT_XY 0 -145)
    TEXT_SIZE 3.5
    TEXT ('result from : '+STR OUTFILE) P1
    LET P1 (P4+PNT_XY 0 -150)
    LINE SOLID HORIZONTAL 0,-116 270  END
    READ STRING '"new graph" is recommended ! ' DEFAULT 'press enter to continue' AAA
    END_IF
LET DAY_P DAY
    TEXT   (' '+STR (INT(DAY_P +.5))+'  '+STR (MUE_D) +'  '+STR (BM_D) +'  '+STR (BMJ_D) +'
'+STR (RKJD_D) +'    '+STR (PSKJD_D) +'         '+STR (PSBMD_D)) P1
    END
  END_IF
conversion_aktuell_merken
LINE GREEN DOTTED END
IF (COL = 0)
    LINE DOTTED GREEN
  ELSE_IF (COL = 1)
    LINE DOTTED YELLOW
  ELSE_IF (COL = 2)
    LINE DOTTED RED
  ELSE_IF (COL = 3)
    LINE DOTTED BLUE
```

```
    ELSE_IF (COL = 4)
      LINE DOTTED WHITE
    ELSE_IF (COL = 5)
      LINE DOTTED CYAN
    ELSE_IF (COL = 6)
      LINE DOTTED SUSO2
    ELSE_IF (COL = 7)
      LINE DOTTED SUSO3
    ELSE_IF (COL = 8)
      LINE DOTTED SUSO4
    ELSE_IF (COL = 9)
      LINE DOTTED SUSO5
    ELSE
      LINE CENTER_DASH_DASH RED
    END_IF
LINE HORIZONTAL P6 P5
    LINE VERTICAL   P6 P5 END
WINDOW FIT
END_DEFINE
{*********************************************************************}
  DEFINE beginn_plot
LET FAKDAY ((BILDBREITE -20)/(SSE/800)) {FAKDAY automatisch }
    LET FAKBM  ((BILDHOEHE -70)/BMEXIT)    {FAKBM  automatisch }
{ WINDOW -5,10 360,280     Eckpunkte fuer die Kurve }
    WINDOW -5,10 (P5+PNT_XY (SSE/800*FAKDAY+20) (BMEXIT*FAKBM+20))
LINE SOLID WHITE
    LEADER_ARROW 30 ARROW_TYPE
    LEADER_LINE P5  (P5+PNT_XY (SSE/800*FAKDAY) 0) END
    LEADER_LINE P5  (P5+PNT_XY 0 (BMEXIT*FAKBM)) END END
CURRENT_FONT 'hp_block_v'
    TEXT_ADJUST 7
    TEXT_SIZE 6
    TEXT ('BMC = '+STR (BMEXIT) +' gC') (P5+PNT_XY 10 (BMEXIT*FAKBM))   END
    TEXT_ADJUST 3
    TEXT ('day = '+STR (SSE)+' ~ '+STR ((INT(SSE/365.242199*10 +.5))/10)+' years') (P5+PNT_XY
(SSE/800*FAKDAY) 10)   END
TEXT_ADJUST 1
    CURRENT_FONT 'hp_i3098_v'
LET DAY (SS)
    LET DAYD (SSD)
    LET P1 (P1+PNT_XY 0 -5)
    TEXT_SIZE 3.5
TEXT 'c  Copyright Susanne Gatti' 0,43.5 END
    CIRCLE CENTER SOLID WHITE 1.3,44.73 3 END
END_DEFINE
{*********************************************************************}
DEFINE punkt_zeichnen
    { Null - Punkt Ergebnis mit LET P5 (0,50) ist festgelegt }
IF (COL = 0)
    LINE LONG_DASHED GREEN
    ELSE_IF (COL = 1)
    LINE LONG_DASHED YELLOW
    ELSE_IF (COL = 2)
    LINE LONG_DASHED RED
    ELSE_IF (COL = 3)
    LINE LONG_DASHED BLUE
    ELSE_IF (COL = 4)
    LINE LONG_DASHED WHITE
    ELSE_IF (COL = 5)
    LINE LONG_DASHED CYAN
    ELSE_IF (COL = 6)
    LINE LONG_DASHED SUSO2
    ELSE_IF (COL = 7)
```

```
      LINE LONG_DASHED SUSO3
    ELSE_IF (COL = 8)
      LINE LONG_DASHED SUSO4
    ELSE_IF (COL = 9)
      LINE LONG_DASHED SUSO5
    ELSE
      LINE CENTER_DASH_DASH RED
    END_IF
LET P6 (P5+PNT_XY (DAY / 800 * FAKDAY) (BMC * FAKBM))
    POINT P6
    END
  END_DEFINE
{*******************************************************************}
  DEFINE zeilen_druck
{   TEXT_SIZE 3.5
    TEXT   ('   '+STR DAY +'   '+STR (MUE) +'   '+STR (BMC) +'   '+STR (BMJ) +'   '+STR (RKJD) +'
'+STR (PSKJD) +'   '+STR (PSBMD) )  P1
    END}
    punkt_zeichnen
OPEN_OUTFILE 1 APPEND OUTFILE
WRITE_FILE 1   ('"+STR DAY +'   '+STR (MUE) +'   '+STR (BMC) +'   '+STR (BMJ) +'   '+STR (RKJD)
+'   '+STR (PSKJD) +'   '+STR (PSBMD) )
CLOSE_FILE 1
END_DEFINE
{*******************************************************************}
  DEFINE conversion_merken
CURRENT_DIRECTORY 'C:/ARCHIV/ME10/GROWTH/SAVE'
  OPEN_OUTFILE 2 DEL_OLD '!_CONV.SAV'
conf_schreiben
  END_DEFINE
{***********************}
DEFINE conversion_aktuell_merken
CURRENT_DIRECTORY 'C:/ARCHIV/ME10/GROWTH/SAVE'
  OPEN_OUTFILE 2 DEL_OLD ("+STR OUTFILE +'.SAV')
conf_schreiben
  END_DEFINE
{***********************}
  DEFINE conf_schreiben
WRITE_FILE 2 '{***** CONVERSION ********************}'
    WRITE_FILE 2 '{   Anfangsvariablen merken + setzen }'
    WRITE_FILE 2 'DEFINE daten_conversion'
    WRITE_FILE 2 ' '
    WRITE_FILE 2 ('LET meth (' +STR (meth)  +')' )
    WRITE_FILE 2 ' '
    WRITE_FILE 2 ('LET PSRA (' +STR (PSRA)  +')' )
    WRITE_FILE 2 ('LET PSRB (' +STR (PSRB)  +')' )
    WRITE_FILE 2 ('LET PSRA2 (' +STR (PSRA2)  +')' )
    WRITE_FILE 2 ('LET PSRB2 (' +STR (PSRB2)  +')' )
    WRITE_FILE 2 ('LET critBM (' +STR (critBM)  +')' )
    WRITE_FILE 2 ' '
    WRITE_FILE 2 ('LET MSPA (' +STR (MSPA)  +')' )
    WRITE_FILE 2 ('LET MSPB (' +STR (MSPB)  +')' )
    WRITE_FILE 2 ' '
    WRITE_FILE 2 ('LET IM (' +STR (IM) +')' )
    WRITE_FILE 2 ('LET SS (' +STR (SS) +')' )
    WRITE_FILE 2 ('LET SSD (' +STR (SSD) +')' )
    WRITE_FILE 2 ('LET SSE (' +STR (SSE) +')' )
    WRITE_FILE 2 ('LET BMEXIT (' +STR (BMEXIT) +')' )
    WRITE_FILE 2 ' '
    WRITE_FILE 2 ('LET AFDMC (' +STR (AFDMC) +')' )
    WRITE_FILE 2 ('LET MGCG (' +STR (MGCG) +')' )
    WRITE_FILE 2 ('LET GCKJ (' +STR (GCKJ) +')' )
    WRITE_FILE 2 ('LET MLOG (' +STR (MLOG) +')' )
```

```
      WRITE_FILE 2 ('LET MGOJ (' +STR (MGOJ) +')' )
      WRITE_FILE 2 ('LET WMD (' +STR (WMD) +')' )
      WRITE_FILE 2 ('LET DMA (' +STR (DMA) +')' )
      WRITE_FILE 2 ('LET WMA (' +STR (WMA) +')' )
      WRITE_FILE 2 ('LET MGOM (' +STR (MGOM) +')' )
      WRITE_FILE 2 ' '
      WRITE_FILE 2 ("LET OUTFILE '" +STR OUTFILE +"'" )
      WRITE_FILE 2 ' '
.....WRITE_FILE 2 ('LET FAKBM (' +STR (FAKBM) +')' )
      WRITE_FILE 2 ('LET FAKDAY (' +STR (FAKDAY) +')' )
.....WRITE_FILE 2 ' '
      WRITE_FILE 2 'END_DEFINE'
      WRITE_FILE 2 ' '
      WRITE_FILE 2 '{*******************************}'
      WRITE_FILE 2 ' '
      WRITE_FILE 2 'DEFINE daten_confidence
      WRITE_FILE 2 ' '
      WRITE_FILE 2 ('LET regr (' +STR (regr) +')' )
      WRITE_FILE 2 ' '
      WRITE_FILE 2 ('LET conf_t (' +STR (conf_t) +')' )
      WRITE_FILE 2 ('LET conf_n (' +STR (conf_n) +')' )
      WRITE_FILE 2 ('LET conf_stdv (' +STR (conf_stdv) +')' )
      WRITE_FILE 2 ('LET conf_xmean (' +STR (conf_xmean) +')' )
      WRITE_FILE 2 ('LET conf_sum (' +STR (conf_sum) +')' )
      WRITE_FILE 2 ' '
      WRITE_FILE 2 'END_DEFINE'
      WRITE_FILE 2 ' '
      WRITE_FILE 2 '{******************}'
      WRITE_FILE 2 ' '
      WRITE_FILE 2 'daten_confidence'
      WRITE_FILE 2 'daten_conversion'
      WRITE_FILE 2 'SM_GROWTH'
      WRITE_FILE 2 ' '
      WRITE_FILE 2 '{*********************************}'
CLOSE_FILE 2
END_DEFINE
{*********************************************************************}
DEFINE kopf_schreiben
      {schreibt den Kopf des Ergebnisfiles, das spaeter in excel gebraucht wird}
   OPEN_OUTFILE 1 DEL_OLD OUTFILE
WRITE_FILE 1 ('method: log (1); lin (2); exp (3); ln (4);  ln->lin (5); meth =    '+STR meth)
WRITE_FILE 1 ('for Ps/R vs body mass [kJ] a=   '    +STR  PSRA)
WRITE_FILE 1 ('for Ps/R vs body mass [kJ] b=   '    +STR  PSRB)
WRITE_FILE 1 ('for Ps/R vs body mass [kJ] a2=  '    +STR  PSRA2)
WRITE_FILE 1 ('for Ps/R vs body mass [kJ] b2=  '    +STR  PSRB2)
WRITE_FILE 1 ('critical BM [gC] crit BM=   '      +STR  critBM)
WRITE_FILE 1 ('for: log msp rr = a+b*log M  a=   '    +STR MSPA)
WRITE_FILE 1 ('for: log msp rr = a+b*log M  b=   '    +STR MSPB)
WRITE_FILE 1 ('initial body mass [gC] =   '        +STR IM)
WRITE_FILE 1 ('max. body mass [gC] =   '            +STR BMEXIT)
WRITE_FILE 1 ('stepsize [days] =   '        +STR SS)
WRITE_FILE 1 ('stepsize display [days] =   '       +STR SSD)
WRITE_FILE 1 ('stepsize end [days] =   '         +STR SSE)
WRITE_FILE 1 ('AFDM -> C [g->g or mg->mg] =   '     +STR AFDMC)
WRITE_FILE 1 ('mg C-> gAFDM =   '        +STR MGCG)
WRITE_FILE 1 ('gC->kJ =   '        +STR GCKJ)
WRITE_FILE 1 ('mlO2->gC =   '        +STR MLOG)
WRITE_FILE 1 ('mgO2->J =   '        +STR MGOJ)
WRITE_FILE 1 ('mgO2->mgC =   '         +STR MGOM)
WRITE_FILE 1 ('WM->DM =   '        +STR WMD)
WRITE_FILE 1 ('DM->AFDM =   '        +STR DMA)
WRITE_FILE 1 ('WM->AFDM =   '        +STR WMA)
WRITE_FILE 1 ("Filename:    "         +STR OUTFILE)
```

```
WRITE_FILE 1 ''
WRITE_FILE 1 ('regression: fit (1); up95 (2); low95 (3); regr=    ' +STR regr)
WRITE_FILE 1 ('conf_t=   '    +STR conf_t)
WRITE_FILE 1 ('conf_n=   '    +STR conf_n)
WRITE_FILE 1 ('conf_stdv=   ' +STR conf_stdv)
WRITE_FILE 1 ('conf_sum=   '  +STR conf_sum)
WRITE_FILE 1 ('conf_xmean=   ' +STR conf_xmean)
WRITE_FILE 1 ''
WRITE_FILE 1 ''
WRITE_FILE 1 'day   MUE   BMC   BM[kJ]   R[kJ*ind-1*d-1]   Ps[kJ*ind-1*d-1]   Ps/BM[kJ*kJ-1*d-1]'
CLOSE_FILE 1
END_DEFINE
{******************************************************************************************}

{***** MENUE1.MAC  4.04 *******************************************************************}
DEFINE SM_GROWTH
    Tm_create_1
    T_clear_menu Menu_control_icons
    MENU BLACK SUSO1  CENTER 'let it grow' 'calculate'         1 3
MENU WHITE Bcol1 'outfile = '  'IN_OUTFILE'                   2 1
    MENU WHITE Bcol2 ("+STR OUTFILE) 'IN_OUTFILE'        2 2
IF (meth = 1)
    MENU Colo0 Bcol3 'method   ' 'methode'         3 1
    MENU Colo0 Bcol3 'log      ' 'methode'         3 2
    END_IF
IF (meth = 2)
    MENU Colo0 Bcol3 'method   ' 'methode'         3 1
    MENU Colo0 Bcol3 '  lin  ' 'methode'         3 2
    END_IF
IF (meth = 3)
    MENU Colo0 Bcol7 'method   ' 'methode'         3 1
    MENU Colo0 Bcol7 '    exp ' 'methode'         3 2
    END_IF
IF (meth = 4)
    MENU Colo0 Bcol3 'method   ' 'methode'         3 1
    MENU Colo0 Bcol3 '      ln' 'methode'         3 2
    END_IF
IF (meth = 5)
    MENU Colo1 Bcol2 'method   ' 'methode'         3 1
    MENU Colo1 Bcol2 ' ln -> lin ' 'methode'         3 2
    END_IF
IF (regr = 1)
    MENU Colo0 Bcol7 'regression' 'regression'         4 1
    MENU Colo0 Bcol7 ' fitted y ' 'regression'         4 2
    END_IF
IF (regr = 2)
    MENU Colo0 Bcol3 'regression' 'regression'         4 1
    MENU Colo0 Bcol3 'up 95    ' 'regression'         4 2
    END_IF
IF (regr = 3)
    MENU Colo0 Bcol3 'regression' 'regression'         4 1
    MENU Colo0 Bcol3 '  low 95' 'regression'         4 2
    END_IF
IF    (GRAPH = 0)
    MENU Colo0 Bcol1 'new graph ' 'graph_schalter'         5 1
    ELSE_IF (GRAPH = 1)
    MENU   Colo0 Bcol2 'keep graph' 'graph_schalter'         5 1
    ELSE
    MENU          '    ' '      '         5 1
    END_IF
IF    (COL = 0)
    MENU BLACK GREEN ' color ' 'LET COL (1) SM_GROWTH'   5 2
    ELSE_IF (COL = 1)
```

```
        MENU BLACK YELLOW ' color  ''LET COL (2) SM_GROWTH'   5 2
          ELSE_IF (COL = 2)
        MENU WHITE RED    ' color  ''LET COL (3) SM_GROWTH'   5 2
          ELSE_IF (COL = 3)
        MENU WHITE BLUE   ' color  ''LET COL (4) SM_GROWTH'   5 2
          ELSE_IF (COL = 4)
        MENU BLACK WHITE  ' color  ''LET COL (5) SM_GROWTH'   5 2
          ELSE_IF (COL = 5)
        MENU BLACK CYAN   ' color  ''LET COL (6) SM_GROWTH'   5 2
          ELSE_IF (COL = 6)
        MENU WHITE SUSO2  ' color  ''LET COL (7) SM_GROWTH'   5 2
          ELSE_IF (COL = 7)
        MENU BLACK SUSO3  ' color  ''LET COL (8) SM_GROWTH'   5 2
          ELSE_IF (COL = 8)
        MENU BLACK SUSO4  ' color  ''LET COL (9) SM_GROWTH'   5 2
          ELSE_IF (COL = 9)
        MENU BLACK SUSO5  ' color  ''LET COL (0) SM_GROWTH'   5 2
          ELSE
        MENU          '     '  '    '            5 2
          END_IF
MENU          '       '  '  '                      6 1
        MENU          '       '  '  '                    6 2
MENU WHITE Bcol7  'Ps/R vs M ' '    '              7 1
        MENU                   '       ' '  '          7 2
MENU          '     a:'  'IN_PSRA'              8 1
        MENU          ("+STR(PSRA)) 'IN_PSRA'          8 2
MENU          '     b:'  'IN_PSRB'              9 1
        MENU          ("+STR(PSRB)) 'IN_PSRB'          9 2
MENU          '     a2:'        'IN_PSRA2'      10 1
        MENU          ("+STR(PSRA2)) 'IN_PSRA2'      10 2
MENU          '     b2:'        'IN_PSRB2'      11 1
        MENU          ("+STR(PSRB2)) 'IN_PSRB2'      11 2
MENU          '  critBM:'  'IN_critBM'          12 1
        MENU          ("+STR(critBM)) 'IN_critBM'      12 2
MENU          '     '  '    '              13 1
        MENU          '     '  '    '            13 2
MENU WHITE Bcol7  'msprr vs M' "              14 1
        MENU          '    ' "                  14 2
MENU          '     a:'  'IN_MSPA'              15 1
        MENU          ("+STR(MSPA)) 'IN_MSPA'          15 2
MENU          '     b:'  'IN_MSPB'              16 1
        MENU          ("+STR(MSPB)) 'IN_MSPB'          16 2
MENU          '     '  '    '              17 1
        MENU          '     '  '    '            17 2
MENU WHITE Bcol2 'ini M:(gC)' 'IN_IM'        18 1
        MENU          ("+STR(IM)) 'IN_IM'          18 2
MENU WHITE Bcol2 'end M:(gC)'  'IN_BMEXIT'        19 1
        MENU          ("+STR BMEXIT) 'IN_BMEXIT'          19 2
MENU WHITE Bcol2 'stepsize: ' 'IN_SS'          20 1
        MENU          ("+STR(SS)) 'IN_SS'              20 2
MENU WHITE Bcol2 'step disp:' 'IN_SSD'          21 1
        MENU          ("+STR(SSD)) 'IN_SSD'          21 2
MENU WHITE Bcol2 'step end: ' 'IN_SSE'          22 1
        MENU          ("+STR (SSE)) 'IN_SSE'              22 2
MENU          '     '  ' '    '              23 1
        MENU          '       '  '  '              23 2
MENU WHITE Bcol2 'save data ' 'conversion_merken'          24 1
MENU WHITE Bcol2 'input data' 'CURRENT_DIRECTORY
"C:/ARCHIV/ME10/GROWTH/SAVE/"Fbt_dtabs_all_on 0 INPUT' 24 2
MENU WHITE Bcol2 'save graph' 'CURRENT_DIRECTORY
"C:/ARCHIV/ME10/GROWTH/SAVE/GRAPHS" STORE MI ALL'   25 1
MENU WHITE Bcol2 'load graph' 'DAC CURRENT_DIRECTORY
"C:/ARCHIV/ME10/GROWTH/SAVE/GRAPHS"Fbt_dtabs_all_on 0 LOAD' 25 2
```

```
END_DEFINE
{*********************************************************************}
DEFINE SM_CONVERSION
    Tm_create_1
    T_clear_menu Menu_control_icons
    MENU Colo1 Bcol4 CENTER 'conversion menue' '      '    1 3
MENU            '      ' '       '            2 1
    MENU            '       ' '       '            2 2
MENU            '       ' '       '            3 1
    MENU            '       ' '       '            3 2
MENU            '       ' '       '            4 1
    MENU            '       ' '       '            4 2
MENU            '       ' '       '            5 1
    MENU            '       ' '       '            5 2
MENU BLACK Bcol7  'conversion' "                6 1
    MENU            '       ' "                6 2
MENU            ' AFDM->C'  'IN_AFDMC'          7 1
    MENU            ("+STR(AFDMC)) 'IN_AFDMC'            7 2
MENU            'mgC->gAFDM'  'IN_MGCG'          8 1
    MENU            ("+STR(MGCG)) 'IN_MGCG'            8 2
MENU            ' gC->kJ'  'IN_GCKJ'          9 1
    MENU            ("+STR(GCKJ)) 'IN_GCKJ'            9 2
MENU            ' mgC->kJ'      "            10 1
    MENU            ("+STR(GCKJ/1000)) "            10 2
MENU            ' mlO2->gC'  'IN_MLOG'          11 1
    MENU            ("+STR(MLOG)) 'IN_MLOG'            11 2
MENU            ' mgO2->J'  'IN_MGOJ'          12 1
    MENU            ("+STR(MGOJ)) 'IN_MGOJ'            12 2
MENU            'mgO2->mgC'  'IN_MGOM'          13 1
    MENU            ("+STR(MGOM)) 'IN_MGOM'            13 2
MENU            ' WM->DM'  'IN_WMD'          14 1
    MENU            ("+STR(WMD)) 'IN_WMD'            14 2
MENU            ' DM->AFDM'  'IN_DMA'          15 1
    MENU            ("+STR(DMA)) 'IN_DMA'            15 2
MENU            ' WM->AFDM'  'IN_WMA'          16 1
    MENU            ("+STR(WMA)) 'IN_WMA'            16 2
MENU            '       ' '       '            17 1
    MENU            '       ' '       '            17 2
MENU            '       ' '       '            18 1
    MENU            '       ' '       '            18 2
MENU            '       ' '       '            19 1
    MENU            '       ' '       '            19 2
MENU            '       ' '       '            20 1
    MENU            '       ' '       '            20 2
MENU            '       ' '       '            21 1
    MENU            '       ' '       '            21 2
MENU            '       ' '       '            22 1
    MENU            '       ' '       '            22 2
MENU            '       ' '       '            23 1
    MENU            '       ' '       '            23 2
MENU            '       ' '       '            24 1
    MENU            '       ' '       '            24 2
MENU            '       ' '       '            25 1
    MENU            '       ' '       '            25 2
END_DEFINE
{*********************************************************************}
DEFINE SM_CONFIDENCE
    Tm_create_1
    T_clear_menu Menu_control_icons
    MENU Colo1 Bcol4 CENTER 'confidence menue' '      '    1 3
MENU            '      ' '       '            2 1
    MENU            '       ' '       '            2 2
MENU            '       ' '       '            3 1
```

```
    MENU          '      ' '     '           3 2
MENU          '      '  '     '           4 1
    MENU          '      ' '    '           4 2
MENU          '      '  '    '           5 1
    MENU          '      '  '    '           5 2
MENU BLACK Bcol7 'confidence' "              6 1
    MENU          '      ' "              6 2
MENU          '   conf_t'    'IN_CONF_T'       7 1
    MENU          ('"+STR(conf_t)) 'IN_CONF_T'        7 2
MENU          '  conf_n'    'IN_CONF_N'       8 1
    MENU          ('"+STR(conf_n)) 'IN_CONF_N'         8 2
MENU          ' conf_stdv'     'IN_CONF_STDV'    9 1
    MENU          ('"+STR(conf_stdv)) 'IN_CONF_STDV'    9 2
MENU          'conf_xmean'      'IN_CONF_XMEAN'  10 1
    MENU          ('"+STR(conf_xmean)) 'IN_CONF_XMEAN'  10 2
MENU          ' conf_sum'    'IN_CONF_SUM'     11 1
    MENU          ('"+STR(conf_sum)) 'IN_CONF_SUM'     11 2
MENU          '     ' '    '           12 1
    MENU          '     '  '    '           12 2
MENU          '     ' '     '           13 1
    MENU          '      '  '    '           13 2
MENU          '     ' '    '           14 1
    MENU          '     '  '     '           14 2
MENU          '     '  '    '           15 1
    MENU          '     '  '     '           15 2
MENU          '     '  '    '           16 1
    MENU          '     '  '     '           16 2
MENU          '     '  '    '           17 1
    MENU          '     '  '     '           17 2
MENU          '     '  '    '           18 1
    MENU          '     '  '     '           18 2
MENU          '     '  '    '           19 1
    MENU          '     '  '     '           19 2
MENU          '     '  '    '           20 1
    MENU          '     '  '     '           20 2
MENU          '     '  '    '           21 1
    MENU          '     '  '     '           21 2
MENU          '     '  '    '           22 1
    MENU          '     '  '     '           22 2
MENU          '     '  '    '           23 1
    MENU          '     '  '     '           23 2
MENU          '     '  '    '           24 1
    MENU          '     '  '     '           24 2
MENU          '     '  '    '           25 1
    MENU          '     '  '     '           25 2
END_DEFINE
{*****************************************************************************}
DEFINE Sm_screen_macro
 LET Lastmen 'Sm_screen_macro'
 MENU_BUFFER ON
 CURRENT_MENU Screen_menu_layout_name
 MENU Colo1 Bcol0 " " BOX 1 1 39 1
 MENU Colo0 Bcol5 'HAUPT' 'Dsp_menu' 1 1
 MENU 'LAB / DAC' 'EDIT_PART "/" DELETE ALL CONFIRM ' 2 1
 MENU " " 3 1
 MENU WHITE Bcol3 'to menue ' '        ' 4 1
 MENU WHITE Bcol1 'conversion' 'SM_CONVERSION' 5 1
 MENU WHITE Bcol1 'confidence' 'SM_CONFIDENCE' 6 1
 MENU WHITE Bcol1 'growth    ' 'SM_GROWTH'   7 1
 MENU WHITE Bcol1 'top models' 'TOP_MODELS'   8 1
 MENU WHITE Bcol1 'top graphs' 'TOP_GRAPHS'   9 1
 MENU " " 10 1
 MENU Colo1 Bcol4 'ME10 EXIT' 'EXIT_MACRO' 11 1
```

```
MENU Colo1 Bcol4 'DELETE'   'DELETE'    12 1
MENU Colo1 Bcol4 'END' 'END'            13 1
MENU " " 14 1
MENU Colo1 Bcol2'CONFIRM' 'CONFIRM' 15 1
MENU " " 16 1
MENU Colo1 Bcol3 'DATEI EDIT' 17 1
MENU Colo1 Bcol2
'.\RESULT'
'CURRENT_DIRECTORY "C:\ARCHIV\ME10\GROWTH/RESULT" Sm_file_1 Fbt_dtabs_all_on 0' 18 1
MENU Colo1 Bcol2
'.\SAVE '
'CURRENT_DIRECTORY "C:\ARCHIV\ME10\GROWTH/SAVE" Sm_file_1 Fbt_dtabs_all_on 0' 19 1
MENU Colo1 Bcol2
'.\growth'
'CURRENT_DIRECTORY "C:\ARCHIV\ME10\growth" Sm_file_1 Fbt_dtabs_all_on 0' 20 1
MENU " " 21 1
MENU Colo0 Bcol7 'INPUT Grow' "INPUT 'C:/ARCHIV/ME10/GROWTH/START.MAC" 22 1
MENU " " 23 1
MENU " " 24 1
MENU " " 25 1
MENU WHITE SUSO1 'WHITESUSO1' " 26 1
MENU BLACK SUSO1 'BLACKSUSO1' " 27 1
MENU WHITE Bcol7 'WHITEBcol7' " 28 1
MENU BLACK Bcol7 'BLACKBcol7' " 29 1
MENU Colo0 Bcol0 'Colo0Bcol0' " 30 1
MENU Colo0 Bcol7 'Colo0Bcol7' " 31 1
MENU Colo0 Bcol6 'Colo0Bcol6' " 32 1
MENU Colo0 Bcol5 'Colo0Bcol5' " 33 1
MENU Colo0 Bcol4 'Colo0Bcol4' " 34 1
MENU Colo0 Bcol3 'Colo0Bcol3' " 35 1
MENU Colo1 Bcol2 'Colo1Bcol2' " 36 1
MENU Colo0 Bcol1 'Colo0Bcol1' " 37 1
MENU Colo0 Bcol5 'HAUPT' 'Dsp_menu' 38 1 Macro_menu_add
END_DEFINE
{*******************************************************************************************}

{***** MENUE2.MAC * 4.04 ********************************************************************}

DEFINE TOP_MODELS
CURRENT_DIRECTORY 'C:/ARCHIV/ME10/GROWTH/SAVE/MODELS'
Tm_create_1
T_clear_menu Menu_control_icons
MENU Colo1 Bcol4 CENTER 'top models menue' '      '   1 3
MENU            '       ' '      '          2 1
    MENU         '       ' '      '   '          2 2
MENU BLACK SUSO1 'Hali pani' ' '    '                       3 1
    MENU          'Hp_weight '   3 2
MENU          'Hp_unweigh' '     '          4 1
    MENU          'Hp_up slop'  '     '          4 2
MENU          'Hp_lowslop'  '     '          5 1
    MENU          'Hp_small '  '     '          5 2
MENU BLACK SUSO1 'Stylocordy'  '    ' '       '          6 1
    MENU BLACK SUSO1 'la boreal.  ' '     '          6 2
MENU          'Sb_weight '       "INPUT '!_SB_SB_200_LN1B.SAV'      SM_GROWTH"      7 1
    MENU          'Sb_mean_1b'   "INPUT '!_SB_MEAN_200_LN1B.SAV'     SM_GROWTH"      7 2
MENU          'Sb_unweigh'    "INPUT '!_SB_SB_200_LN2B.SAV'      SM_GROWTH"      8 1
    MENU          'Sb_mean_2b'   "INPUT '!_SB_MEAN_200_LN2B.SAV'     SM_GROWTH"      8 2
MENU          'Sb_up slop' "INPUT '!_SB_SB_200_LN3B.SAV'      SM_GROWTH"      9 1
    MENU          'Sb_mean_3b'   "INPUT '!_SB_MEAN_200_LN3B.SAV'     SM_GROWTH"      9 2
MENU          'Sb_lowslop'    "INPUT '!_SB_SB_200_LN4B.SAV'      SM_GROWTH"      10 1
    MENU          'Sb_mean_4b'   "INPUT '!_SB_MEAN_200_LN4B.SAV'     SM_GROWTH"      10 2
MENU          'Sb_200_ln1'    "INPUT '!_SB_SB_200_LN1.SAV'      SM_GROWTH"      11 1
    MENU          'Sb_200_ln2'    "INPUT '!_SB_SB_200_LN2.SAV'      SM_GROWTH"      11 2
```

```
MENU          'Sb_200_ln3'      "INPUT '!_SB_SB_200_LN3.SAV'    SM_GROWTH"      12 1
      MENU        'Sb_200_ln4'      "INPUT '!_SB_SB_200_LN4.SAV'    SM_GROWTH"      12 2
MENU BLACK SUSO1 'Cinachyra'                        '  '          13 1
      MENU BLACK SUSO1 'antarctica'                '     '          13 2
MENU          'ca_02_m ' '   '              14 1
      MENU        'ca_03_m ' '   '              14 2
MENU          'ca_04_m ' '   '            15 1
      MENU        'ca_05_m ' '   '            15 2
MENU          'ca_06_m ' '   '          16 1
      MENU        'ca_07_m ' '   '          16 2
MENU          'ca_08_m ' '   '        17 1
      MENU        'ca_09_m ' '   '        17 2
MENU BLACK SUSO1 'hexa      ' '    '          18 1
      MENU        'hexa_01_m' '   '          18 2
MENU          'hexa_02_m' '   '        19 1
      MENU        'hexa_03_m' '   '        19 2
MENU          'hexa_04_m' '   '      20 1
      MENU        'hexa_05_m' '   '      20 2
MENU          'hexa_06_m' '   '    21 1
      MENU        'hexa_07_m' '   '    21 2
MENU          'hexa_08_m' '   '  22 1
      MENU        'hexa_09_m' '   '  22 2
MENU BLACK SUSO1 '        ' '   '    23 1
      MENU        'gruen   ' "INPUT 'gruen.sav' SM_GROWTH" 23 2
MENU          'gelb   ' "INPUT 'gelb.sav'  SM_GROWTH" 24 1
      MENU        'rot    ' "INPUT 'rot.sav'   SM_GROWTH" 24 2
MENU          'blau   ' "INPUT 'blau.sav' SM_GROWTH" 25 1
      MENU        'weiss  ' "INPUT 'weiss.sav' SM_GROWTH" 25 2
END_DEFINE
{*************************************************************************}
DEFINE TOP_GRAPHS
      CURRENT_DIRECTORY 'C:/ARCHIV/ME10/GROWTH/SAVE/GRAPHS'
      Tm_create_1
      T_clear_menu Menu_control_icons
      MENU Colo1 Bcol4 CENTER 'top graphs menue' '     '   1 3
MENU          '      ' '   '        2 1
      MENU        '    ' '   '      2 2
MENU BLACK Bcol7 'Hp      ' '   '        3 1
      MENU        'hp_01_g ' '   '        3 2
MENU          'hp_02_g ' '   '      4 1
      MENU        'hp_03_g ' '   '      4 2
MENU          'hp_04_g ' '   '    5 1
      MENU        'hp_05_g ' '   '    5 2
MENU          'hp_06_g ' '   '  6 1
      MENU        'hp_07_g ' '   '  6 2
MENU          'hp_08_g ' '   '  7 1
      MENU        'hp_09_g ' '   '  7 2
MENU BLACK Bcol7 'Sb      ' '   '   .  8 1
      MENU        'sb_01_g ' '   '      8 2
MENU          'sb_02_g ' '   '    9 1
      MENU        'sb_03_g ' '   '    9 2
MENU          'sb_04_g ' '   '  10 1
      MENU        'sb_05_g ' '   '  10 2
MENU          'sb_06_g ' '   '  11 1
      MENU        'sb_07_g ' '   '  11 2
MENU          'sb_08_g ' '   '  12 1
      MENU        'sb_09_g ' '   '  12 2
MENU BLACK Bcol7 'Ca      ' '   '  13 1
      MENU        'ca_01_g ' '   '  13 2
MENU          'ca_02_g ' '   '  14 1
      MENU        'ca_03_g ' '   '  14 2
MENU          'ca_04_g ' '   '  15 1
      MENU        'ca_05_g ' '   '  15 2
```

```
MENU          ' ca_06_g ' '    '              16 1
     MENU          ' ca_07_g ' '    '             16 2
MENU          ' ca_08_g ' '    '          17 1
     MENU          ' ca_09_g ' '    '            17 2
MENU BLACK Bcol7 'hexa      ' '    '          18 1
     MENU          'hexa_01_g ' '    '          18 2
MENU          'hexa_02_g ' '    '          19 1
     MENU          'hexa_03_g ' '    '          19 2
MENU          'hexa_04_g ' '    '          20 1
     MENU          'hexa_05_g ' '    '           20 2
MENU          'hexa_06_g ' '    '          21 1
     MENU          'hexa_07_g ' '    '            21 2
MENU          'hexa_08_g ' '    '          22 1
     MENU          'hexa_09_g ' '    '            22 2
MENU BLACK Bcol7 '        ' '    '          23 1
     MENU          ' GGRBW   ' "DAC LOAD 'GGRBW.MI' WF SM_GROWTH" 23 2
MENU          ' gelb    ' '    '          24 1
     MENU          ' rot     ' '    '          24 2
MENU          ' blau    ' '    '          25 1
     MENU          ' weiss   ' '    '          25 2
END_DEFINE
{*****************************************************************************************************}

{***************** START.MAC for GROWTH  4.04*****************************************************}
CURRENT_DIRECTORY 'C:/ARCHIV/ME10/GROWTH'
{ RENAME_PART '                   ** su-s*nnes AMIGO** }
   LET BILDBREITE (300)
   LET BILDHOEHE  (280)
LET GRAPH  (0)
   LET COL    (0)
   LET WACHE1 (1)
   LET KEEPGR (0)
   LET PSRM (0)
INPUT 'GROWTH.QEL'
   INPUT 'GROWTH.MAC'
   INPUT 'MENUE1.MAC'
   INPUT 'MENUE2.MAC'
   INPUT 'IN_OUT.QEL'
   INPUT './SAVE/I_CONV.SAV'
I_set_font 'HP_BLK_V.FNT'
   TEXT_FILL on
SM_GROWTH
   Sm_screen_macro
   DELETE ALL CONFIRM
   LOAD 'SUSONNE.BI'
   WINDOW FIT
{*****************************************************************************************************}
```

"Berichte zur Polarforschung"

Eine Titelübersicht der Hefte 1 bis 376 (1981 - 2000) erschien zuletzt im Heft 413 der nachfolgenden Reihe "Berichte zur Polar- und Meeresforschung". Ein Verzeichnis aller Hefte beider Reihen sowie eine Zusammenstellung der Abstracts in englischer Sprache finden sich im Internet unter der Adresse:

http://www.awi-bremerhaven.de/Resources/publications.html

Ab dem Heft-Nr. 377 erscheint die Reihe unter dem Namen: "Berichte zur Polar- und Meeresforschung".

Heft-Nr. 377/2000 – „Rekrutierungsmuster ausgewählter Wattfauna nach unterschiedlich strengen Wintern" von Matthias Strasser.

Heft-Nr. 378/2001 – „Der Transport von Wärme, Wasser und Salz in den Arktischen Ozean", von Boris Cisewski.

Heft-Nr. 379/2001 – „Analyse hydrographischer Schnitte mit Satellitenaltimetrie", von Martin Losch.

Heft-Nr. 380/2001 – „Die Expeditionen ANTARKTIS XVI/1-2 des Forschungsschiffes POLARSTERN 1998/1999", herausgegeben von Eberhard Fahrbach und Saad El Naggar.

Heft-Nr. 381/2001 – „UV-Schutz- und Reparaturmechanismen bei antarktischen Diatomeen und *Phaeocystis antarctica*", von Lieselotte Riegger.

Heft-Nr. 382/2001 – "Age determination in polar Crustacea using the autofluorescent pigment lipofuscin", by Bodil Bluhm.

Heft-Nr. 383/2001 – „Zeitliche und räumliche Verteilung, Habitatspräferenzen und Populationsdynamik benthischer Copepoda Harpacticoida in der Potter Cove (King George Island, Antarktis)", von Gritta Veit-Köhler.

Heft-Nr. 384/2001 – „Beiträge aus geophysikalischen Messungen in Dronning Maud Land, Antarktis, zur Auffindung eines optimalen Bohrpunktes für eine Eiskerntiefbohrung", von Daniel Steinhage.

Heft-Nr. 385/2001 – „Actinium-227 als Tracer für Advektion und Mischung in der Tiefsee", von Walter Geibert.

Heft-Nr. 386/2001 – „Messung von optischen Eigenschaften troposphärischer Aerosole in der Arktis", von Rolf Schumacher.

Heft-Nr. 387/2001 – „Bestimmung des Ozonabbaus in der arktischen und subarktischen Stratosphäre", von Astrid Schulz.

Heft-Nr. 388/2001 – "Russian-German Cooperation SYSTEM LAPTEV SEA 2000: The Expedition LENA 2000", edited by Volker Rachold and Mikhail N. Grigoriev.

Heft-Nr. 389/2001 – "The Expeditions ARKTIS XVI/1 and ARKTIS XVI/2 of the Rearch Vessel ‚Polarstern' in 2000", edited by Gunther Krause and Ursula Schauer.

Heft-Nr. 390/2001 – "Late Quaternary climate variations recorded in North Atlantic deep-sea benthic ostracodes", by Claudia Didié.

Heft-Nr. 391/2001 – "The polar and subpolar North Atlantic during the last five glacial-interglacial cycles", by Jan P. Helmke.

Heft-Nr. 392/2001 – „Geochemische Untersuchungen an hydrothermal beeinflußten Sedimenten der Bransfield Straße (Antarktis)", von Anke Dählmann.

Heft-Nr. 393/2001 – "The German-Russian Project on Siberian River Run-off (SIRRO): Scientific Cruise Report of the Kara-Sea Expedition 'SIRRO 2000' of RV ‚Boris Petrov' and first results", edited by Ruediger Stein and Oleg Stepanets.

Heft-Nr. 394/2001 – „Untersuchungen der Photooxidantien Wasserstoffperoxid, Methylhydroperoxid und Formaldehyd in der Troposphäre der Antarktis ", von Katja Riedel.

Heft-Nr. 395/2001 – "Role of benthic cnidarians in the energy transfer processes in the Southern Ocean marine ecosystem (Antarctica)", by Covadonga Orejas Saco del Valle.

Heft-Nr. 396/2001 – "Biogeochemistry of Dissolved Carbohydrates in thew Arctic", by Ralph Engbrodt.

Heft-Nr. 397/2001 – "Seasonality of marine algae and grazers of an Antarctic rocky intertidal, with emphasis on the role of the limpet *Nacilla concinna* Strebel (Gastropoda: Patellidae)", by Dohong Kim.

Heft-Nr. 398/2001 – "Polare Stratosphärenwolken und mesoskalige Dynamik am Polarwirbelrand", von Marion Müller.

Heft-Nr. 399/2001 – "North Atlantic Deep Water and Antarctic Bottom Water: Their Interaction and Influence on Modes of the Global Ocean Circulation", by Holger Brix.

Heft-Nr. 400/2001 – "The Expeditions ANTARKTIS XVIII/1-2 of the Research Vessel 'Polarstern' in 2000", edited by Victor Smetacek, Ulrich Bathmann, Saad El Naggar.

Heft-Nr. 401/2001 – "Variabilität von CH_2O (Formaldehyd) - untersucht mit Hilfe der solaren Absorptionsspektroskopie und Modellen", von Torsten Albrecht.

Heft-Nr. 402/2001 – "The Expedition ANTARKTIS XVII/3 (EASIZ III) of RV 'Polarstern' in 2000", edited by Wolf E. Arntz and Thomas Brey.

Heft-Nr. 403/2001 – "Mikrohabitatansprüche benthischer Foraminiferen in Sedimenten des Südatlantiks", von Stefanie Schumacher.

Heft-Nr. 404/2002 – "Die Expedition ANTARKTIS XVII/2 des Forschungsschiffes 'Polarstern' 2000", herausgegeben von Jörn Thiede und Hans Oerter.

Heft-Nr. 405/2002 – "Feeding Ecology of the Arctic Ice-Amphipod *Gammarus wilkitzkii*. Physiological, Morphological and Ecological Studies", by Carolin E. Arndt.

Heft-Nr. 406/2002 – "Radiolarienfauna im Ochotskischen Meer - eine aktuopaläontologische Charakterisierung der Biozönose und Taphozönose", von Anja Nimmergut.

Heft-Nr. 407/2002 – "The Expedition ANTARKTIS XVIII/5b of the Research Vessel 'Polarstern' in 2001", edited by Ulrich Bathmann.

Heft-Nr. 408/2002 – "Siedlungsmuster und Wechselbeziehungen von Seepocken (Cirripedia) auf Muschelbänken (*Mytilus edulis* L.) im Wattenmeer", von Christian Buschbaum.

Heft-Nr. 409/2002 – "Zur Ökologie von Schmelzwassertümpeln auf arktischem Meereis - Charakteristika, saisonale Dynamik und Vergleich mit anderen aquatischen Lebensräumen polarer Regionen", von Marina Carstens.

Heft-Nr. 410/2002 – "Impuls- und Wärmeaustausch zwischen der Atmosphäre und dem eisbedeckten Ozean", von Thomas Garbrecht.

Heft-Nr. 411/2002 – "Messung und Charakterisierung laminarer Ozonstrukturen in der polaren Stratosphäre", von Petra Wahl.

Heft-Nr. 412/2002 – "Open Ocean Aquaculture und Offshore Windparks. Eine Machbarkeitsstudie über die multifunktionale Nutzung von Offshore-Windparks und Offshore-Marikultur im Raum Nordsee", von Bela Hieronymus Buck.

Heft-Nr. 413/2002 – "Arctic Coastal Dynamics. Report of an International Workshop. Potsdam (Germany) 26-30 November 2001", edited by Volker Rachold, Jerry Brown and Steve Solomon.

Heft-Nr. 414/2002 – "Entwicklung und Anwendung eines Laserablations-ICP-MS-Verfahrens zur Multielementanalyse von atmosphärischen Einträgen in Eisbohrkernen", von Heiko Reinhardt.

Heft-Nr. 415/2002 – "Gefrier- und Tauprozesse im sibirischen Permafrost – Untersuchungsmethoden und ökologische Bedeutung", von Wiebke Müller-Lupp.

Heft-Nr. 416/2002 – "Natürliche Klimavariationen der Arktis in einem regionalen hochauflösenden Atmosphärenmodell", von Wolfgang Dorn.

Heft-Nr. 417/2002 – "Ecological comparison of two sandy shores with different wave energy and morphodynamics in the North Sea", by Iris Menn.

Heft-Nr. 418/2002 – "Numerische Modellierung turbulenter Umströmungen von Gebäuden", von Simón Domingo López.

Heft-Nr. 419/2002 – "Scientific Cruise Report of the Kara-Sea Expedition 2001 of RV 'Academik Petrov': The German-Russian Project on Siberian River Run-off (SIRRO) and the EU Project 'ESTABLISH'", edited by Ruediger Stein and Oleg Stepanets.

Heft-Nr. 420/2002 – "Vulkanologie und Geochemie pliozäner bis rezenter Vukanite beiderseits der Bransfield-Straße / West-Antarktis", von Andreas Veit.

Heft-Nr. 421/2002 – "POLARSTERN ARKTIS XVII/2 Cruise Report: AMORE 2001 (Arctic Mid-Ocean Ridge Expedition)", by J. Thiede et al.

Heft-Nr. 422/2002 – "The Expedition 'AWI' of RV 'L'Atalante' in 2001", edited by Michael Klages, Benoit Mesnil, Thomas Soltwedel and Alain Christophe with contributions of the participants.

Heft-Nr. 423/2002 – "Über die Tiefenwasserausbreitung im Weddellmeer und in der Scotia-Sea: Numerische Untersuchungen der Transport- und Austauschprozesse in der Weddell-Scotia-Konfluenz-Zone", von Michael Schodlok.

Heft-Nr. 424/2002 – "Short- and Long-Term Environmental Changes in the Laptev Sea (Siberian Arctic) During the Holocene", von Thomas Müller-Lupp.

Heft-Nr. 425/2002 – "Characterisation of glacio-chemical and glacio-meteorological parameters of Amundsenisen, Dronning Maud Land, Antarctica", by Fidan Göktas.

Heft-Nr. 426/2002 – "Russian-German Cooperation SYSTEM LAPTEV SEA 2000: The Expedition LENA 2001", edited by Eva-Maria Pfeiffer and Mikhail N. Grigoriev.

Heft-Nr. 427/2002 – "From the Inner Shelf to the Deep Sea: Depositional Environments on the Antarctic Peninsula Margin - A Sedimentological and Seismostratigraphic Study (ODP Leg 178)", by Tobias Mörz.

Heft-Nr. 428/2002 – "Concentration and Size Distribution of Microparticles in the NGRIP Ice Core (Central Greenland) during the Last Glazial Period", by Urs Ruth.

Heft-Nr. 429/2002 – "Interpretation von FCKW-Daten im Weddellmeer", von Olaf Klatt.

Heft-Nr. 430/2002 – "Thermal History of the Middle and Late Miocene Southern Ocean - Diatom Evidence", by Bernd M. Censarek.

Heft-Nr. 431/2002 – "Radium-226 and Radium-228 in the Atlantic Sector of the Southern Ocean", by Claudia Hanfland.

Heft-Nr. 432/2002 – "Population dynamics and ecology of the surf clam *Donax serra* (Bivalvia, Donacidae) inhabiting beaches of the Benguela upwelling system", by Jürgen Laudien.

Heft-Nr. 433/2002 – "Die Expedition ARKTIS XVII/1 des Forschungsschiffes POLARSTERN 2001", herausgegeben von Eberhard Fahrbach.

Heft-Nr. 434/2002 – "The Rôle of Sponges in High-Antarctic Carbon and Silicon Cycling – a Modelling Approach", by Susanne Gatti.